

Investigation of the Interphase Behavior of Different Bronze Alloys in Archaeological Soil of Cyprus

Elif Dođru

Submitted to the
Institute of Graduate Studies and Research
in partial fulfillment of the requirements for the degree of

Master of Science
in
Chemistry

Eastern Mediterranean University
January 2020
Gazimađusa, North Cyprus

Approval of the Institute of Graduate Studies and Research

Prof. Dr. Ali Hakan Ulusoy
Director

I certify that this thesis satisfies all the requirements as a thesis for the degree of Master of Science in Chemistry.

Prof. Dr. İzzet Sakallı
Chair, Department of Chemistry

We certify that we have read this thesis and that in our opinion it is fully adequate in scope and quality as a thesis for the degree of Master of Science in Chemistry.

Asst. Prof. Dr. Bülent Kızılduman
Co-Supervisor

Prof. Dr. Huriye İcil
Supervisor

Examining Committee

1. Prof. Dr. Huriye İcil

2. Assoc. Prof. Dr. Nur P. Aydınlık

3. Asst. Prof. Dr. Süleyman Aşır

ABSTRACT

The analysis of archaeological bronze artifacts for the identification of corrosion products and the evaluation of possible causes of these products is carried out by a combination of different disciplines. Corrosion products seen on bronze objects have often destructive effects on the artifacts due to their complex structure and put the artifacts in a cycle of irreversible deterioration. Because each artifact is original, it is necessary to examine each one separately in order to understand and stop the cause of this destructive process.

In this thesis, it is aimed to identify corrosion products resulting from the chemical and electrochemical corrosion processes of the 6 bronze bowl, selected by hoard, in a pithos from Late Bronze Age and to explain the effect of environmental-structural factors. In line with this goal, Cyclic Voltammetry (CV) for electrochemical analysis of corrosion product samples, 3 of each and 18 total, and Fourier Infrared Spectroscopy (FT-IR) were used for spectroscopic examination.

Electrochemical analyses and spectroscopic examinations of bronze artifacts have identified the presence of different types of copper alloy corrosion products. Consequently, corrosion types of 6 bronze bowls from the Late Bronze Age period were identified and it was observed that they were directly and indirectly related to environmental factors in the formation of these corrosion products.

Keywords: bronze, corrosion, infrared spectroscopy, cyclic voltammetry

ÖZ

Arkeolojik bronz eserlerin korozyon ürünlerinin tanımlanmasına yönelik analiz ve bu ürünlerin olası sebeplerinin değerlendirilmesi disiplinlerarası bir çalışma ile gerçekleştirilmiştir. Bronz objeler üzerinde görülmekte olan korozyon ürünleri kompleks yapıları sebebi ile eserler üzerinde çoğunlukla yıkıcı etkilere sahip olup, eserleri geri dönüşümü olmayan bir bozulma döngüsüne sokmaktadır. Her bir eserin özgün olmasından dolayı, bu yıkıcı sürecin sebebini anlamak ve durdurmak için detaylı araştırmalar yapılması gerekmektedir.

Bu tezde, bir pitos içerisinde bulunan ve Geç Tunç Dönemi'ne ait altı adet bronz kaseinin korozyon ürünleri iki farklı spektroskopik metot ile detaylı incelenmiştir.. Bu amaçla, altı farklı kaseden üçer örnek alınmak suretiyle toplam 18 adet korozyon ürünü örnekleri, Fourier Dönüşümlü Kızılötesi Spektroskopisi (FT-IR) ve Dönüşümlü Voltametri spektroskopik yöntemleri ile detaylı incelenmiştir.

Elektrokimyasal analizleri ve spektroskopik incelemeleri gerçekleştirilmiş olan bronz eserlere ait örneklerde farklı türde, bakır alaşımlarına ait korozyon ürünlerinin varlığı belirlenmiştir. Geç Tunç Çağı dönemine ait altı adet bronz kaseinin korozyon türleri tespit edilmiş ve bu korozyon ürünlerinin oluşumunda çevresel faktörler ile doğrudan ve dolaylı olarak ilişkisi detaylı olarak tartışılmıştır.

Anahtar Kelimeler: bronz, korozyon, infrared spektroskopisi, dönüşümlü voltametri

To My Mom...

ACKNOWLEDGEMENT

I would like to thank my supervisor Prof. Dr. Huriye İcil for giving me valuable advice and support always when needed. Besides my supervisor, I would like to thank my co-supervisor Asst. Prof. Bülent Kızılduman for his good advice, insightful comments and for helping me throughout my academic life.

I am indebted to my lovely friend Duygu Malyalı who have always been there for support and sharing her knowledge with me. Special thanks to DAKMAR family, Arwa Abou Rajab and Meltem Dinleyici.

Last but not least, I would like to thank Rüşhan Giriş for supporting me through this master's duration and always.

TABLE OF CONTENTS

ABSTRACT.....	iii
ÖZ	iv
DEDICATION.....	v
ACKNOWLEDGEMENT	vi
LIST OF TABLES	ix
LIST OF FIGURES	x
LIST OF SYMBOLS AND ABBREVIATIONS	xi
1 INTRODUCTION	1
2 THEORETICAL	3
2.1 Raw Material Resources in Cyprus Late Bronze Age Metallurgy.....	3
2.1.1 Copper.....	4
2.1.2 Arsenic	5
2.1.3 Lead.....	5
2.1.4 Tin	6
2.2 Copper Alloys	6
2.2.1 Bronze	7
2.3 The Late Bronze Age Hoard of Kral Tepesi	8
2.3.1 2004 Kral Tepesi Bronzes' Content.....	11
2.3.2 2004 Kral Tepesi Mineral Origin Analysis of Bronzes	13
2.4 Corrosion and Patina in Copper Alloys	15
2.4.1 Corrosion Types	16
2.4.1.1 Chemical Corrosion	16
2.4.1.2 Electrochemical Corrosion.....	16

2.4.2 Patina Types	17
2.4.2.1 Oxides	19
2.4.2.2 Chlorides	20
2.4.2.3 Carbonates.....	22
2.4.2.4 Sulphates	22
2.4.2.5 Sulphides	23
2.4.2.6 Phosphates.....	23
2.4.2.7 Hydroxides	23
2.4.2.8 Nitrates	23
2.4.3 Causes of Copper Alloy Corrosion	24
2.4.3.1 Structural Impact.....	24
2.4.3.2 Atmosphere	24
2.4.3.3 Oxygen	25
2.4.3.4 Water	25
2.4.3.5 Humidity	25
2.4.3.6 Temperature	26
2.4.3.7 Microbiological Organisms.....	26
2.4.3.8 Ph	27
2.4.3.9 Soil	27
3 EXPERIMENTAL	29
3.1 Metarials.....	29
3.2 Instruments.....	38
3.3 Methods.....	38
4 DATA.....	40
4.1 Fourier transform infrared spectroscopy.....	40

4.2 Cyclic Voltammetry	58
5 RESULTS AND DISCUSSION	78
5.1 Fourier transform infrared spectroscopy	78
5.2 Cyclic Voltammetry	83
6 CONCLUSION	91
REFERENCES.....	92

LIST OF TABLES

Table 1: Copper properties.....	4
Table 2: Arsenic properties.....	5
Table 3: Lead properties.....	5
Table 4: Tin properties.....	6
Table 5: XRF results of bronzes.....	12
Table 6: Result of lead-isotopes and trace element.....	14
Table 7: Corrosion products of copper and copper alloys.....	18
Table 8: Conditions of metal artifacts according to different pH of soil.....	27
Table 9: Microscopic images of samples.....	30
Table 10: Cyclic voltammetry data of samples and reference compounds in solid state.....	86
Table 11: Corrosion product types of all samples.....	88

LIST OF FIGURES

Figure 1: Hoard on the Kral Tepesi in situ.....	8
Figure 2: Schematic drawing of the location of the hoard objects within the pithos and selected bowls with their excavation number.....	9
Figure 3: The view of the hoard, after being taken out from the pithos and selected bowls with their excavation number.....	10
Figure 4: Copper alloy deterioration due to ‘bronze disease’	21
Figure 5: 3 samples of every each bowls’ location.....	31
Figure 6: 3 samples of KT/04/11/05’s locations and their microscopic images.....	32
Figure 7: 3 samples of KT/04/11/06’s locations and their microscopic images.....	33
Figure 8: 3 samples of KT/04/11/07’s locations and their microscopic images.....	34
Figure 9: 3 samples of KT/04/11/08’s locations and their microscopic images.....	35
Figure 10: 3 samples of KT/04/11/10’s locations and their microscopic images.....	36
Figure 11: 3 samples of KT/04/11/22’s locations and their microscopic images.....	37
Figure 12: Infrared Spectrum of KT/04/11/05 A.....	41
Figure 13: Infrared Spectrum of KT/04/11/05 B.....	42
Figure 14: Infrared Spectrum of KT/04/11/06 A.....	43
Figure 15: Infrared Spectrum of KT/04/11/06 B.....	44
Figure 16: Infrared Spectrum of KT/04/11/06 C.....	45
Figure 17: Infrared Spectrum of KT/04/11/07 A.....	46
Figure 18: Infrared Spectrum of KT/04/11/07 B.....	47
Figure 19: Infrared Spectrum of KT/04/11/07 C.....	48
Figure 20: Infrared Spectrum of KT/04/11/08 A.....	49
Figure 21: Infrared Spectrum of KT/04/11/08 B.....	50

Figure 22: Infrared Spectrum of KT/04/11/08 C.....	51
Figure 23: Infrared Spectrum of KT/04/11/10 A.....	52
Figure 24: Infrared Spectrum of KT/04/11/10 B.....	53
Figure 25: Infrared Spectrum of KT/04/11/10 C.....	54
Figure 26: Infrared Spectrum of KT/04/11/22 A.....	55
Figure 27: Infrared Spectrum of KT/04/11/22 B.....	56
Figure 28: Infrared Spectrum of KT/04/11/22 C.....	57
Figure 29: Cyclic voltammetry curve for KT/11/04/05 A	59
Figure 30: Cyclic voltammetry curve for KT/11/04/05 B.....	60
Figure 31: Cyclic voltammetry curve for KT/11/04/06 A.....	61
Figure 32: Cyclic voltammetry curve for KT/11/04/06 B.....	62
Figure 33: Cyclic voltammetry curve for KT/11/04/07 A.....	63
Figure 34: Cyclic voltammetry curve for KT/11/04/07 B.....	64
Figure 35: Cyclic voltammetry curve for KT/11/04/08 A.....	65
Figure 36: Cyclic voltammetry curve for KT/11/04/08 B.....	66
Figure 37: Cyclic voltammetry curve for KT/11/04/08 C.....	67
Figure 38: Cyclic voltammetry curve for KT/11/04/10 A.....	68
Figure 39: Cyclic voltammetry curve for KT/11/04/10 B.....	69
Figure 40: Cyclic voltammetry curve for KT/11/04/10 C.....	70
Figure 41: Cyclic voltammetry curve for KT/11/04/22 A.....	71
Figure 42: Cyclic voltammetry curve for KT/11/04/22 B.....	72
Figure 43: Cyclic voltammetry curve for KT/11/04/22 C.....	73
Figure 44: Cyclic voltammetry curve for $CuCl$	74
Figure 45: Cyclic voltammetry curve for $CuCl_2$	75
Figure 46: Cyclic voltammetry curve for CuO	76

Figure 47: Cyclic voltammetry curve for $CuSO_4$77

Figure 48: Selected bowls' main corrosion types and possible causes.....89

LIST OF SYMBOLS AND ABBREVIATIONS

amu	atomic mass unit
BP	boiling point
cm	centimetre
CV	Cyclic Voltammetry
FT-IR	Fourier transform infrared spectroscopy
E _{pc}	cathodic potential.
E _{pa}	anodic potential.
E _p	peak potential separations.
eV	Electron volt
<i>kJ</i>	kilojoule
KBr	Potassium bromide
mm	millimeter
mol	Mole
MP	melting point
V	voltage
ΔG	Gibbs free energy
%	per cent
°C	Celsius

Chapter 1

INTRODUCTION

Even though archaeological bronze artifacts have similar chemical composition and microstructure, the situation of each archaeological work is more complex than the other because they all have a unique individual story and interaction with the soil.

(Memet, 2007). Given the variation of environmental elements and the diversity of alloy metals; it is not possible to make a generalization on the protection / degradation behavior of archaeological bronze artifacts. Therefore, it is very important to determine a descriptive method for dealing with the corrosion stratigraphy of the works. (Dillmann et al., 2014)

Characterization of corrosion products has been carried out for a long time to develop the conservation strategies and restoration procedures of archaeological copper alloys (Piccardo and Robbiola, 2007). Davy (1826) conducted the first scientific study on the analysis of deterioration of copper and copper alloys in 1826. In the early 1900s, the composition of natural patinas was defined by the Vernon and Whitby (1929), after that studied the formation and mechanisms of natural patina on copper (Graedel, 1987; Franey and Davis, 1987).

Infrared Spectroscopy, which has long been used in the identification of archaeological materials, is also used for characterization of patina (Derric et al.,

2000). Tennet and Antonio (1981) characterized the bronze disease and products by using IR technique. Since then, the use of IR technique is preferred to obtain information about molecular structures, functional groups and chemical compounds of copper alloys' corrosion products. (Koltai, 1984; Bettembourg, 1993 ; Mazzeo and Joseph, 2005 ; Berger, 2012 ; Di Carlo et al., 2017).

Cyclic voltammetry, which is generally focused on metal corrosion problems in the use of electrochemical methods, is one of the most widely used electrochemical techniques (Doménech-Carbó, et al. 2009). However, the use of cyclic voltammetry for the electrochemical behavior of archaeological copper alloys has been taking place since 2004 (Souissi et al., 2004). Serghini and his team performed spectroscopic and electrochemical characterizations of some archeological bronze patinas in 2005. (Serghini-Idrissi et al. , 2005)

The purpose of this study is to characterize the corrosion products of 6 bronze bowls from Late Bronze Age which were found in 2004, by using electrochemical and spectroscopic techniques. By using FT-TR and cyclic voltammetry techniques, the environmental impacts of the patinas¹ during the formation process will also be examined.

¹ Patinas can be in two different types: historical and artistic (Robbiola and Portier, 2006). However, since there is no evidence of artistic patination prior to the pre-classical antiquity period (La-Niece, 2013), patinas of selected artifacts for this thesis has stated natural.

Chapter 2

THEORETICAL

2.1 Raw Material Resources in Cyprus Late Bronze Age Metallurgy

Mining in Cyprus has started in the Chalcolithic Age (Kızılduman, 2000). The first metal objects of the chalcolithic period were copper and they were produced from Cyprus' local sources (Kassianidou, 2012). However, it is known that Cypriot metallurgy and copper mining were primitive in the Chalcolithic period (Gale, 1991).

Cyprus, known for its richness in copper and other natural resources, (Toumazou et al., 1998) its metallurgy and the development of copper production has developed with the desire to meet the demand from foreign markets (Knapp, 1988; Gale, 1991).

In the Bronze Age when Cyprus was active and central in copper trade (Stos-Gale and Gale, 2010 - Knapp 1985), especially at Late Bronze Age, the island's wealth was mainly depended on the copper reserves (Steel, 2014) and it provided unprecedented prosperity (Knapp, 2003).

Due to the lack of lead and tin ore in the island, during the antiquity period copper was almost the only metal produced. (Stos-Gale and Gale, 2010).

2.1.1 Copper

Copper can be found either as mineral or as ore in nature. Despite that the copper was known from prehistoric period, the name of this element was arisen from 'Cuprum' for Cyprus (Norman, 2019).

Copper, naturally, can be found mostly in stream deposits or in the eroded upper layers of copper ores, and is a material that can be oxidized (Kızılduman, 2000).

The natural copper is abundant in Cyprus (Moorey, 1994). Cyprus type copper deposits are located in the Trodos massifs and slopes (Kızılduman, 2000), and copper minerals that are found in Cyprus consist of Azurite, Bornite, Delafosit, Chalcocite, Kovelite, Malachite and Tenorite (Tylecote, 1982). Cyprus was seen as a production center for copper producing during the antiquity period. (Forbes, 1950).

Some important properties of copper element are given in Table 1 (Greenwood and Earnshaw, 2012)

Table 1: Copper properties

Property	Copper
Symbol	Cu
Atomic number	29
Atomic weight/ amu	63.546
MP/ °C	1083
BP/ °C	2570

2.1.2 Arsenic

In prehistoric period, arsenic was recognized for its toxic sulfides (Norman, 2019). Main arsenic minerals are known as realgar, orpiment, arsenopyrite and arsenolite (Kızılduman, 2000). It is known that arsenic is present in copper mineral deposits in Cyprus (Panayiotu, 1980). Some important properties of the element arsenic are presented in Table 2 below (Greenwood and Earnshaw, 2012).

Table 2: Arsenic properties

Property	Arsenic
Symbol	As
Atomic number	33
Atomic weight / amu	74.921

2.1.3 Lead

Lead is the heaviest element among the minerals used in alloys. It is a soft metal that can be easily shaped and forged with a high corrosion resistance (Kızılduman, 2000). There are galenite ore deposits in Cyprus, one of the most well-known lead minerals (Gale and Stos-Gale, 1985). There may also be lead in copper ore in Cyprus (Gale and Stos Gale, 1982).

Some important features of the lead element are given in Table 3 (Greenwood and Earnshaw, 2012)

Table 3: Lead properties

Property	Lead
Symbol	Pb
Atomic number	82
Atomic weight / amu	207.2

2.1.4 Tin

The general source of tin in ancient history was the mineral cassiterite which is an oxide of tin (Hodges, 1964). Since tin is used to prevent oxidation of various mines, it is also used to make bronze, which is one of copper alloys, which is the most suitable additive for hardening of copper as it is used (Kızılduman, 2000). It is known that tin ores are imported for the addition of tin to copper alloys (Forbes, 1950; Hodges, 1964; Gale, 1991) due to very low amount of chalcopyrite ore in Cyprus reserves (Rapp, 1982) in which this ratio does not have any economic value. Some important properties of the element tin are given in Table 4 (Greenwood and Earnshaw, 2012).

Table 4: Tin properties

Property	Tin
Symbol	Sn
Atomic number	50
Atomic weight	118710

2.2 Copper Alloys

Pure copper is a very soft metal with little strength (Hodges, 1964). Therefore, it was not suitable for use in the construction of tools and tools requiring durability and hardness (Ehsani, 2015). In order to increase the mechanical strength of the material, ease and harden the casting process, different copper alloys were also made by adding zinc, arsenic, tin and lead (Knotkova and Kreislova, 2007).

In the ancient times (Bronze Age, 3300-2800 BC) while bronze (copper and tin alloy) was obtained directly from complex ores, brass (copper and zinc alloy) began to be used in 1000 BC. (Ehsani, 2015) .

The most used and known copper alloy is bronze (Gnesin, 2015), which is also very commonly observed in archaeological copper alloy artifacts and objects (Knotkova and Kreislova, 2007).

2.2.1 Bronze²

Tin is the most suitable mine for hardening the copper which is soft (Esin, 1969). There are different opinions about the ratio of tin added to create bronze. Bachmann (1982) says that the 0.1-0.5% of the shear in copper is caused by minerals from the ore deposit. Buchholz (1967) believes that artifacts containing 1-7% tin in copper in Cyprus are made of bronze alloy, while Esin (1969) thought that it might be desired to made real bronze when the ratio of copper exceeds 6%. On the other hand, it is also stated that bronze is formed by remelting copper and approximately 12% tin in ceramic furnaces (Ehsani, 2015).

Although alloys with a tin ratio of 10% are considered to be the best grade bronze (Esin 1969), the physical properties of the bronzes change rapidly as the added ratio starts to rise to 10% or higher (Meeks, 1993).

² Arsenical coppers are classified two groups according to the mixture rate they have.; arsenical copper and arsenical bronze (Courcier, 2014).Bronze with 1-2% tin and 1-4% arsenic are arsenic bronzes (Hodges, 1964).Copper with 0.1 - 0.9% arsenic is called arsenical copper (Gadzhiev & Korenevskii, 1984).

The term high-tin bronzes are used for bronzes with tin content between 15% and 27% (Barnard 1961; Caley et al. 1979; Sawada 1979)

2.3 The Late Bronze Age Hoard of Kral Tepesi

Cyprus has a special importance in the Eastern Mediterranean with its harbor and mineral deposits, and Karpaz Peninsula location has always attracted attention with its advantageous reach to overseas environmental cultures (Kızılduman, 2017). The King Tepesi settlement, next to Kaleburnu/Galinoporni on the Karpaz peninsula of Cyprus was discovered by Eastern Mediterranean University academicians during their hiking trip in June 2004 (Bartelheim et al., 2008). A pithos consist 26 metal objects of the hoard, 16 vessels, three offering stands, five sickles, a shovel and a saw (Figure 1-2).

The collection of bronze artefacts discovered during the first intervention, up to the second bronze artefacts to be discovered in 2014 at King's Hill, it was the best preserved and largest collection of bronze artefacts dated to The Late Bronze Age in Cyprus (Kızılduman, 2017) (Figure 3).



Figure 1: Hoard on the Kral Tepesi in situ (Bartelheim et al., 2008).

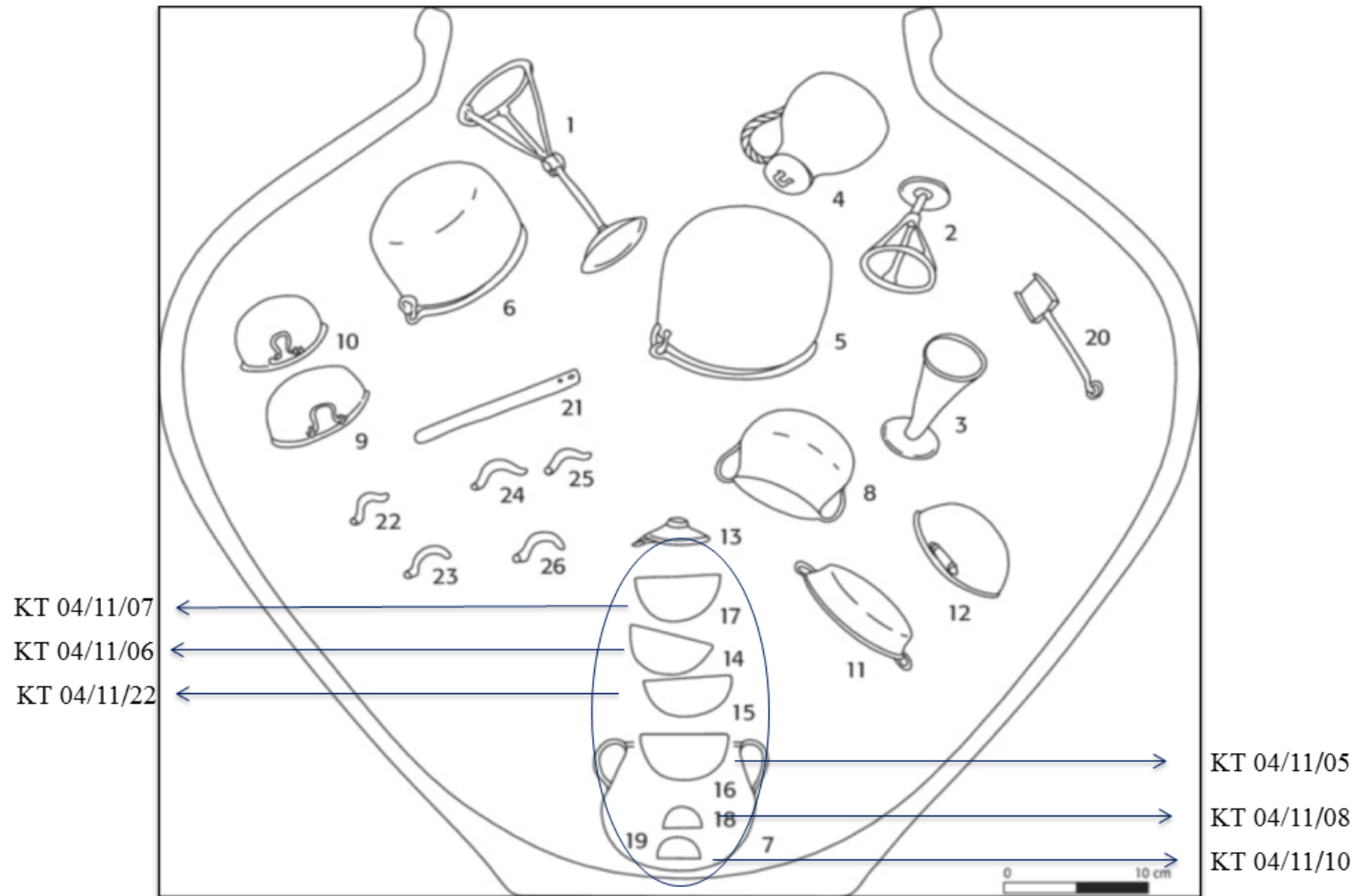


Figure 2: The hoard objects within the pithos on schematic drawing of the location (Bartelheim et al, 2008) and selected bowls with their excavation number.



Figure 3: The view of the hoard, after being taken out from the pithos (Bartelheim et al., 2008) and selected bowls with their excavation number.

However, all the copper alloy artifacts in ‘The Late Bronze Age Hoard of Kaleburnu/Galinoporni on Cyprus’ have been housed in unfavorable conditions throughout their above ground history. Hence, new corrosion formation and degradation are observed in ‘The Late Bronze Age Hoard of Kaleburnu/Galinoporni on Cyprus’.

2.3.1 2004 Kral Tepesi Bronzes’ Content

XRF is one of the most common procedures for determining that consist what kind of material the historical objects are of. XRF-applied samples were taken from inside the objects by drilling 1 mm and it was applied to 26 objects. Table 1 presents the experimental data on XRF.

Table 5: XRF results of bronzes (Bartelheim et al., 2011)

Object No.	Cu%	Fe%	Co%	Ni%	Pb%	Bi%	Ag%	Sn%	Sb%	As%
KT/04/11/01	92	0,03	0,07	<0,01	0,01	0,02	0,028	7,3	0,021	0,51
KT/04/11/02	94	0,18	0,05	<0,01	<0,01	<0,005	0,011	5,5	0,024	0,50
KT/04/11/03	94	0,17	0,05	0,02	<0,01	<0,005	0,006	5,5	0,029	0,44
KT/04/11/04	82	0,10	0,03	0,02	7,9	0,13	0,017	9,7	0,021	<0,01
KT/04/11/05	80	0,50	<0,01	0,04	0,02	<0,005	0,012	18,9	0,024	0,83
KT/04/11/06	76	0,37	0,04	0,04	0,04	<0,005	0,024	22,7	0,030	0,80
KT/04/11/07	88	0,18	0,01	0,04	0,01	<0,005	0,021	11,8	0,029	0,36
KT/04/11/08	80	0,74	<0,01	0,04	0,04	<0,005	0,002	17,8	0,228	1,22
KT/04/11/09	92	0,80	0,02	0,07	0,22	<0,005	0,020	7,3	0,018	0,35
KT/04/11/10	95	0,54	0,01	0,06	0,06	0,06	0,005	3,9	0,005	0,61
KT/04/11/11	83	0,26	<0,01	0,02	0,04	<0,005	0,015	15,9	0,005	0,27
KT/04/11/12	96	0,03	<0,01	0,09	0,06	0,05	0,009	3,8	0,031	0,44
KT/04/11/13	93	0,27	<0,01	0,09	0,01	0,04	0,020	6,4	0,036	0,43
KT/04/11/14	92	0,23	<0,01	0,09	0,07	0,02	0,016	7,0	0,040	0,29
KT/04/11/15	97	0,08	<0,01	0,06	0,04	0,03	0,009	2,9	0,009	0,31
KT/04/11/16	90	0,16	<0,01	0,07	<0,01	<0,005	0,015	9,4	0,022	0,29
KT/04/11/17	94	0,15	0,02	0,05	0,1	0,02	0,007	5,2	0,011	0,39
KT/04/11/18	92	0,08	<0,01	0,08	0,16	0,01	0,024	6,7	0,033	0,46
KT/04/11/19	91	0,14	0,01	0,06	0,25	<0,005	0,003	8,5	0,036	0,52
KT/04/11/20	91	0,04	0,03	0,07	0,07	<0,005	0,018	8,5	0,034	0,50
KT/04/11/21	90	0,02	0,11	<0,01	0,05	<0,005	0,029	9,4	0,028	0,50
KT/04/11/22	75	0,21	0,01	0,05	0,03	<0,005	0,006	23,5	0,020	0,71
KT/04/11/23	89	0,26	0,09	<0,01	<0,01	<0,005	0,008	10,3	0,054	0,50
KT/04/11/24	90	0,11	0,02	0,05	<0,01	0,02	0,012	9,2	0,032	0,10
KT/04/11/25	92	<0,05	0,04	<0,01	0,05	<0,005	0,014	7,1	0,029	0,40

2.3.2 Mineral Origin Analysis of 2004 Kral Tepesi Bronzes

The big part of 26 bronze pieces that found in 2004, were likely to be produced with copper obtained in Cyprus and the other ones were produced by means of using copper from exterior sources other than Cyprus (Kızılduman, 2017).

Samples from all 26 objects were analyzed in the Curt-Engelhorn-Zentrum-Archäometrie using X-Ray-Fluorescence (EDRFA) and Mass Spectrometry to determine trace elements and the signature of lead isotope.

Table 6 shows the result obtained from the analysis of lead-isotopes and trace element.

Table 6: Result of lead-isotopes and trace element (Bartelheim et al., 2011)

Object No.	Object	Isotope	Chemical
KT/04/11/01	Offering stand / incense burner with massive central stem and foot ring	Arabah	Arabah
KT/04/11/02	Offering stand / incense burner with massive central stem and foot ring	Cyprus	Arabah
KT/04/11/03	Offering stand / incense burner with tubular foot	Cyprus	Arabah
KT/04/11/04	Bag-shaped jug with lid and twisted handle	unknown	Arabah
KT/04/11/05	Hemispherical bowl	Cyprus	Cyprus
KT/04/11/06	Hemispherical bowl	Cyprus	Cyprus
KT/04/11/07	Hemispherical bowl	Cyprus	Cyprus
KT/04/11/08	Hemispherical bowl	Cyprus	Cyprus
KT/04/11/09	Bowl with wish-bone shaped handle	Cyprus	Cyprus
KT/04/11/10	Hemispherical bowl	Cyprus	Cyprus
KT/04/11/11	Saw blade with two rivet holes	Cyprus	Cyprus
KT/04/11/12	Deep two-handled pot with hemispherical bottom	Arabah	Cyprus
KT/04/11/13	Shovel with writing or mark	Cyprus	Cyprus
KT/04/11/14	Two-handled bi-conical pot with hemispherical bottom	Arabah	Cyprus
KT/04/11/15	Deep cauldron with undecorated handle bases	Cyprus	Cyprus
KT/04/11/16	Shallow cauldron with decorated handle bases	Cyprus	Cyprus
KT/04/11/17	Sickle with bent handle end	Arabah	Arabah
KT/04/11/18	Sickle with obtuse angle between handle and blade	Unkonown	Arabah
KT/04/11/19	Sickle with bent handle end	Arabah	Arabah
KT/04/11/20	Sickle with bent handle end	Arabah	Arabah
KT/04/11/21	Sickle with obtuse angle between handle and blade	Arabah	Arabah
KT/04/11/22	Hemispherical bowl	Cyprus	Cyprus
KT/04/11/23	Large deep bowl with rounded swinging handle	unknown	Arabah
KT/04/11/24	Large deep bowl with omega-shaped swinging handle	Cyprus	Arabah
KT/04/11/25	Two-handled basin	Arabah	Arabah
KT/04/11/26	Handled large deep bowl	Cyprus	Arabah

2.4 Corrosion and Patina in Copper Alloys

Corrosion is a destructive reaction in which a metal enters chemically or electrochemically with its circumference (Revie, 2008).

The products in consequence of these deterioration duration are alike in composition to the minerals present in nature (Faltermeier, 1995). Thermodynamically, as Gibbs free energy exchange (ΔG), negative reactions occur spontaneously and this tendency increases as the negative valence increases (Revie, 2008). Nantokite formation reaction, a mineral and corrosion, product is given below reaction 1 (Frost, 2003).



In line with the reactions and explanations mentioned above, corrosion can also be referred as the change reaction of metals in order to return to their more stable mineral form (Rodgers, 2004). Corrosion layers can protect metal objects by coating them or they can be destructive. (Watkinson, 2010).

The term patina is used to describe corrosion products created by copper and alloys (Chase, 1991). Today, patina is a term that commonly used to refer to green corrosion products that occur over time in copper and copper alloys such as bronze when exposed to open atmosphere or burial conditions (Weil, 2007).

Noble patina is tin-enriched surface corrosion with high protective properties that protect the original surface on ancient bronze (Gettens, 1970) and they may also include corrosive context such as carbonate, chloride, sulphate (Robbiola and Portier, 2006).

Robbiola and Portier classified the patinas as type 1 and type 2. Type 1 patinas are noble patinas and type 2 patinas have destroyed or blasted bronzes' original surface. Type 2 patinas are thicker and more complex than type 1. (Robbiola and Portier, 2006).

2.4.1 Corrosion Types³

2.4.1.1 Chemical Corrosion

Chemical corrosion occurs only by transferring electrical charge between atoms (Scott, 2002). In chemical (or dry) corrosion, the metal and corrosive agent react directly and can occur at high temperatures (Quaranta, 2009).

Due to the fact that the environment is not conductive, the presence of corrosion products is limited to the surface of the metal. (Cramer and Covino, 1992)

2.4.1.2 Electrochemical Corrosion

The descension of historical and archaeological bronze artifacts is mostly due to electrochemical corrosion (Payer, 1992). Electrochemical corrosion process occurs in anode and cathode zones (Scott, 2002). In order for this process to happen, an ionic bond is required between the anode and the cathode, and this ionic bond is often provided by water (Quaranta, 2009).

The reaction in which the electrons are released (for example, when it forms metal ions) is called oxidation (anodic process). Every anodic process is followed by a

³ Microorganisms do not produce certain corrosion types; In general, they are able to produce H_2S and H_2SO_4 that pose a danger to the coroner layer in order to create sulfide films that affect copper alloys (Little and Lee, 2007; (Cramer and Covino, 1992).)However, rather than direct interaction with metal, they provide interaction between ions used in the corrosion process. (European Federation of Corrosion, 1992).For this reason, microbiological corrosion is not examined in a title and is mentioned in the type of corrosion and patinas they affect.

cathodic process (reduction) in which the released electrons are consumed (Novák, 2007).

In addition, microorganisms can also have an effect on corrosion mechanisms and electrochemical corrosion processes with products produced by their metabolism (Little and Lee, 2007; Cramer and Covino, 1992).

2.4.2 Patina Types

Corrosion products are formed on metal artifacts as a result of deterioration caused by the construction technique, atmospheric or burial factors that it is exposed to (Scott, 2002). Depending on all these factors, corrosion products vary. For instance, sulphides dominate under anaerobic conditions, while carbonates often form in well-ventilated soils. (Schweizer, 1994).

Copper oxides, carbonates and chlorides are the most common compounds found on the surface of archaeological copper and copper alloy artifacts. Some corrosion products of copper and copper alloys are given in Table 7.

Table 7: Corrosion products of copper and copper alloys (Dana, 1951 ; Faltermeier, 1995 ; Scott ,2002 ; Ullman et al.,1985)

Mineral name	Formula	Chemical name	Clour	Cyrstal Structure
Oxides				
Cuprite	Cu_2O	Copper-I-oxide, Cuprous oxide	Red	Cubic
Tenorite	CuO	Copper-II-oxide, Cupric oxide	Black	Monoclinic
Cassiterite	SnO_2	Tin-IV-oxide, Stannic oxide	White	Tetragonal
Chlorides				
Nantokite	$CuCl$	Copper-I-chloride, Cuprous chloride	White or Grey	Isomeric
Paratacamite	$CuCl_2 \cdot 3Cu(OH)_2$	Basic copper chloride	Green	Hexagonal
Atacamite	$Cu_2(OH)_3Cl$	Basic cupric chloride	Dark green	Orthorhombic
Carbonates				
Malachite	$Cu_2(OH)_2CO_3$	Copper-II-hydroxycarbonate	Green	Monoclinic
Azurite	$Cu_3(OH)_2(CO_3)_2$	Copper-II-hydroxycarbonate	Blue	Monoclinic
Sulphates				
Brochantite	$Cu_4(SO_4)(OH)_6$	Basic copper sulphate	Green	Monoclinic
Antlerite	$Cu_3(SO_4)(OH)_4$	Hydroxyl copper sulphate	Green	Orthorhombic
Sulphides				
Covellite	CuS	Copper-II-sulphide	Indigo blue	Hexagonal
Chalcocite	Cu_2S	Copper-I-sulphide	Blackish grey	Monoclinic
Phosphates				
Libethenite	$Cu_2(PO_4)(OH)$	Basic copper phosphate	Dark green	Ortohorhombic
Sampleite	$Cu_3(PO_4)_2$	Copper-II-phosphate, Cupric phosphate	Light blue	Monoclinic
Hydroxides				
Spertiniite	$Cu(OH)_2$	Copper-II-hydroxide, Cupric hydroxide	Blue-Green	Ortohorhombic
Nitrates				
Gerhardtite	$Cu_2(NO_3)(OH)_3$	Basic copper nitrate	Light Green	Orthorhombic

2.4.2.1 Oxides

Cuprite is water-soluble (Scott, 1997), a cubic shaped and crystal formed corrosion product which occurs on the surface of copper alloys (Scott, 2002). Cuprite can easily occur in the burial environment that includes oxygen and moisture or atmospheric conditions, while it can be converted into different minerals due to sulphate (SO_4^{-2}), carbonate (CO_3^{-2}) and chlorine (Cl^{-1}) and other causes in the environment (Scott, 1997). The oxidation reaction rate is controlled by diffusion of copper from the cuprite layer (MacLeod, 1981). Although the initial corrosion is rapid, it forms a stable film layer on the underlying metal that isolates from the outside environment in a way that last corrosion rate extremely slow (MacLeod, 1981). The layer it creates during this development process helps to protect the copper alloy object (Chase, 1994).

Since chloride ions affects speed of many of the electrode processes in the presence of these ions, formation of cuprite may not occur (MacLeod, 1981). Nantokite react slowly with water to produce cuprite over time. (Cronyn, 2003). Nantokite may form cuprite by reacting (reaction 2) in the presence of water only without oxygen (Özen, 1999).



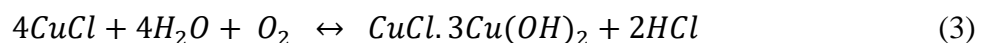
Tenorite is a water-soluble corrosion product such as cuprite (Scott, 1997). Although it is a rare patina compared to cuprite, the presence of tenoritis in the patina composition of archaeological artifacts may indicate that the artifact was exposed to heat in or before the burial environment (Scott, 1997).

Cassiterite forms a corrosion layer on the surface of bronze artifacts known as water patina, which provides a bright surface formation. (Schwizer, 94). In bronze artifacts that tin is high in alloy, tin, which is weaker than copper, acts as a protective task due to its impermeable structure, which is oxidized and called water patina, the mineral cassiterite (Scott, 2002).

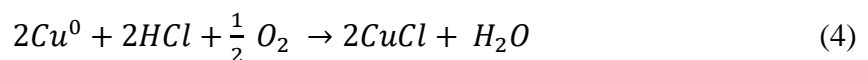
2.4.2.2 Chlorides

Nantokite is a corrosion product with a waxy appearance (Scott, 2002). To create this corrosion product, ionized copper in the anode reacts (reaction 1) with free chloride ions in the environment (Özen,1999). Under the influence of ionic diffusion and electrical migration, chloride ions can penetrate the cuprite layer and react with the underlying metal to form a copper chloride layer (MacLeod, 1981). Nantokite which can remain passive until it reacts with moisture (Rotaru et al., 2010) is the main cause of the active corrosion layer 'Bronze Disease' which is extremely harmful in the presence of humidity and oxygen (Di Carlo et al., 2017; Organ, 1963).

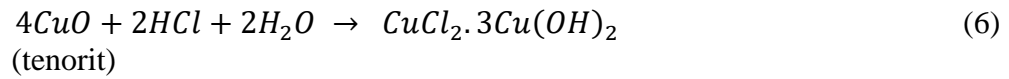
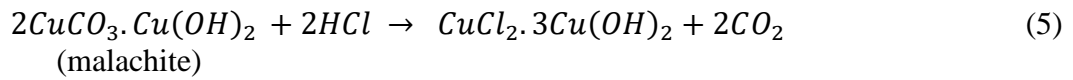
The nantokite formed in the presence of free chlorine ions reacts (reaction 2) in a humid and aerobic environment and converts into paratacamite (Croyn, 2003).



Hydrochloric acid released with paratamite reacts (reaction 4) rapidly with metal in the aerobic environment creating nantokite and water, which leads to the continuity of reaction 3 (Özen, 1999).



Hydrochloric acid (reaction 3), which is released by paratacamite formed by reacting with nantokite, water and oxygen, can also react (reaction 5-6) with +2 valence copper corrosion products to form paracatamite (Care, 1999)



When the nantokite, located deep within the corrosion layers, forms paratacamite, the corrosion layers (Figure 4) deteriorate physically as they are separated by pressure from the growing crystal stack (Cronyn, 2003).

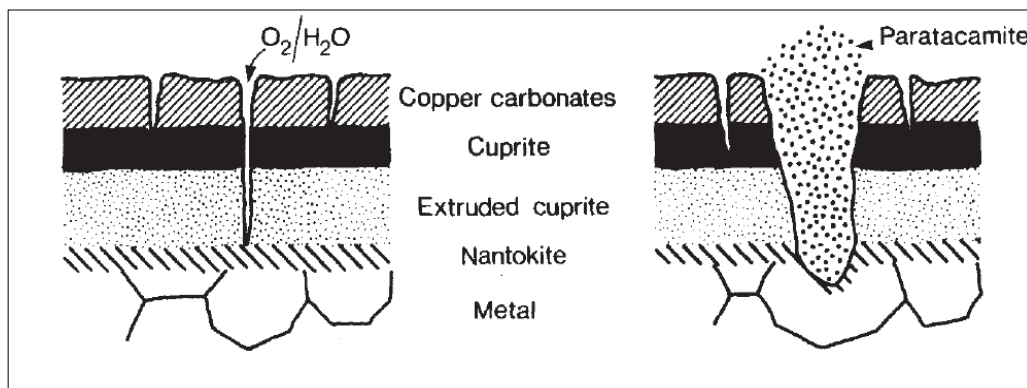


Figure 4: Copper alloy deterioration due to 'bronze disease'

This type of corrosion is called cancer 'bronze disease' because once corrosion reactions begin; unless the conditions causing the deterioration change and no precautions are taken, the deterioration continues until the metal and stable corrosion products are exhausted as a result of consecutive reactions (Özen, 1999).

Atakamit and Paratakamit are different isomers with crystal structures with the same molecular form (Scott, 2002). Nantokite, which is exposed to less than 50% relative humidity, can be transformed into atacamite (Faltermeier, 1995) and the natural formation process of atacamite is quite slow (Feitknecht and Maget, 1949).

2.4.2.3 Carbonates

Malachite is a corrosion product that usually occurs in burial environments and is found in small amounts in copper alloys exposed to atmospheric conditions (Scott, 2000). Two basic copper carbonate malachite and azurite are stable corrosion products in well-ventilated soils as tenorite (Quaranta, 2009). Malachite, which is difficult to perform in a laboratory environment, is an indicator of the authenticity of the artifact because the transition from cuprite to malachite is a natural formation (Scott, 2002).

Azurite is a less common and less stable corrosion product than malachite (Scott, 2002). In the presence of moisture and in cases where carbon dioxide is not present in the environment, azurite can be transformed into malachite (Ghoniem, 2011) which can be accelerated by increasing temperature in the alkaline environment (Scott, 2002).

2.4.2.4 Sulphates

Copper sulfates are usually found in atmospheric artifacts and are rarely seen as patinas on archaeological bronze artifacts (Krapchev, 1976). The presence of brochantite on bronzes is seen on artifacts exposed to high open air with high sulfur dioxide content, but may occur rarely under subterranean conditions (Muros and Scott, 2018 ; Tylecote, 1979) Although it is the most stable corrosion product among copper sulfates in the atmospheric environment (Eggert et al., 2004), this corrosion product can also occur through sulfate reducing bacteria in burial conditions without being exposed to atmospheric environment. (Muros and Scott, 2018). Bronchantite a corrosion product can continue to exist stably in the range of 3.5 to 6.5 pH (Greadel, 1987).

2.4.2.5 Sulphides

Sulphides can develop in low oxygenated water environments or as a product of corrosion caused by museum pollutants (Scott, 2002). Daubree (1875), who described covellite and chalcocite, one of the major sulphide minerals in some Roman coins in 1875, considered sulfate-reducing bacteria as the causes of these corrosion products.

2.4.2.6 Phosphates

Copper phosphate reveals corrosion products as a result of the combination of copper alloy objects in burial conditions with phosphorus sources such as bone (Scott, 2002). The most common copper phosphate seen as a corrosion product is Libethenite (Scott, 2002).

Sodium, calcium and chlorine are required for the formation of sampleite, another phosphate corrosion product. (Scott and Maish, 2010). Sampleite can develop on copper alloys, usually in arid areas, under conditions where groundwater has high soluble salt (Scott, 2002).

2.4.2.7 Hydroxides

Spertiniite as copper hydroxide corrosion product, which is rarely seen in the stable phase and is a transition product during the corrosion process, can collapse into atacamite when it dries (Scott, 2002).

2.4.2.8 Nitrates

The most commonly known copper nitrate is gerhardtite and are very rare as both mineral and corrosion products, due to the water solubility of nitrate salts (Scott, 2002).

2.4.3 Causes of Copper Alloy Corrosion

Various parameters such as geographical location, climate, land use, chemical and physical properties of soil have a significant impact on the deterioration of archaeological artifacts and corrosion rate (Mattson et al., 1996). The composition and microstructure of bronze also play an influential role in patina (Piccardo et al., 2007).

2.4.3.1 Structural Impact

Copper alloys carry a greater risk of corrosion than pure copper (Rodgers, 2004). During productions in archaeological period workshops, element ratios of copper alloys determine whether corrosion products in the corrosion process are passive or unstable depending on ionic and electron transfer mechanisms (Watkinson, 2010). Since it is physically impossible to mix molten metals completely, areas with higher corrosion potential can occur on the surface of the work (Rodgers, 2004).

2.4.3.2 Atmosphere

The atmosphere is an abrasive environment that influences all kinds of products including objects of cultural heritage. (Moncmanová, 2007). The acids formed by the harmful gases in the atmosphere together with rain and moisture react with copper alloys and provide corrosion formation (Marabelli, 1994). Acid rains caused by sulfur dioxide (SO_2^{-2}) and nitrogen dioxide (NO_2^{-}) gases in the atmosphere accelerate reactions that cause corrosion, and with smoke and dust like contaminants, the damaging effect of acid rains on copper alloys increases more (Tansuğ, 2016). Water is found in the atmosphere as a vapor scattered in the air instead of the liquid, unlike the burial environment, and as the temperature increases, the atmosphere can hold more water vapor.

2.4.3.3 Oxygen

Oxygen is an oxidizing agent and because of that takes place in many reactions. (Cronyn, 2003). Oxidation of a material causes chemical changes in the composition of the material, especially on the surface of the material (Moncmanová, 2007). It is the existence or absence of oxygen, which has the basic control of organism activity and is therefore a key role in the deterioration of materials (Cronyn, 2003).

2.4.3.4 Water

Since water can determine the rate of oxygen transport (ventilation-aeration) in the soil, it affects the nature of the corrosion process and plays an important role (Quaranta, 2009). Water penetrating a material can freeze, apply strong pressure to the structure of the material and cause the most damage as it can effectively destroy the surface material with repeated freezing cycles under freezing conditions (Moncmanová, 2007). Furthermore, water is an important component for other electrochemical reactions involving electron movement where it directly affects rate of reaction due to letting chemicals to form ion solutions and allowing electron conduction. (Cronyn,2003). The voltage range in which water is thermodynamically stable depends on the acidity of the solution, i.e. the concentration of hydrogen and hydroxyl ions (Tylecote, 1979).

2.4.3.5 Humidity

The patinas on the archaeological artifacts extracted from the soil are mostly stable and usually corrosion in remain metals is formed by a relative humidity of over 80% (Cronyn, 2003). Humidity and temperature affect the chemical, biological and mechanical processes of decay and in most materials, the increase in relative humidity prepares the appropriate conditions for biodeterioration (Moncmanová, 2007).

There are different opinions related to the effect of moisture in Bronze disease. As low humidity prevents the movement of ionic species, MacLeod (1981) said that relative humidity above 35% can cause bronze disease to be active and accelerate quickly. Cronyn (2003) stated that this can be achieved with a dependency humidity above 40%.

2.4.3.6 Temperature

Day and night temperatures in the atmosphere are constantly changing and therefore there is no stable environment (Tansuđ, 2016). Temperature affects the deterioration processes of a material fractionally and in various ways (Moncmanová, 2007). Although recurrent freeze/thaw conditions cause damage, it increases the rate of chemical reactions and biological growth (Cronyn, 2003).

Soil resistance is inversely proportional to temperature, but the increase in temperature also reduces the solubility of oxygen and rate of cathode reaction (Escalante, 1989). In the soil, deep, well below the air temperature and in a cool environment, the removal of artefacts into a warmer environment brings problems related to temperature (Cronyn, 2003).

2.4.3.7 Microbiological Organisms

Microorganisms that occur naturally in the soil can form biofilm by colonizing the metal surface (McNeil and Little 1999). Under anaerobic conditions, sulphate reductive bacteria play an effective role in corrosion (Quaranta, 2009). There may be a direct correlation between sulfur-rich deposits and bacteria, but these pulses can also be found in copper sulphide deposits on copper alloy under subsoil conditions (Little and Lee, 2007)

2.4.3.8 Ph

Since stable corrosion products have protective properties below a certain pH level, the pH of the soil greatly affects the corrosion process (Memet, 2007). Although low pH values in soil cause thermodynamic instability of external corrosion layers (Reale et al., 2012), corrosion status of metal artifacts according to soil pH is given in Table 8 (Heritage, 2008).

Table 8: Conditions of metal artifacts according to different pH of soil

Burial environment	Materials that could survive
pH below 5.5, oxic	Metalwork is too worn
pH 5.5-7.0, oxic	Metal work well protected
pH above 7.0, oxic	Metalwork is well-preserved
acid to basic, anoxic	Metal work can be well protected, sometimes with metallic surfaces

2.4.3.9 Soil

Soil composition is a form of many factors such as clay content, organic substances, bacteriological activity, soluble salts and water contained within it which leads to different soil types (Schweizer,1994). Therefore, soil is a natural corrosion environment for archaeological bronzes. (Stambolov, 1985). Although the contents of the soils used for agricultural purposes change, the soil compressed by heavy vehicles reduces ventilation. (Mattson et al., 1996). In soils with low oxygen content, sulphate-reducing bacteria can turn sulfate into hazardous hydrogen sulphide. (Memet, 2007). Low pH values in soil cause thermodynamic instability of the outer

corrosion layers (Reale et al., 2012). Since some soil species can buffer rainwater well, soil pH may not be affected by rainfall and may prevent the filtering of soluble salts. (Escalante, 1989)

Chapter 3

EXPERIMENTAL

3.1 Materials

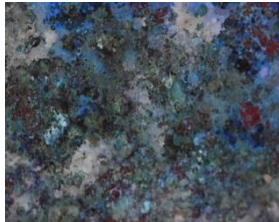














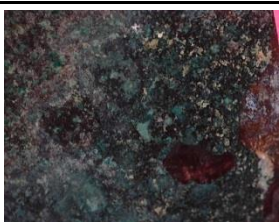
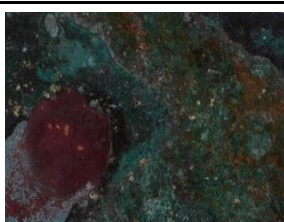

The reason for choosing the studied 6 bronze bowls was to investigate the same artifacts in the Hoard. Those 6 bronze bowls are also manufactured by copper mines that have a Cypriot origin and contain a wide range of tin additive. Moreover, 4 of the 5 high-tin bronzes that were found in the hoard occurred in the bronzes (Table 5-6). 3 samples were analyzed from each of the chosen 6 bowls and the samples were taken from 2 cm^2 regions because it was predicted that the bowl would show different corrosions within itself.

18 samples were investigated for infrared spectroscopy and 15 samples were investigated for cyclic voltammetry⁴ measurements. In addition, pure *CuO*, *CuSO₄*, *CuCl* and *CuCl₂* were investigated with cyclic voltammetry to compare with 15 samples of selected bowls results.

The microscopic images of the 18 samples are provided in Table 8. 3 samples of every each bowls' location and microscopic images are also given in Figure 5-11.

⁴ The inside of 3 bowls (KT/04/11/05, KT/04/11/06, KT/04/11/07) had passive protective patina (type 1 patinas). According to the ethical rules of cultural heritage, since the patinas are directly covering the original surfaces, the amounts of the samples obtained without harming the bowls were only enough for FT-IR measurements.

Table 9: Microscopic images of samples

Sample No.	A	B	C
KT 04/11/05			
KT 04/11/06			
KT 04/11/07			
KT 04/11/08			
KT 04/11/10			
KT 04/11/22			

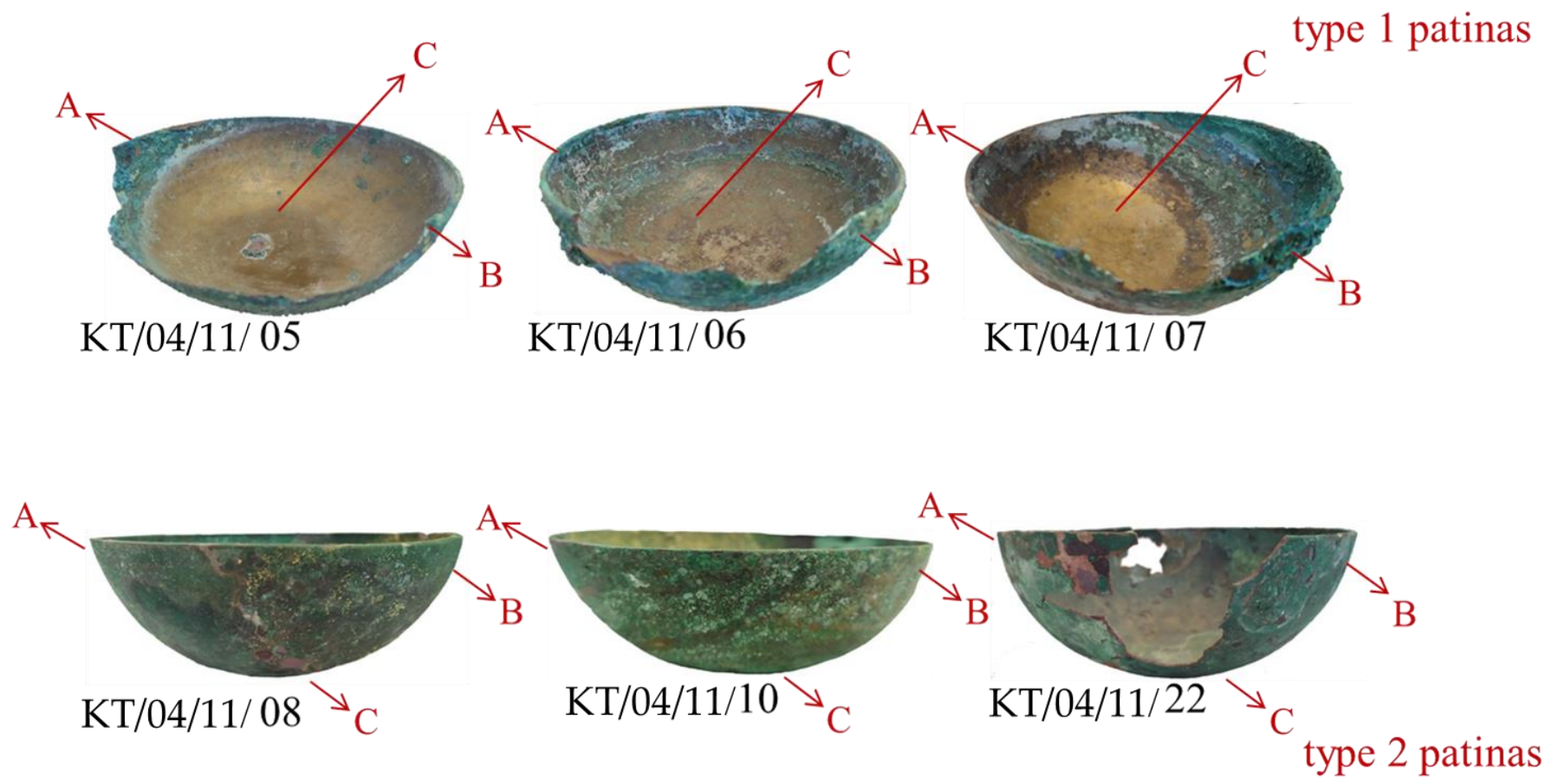


Figure 5: 3 samples of every each bowls' location

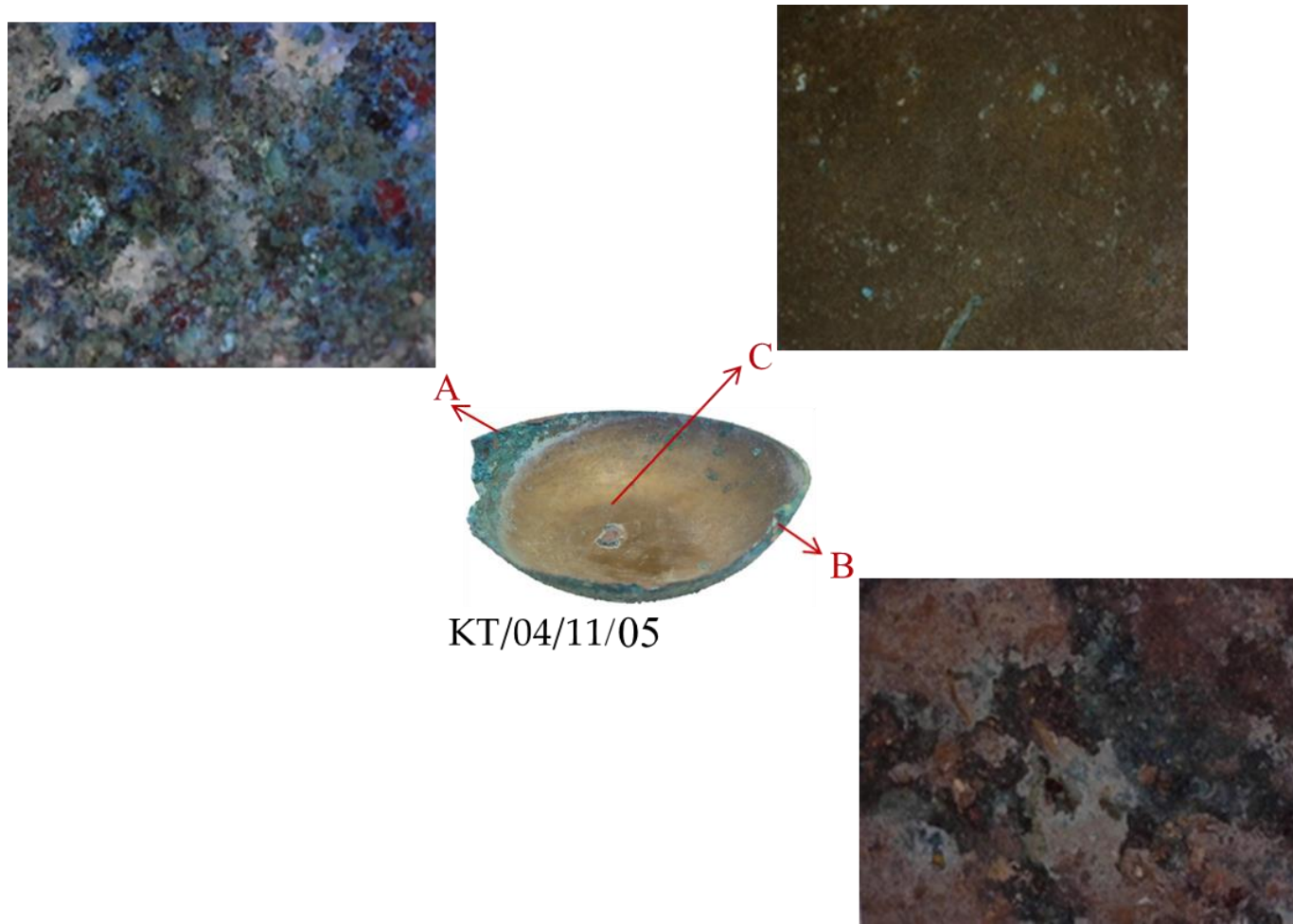


Figure 6: 3 samples of KT/04/11/05's locations and their microscopic images

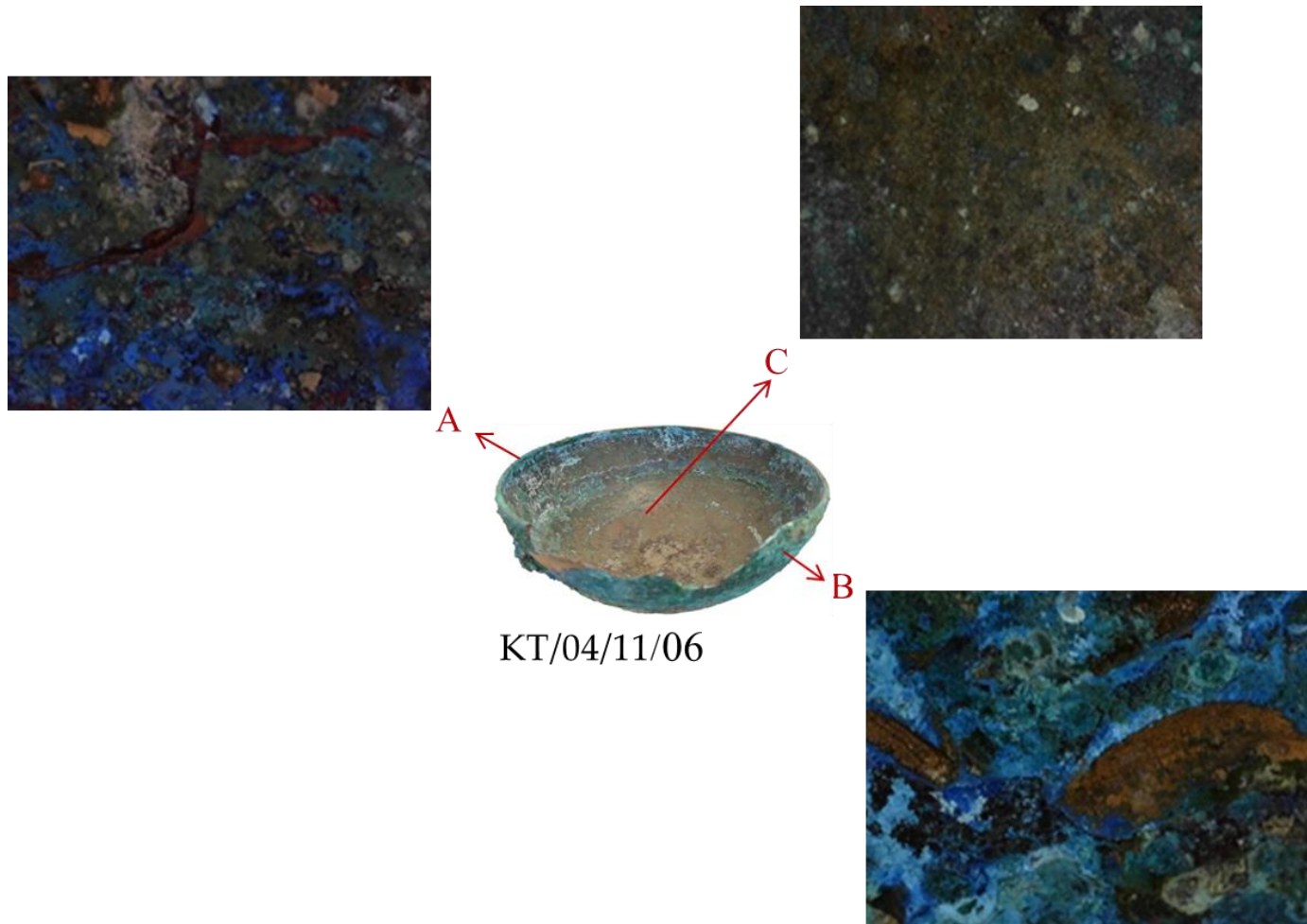


Figure 7: 3 samples of KT/04/11/06's locations and their microscopic images

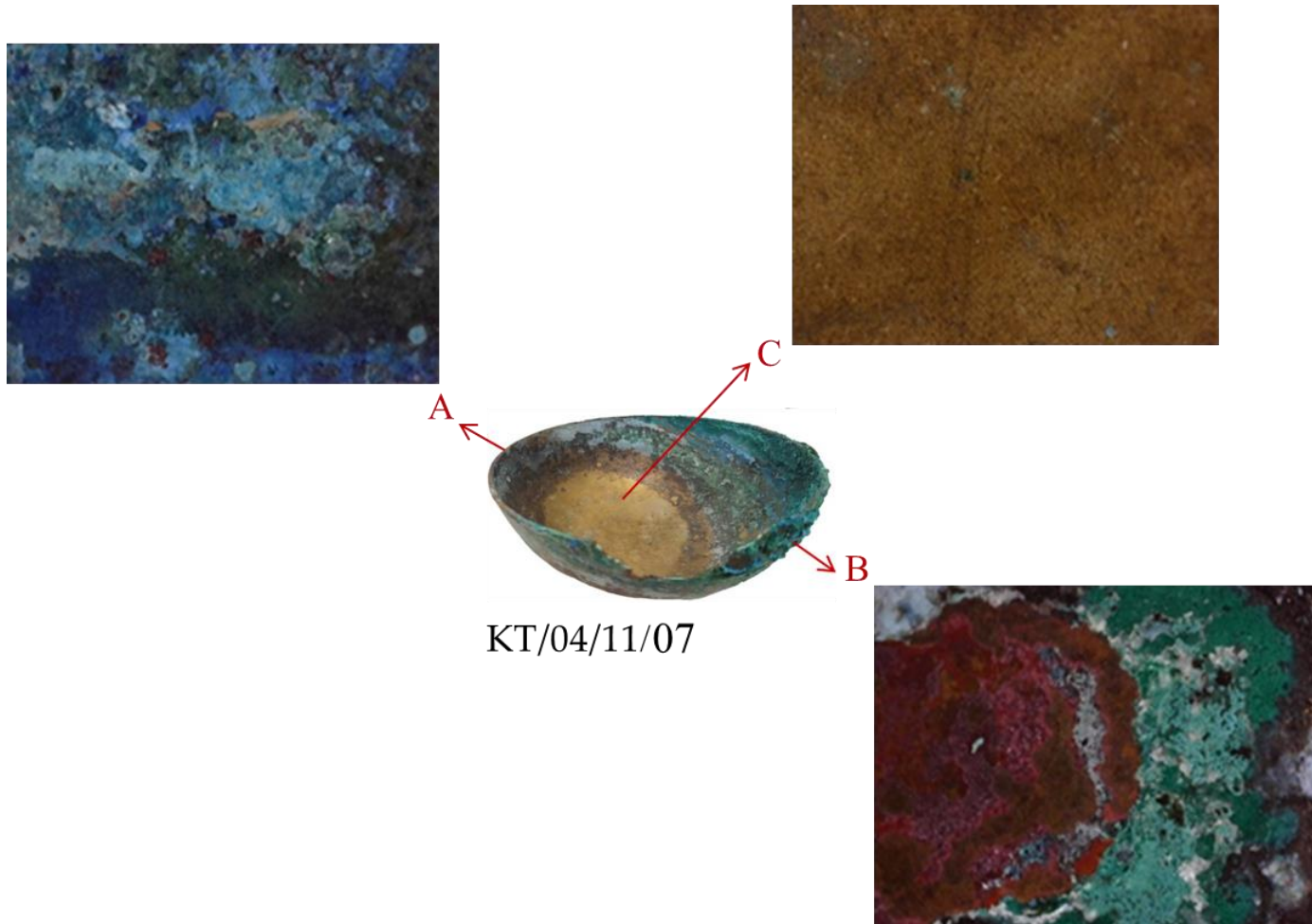


Figure 8: 3 samples of KT/04/11/07's locations and their microscopic images

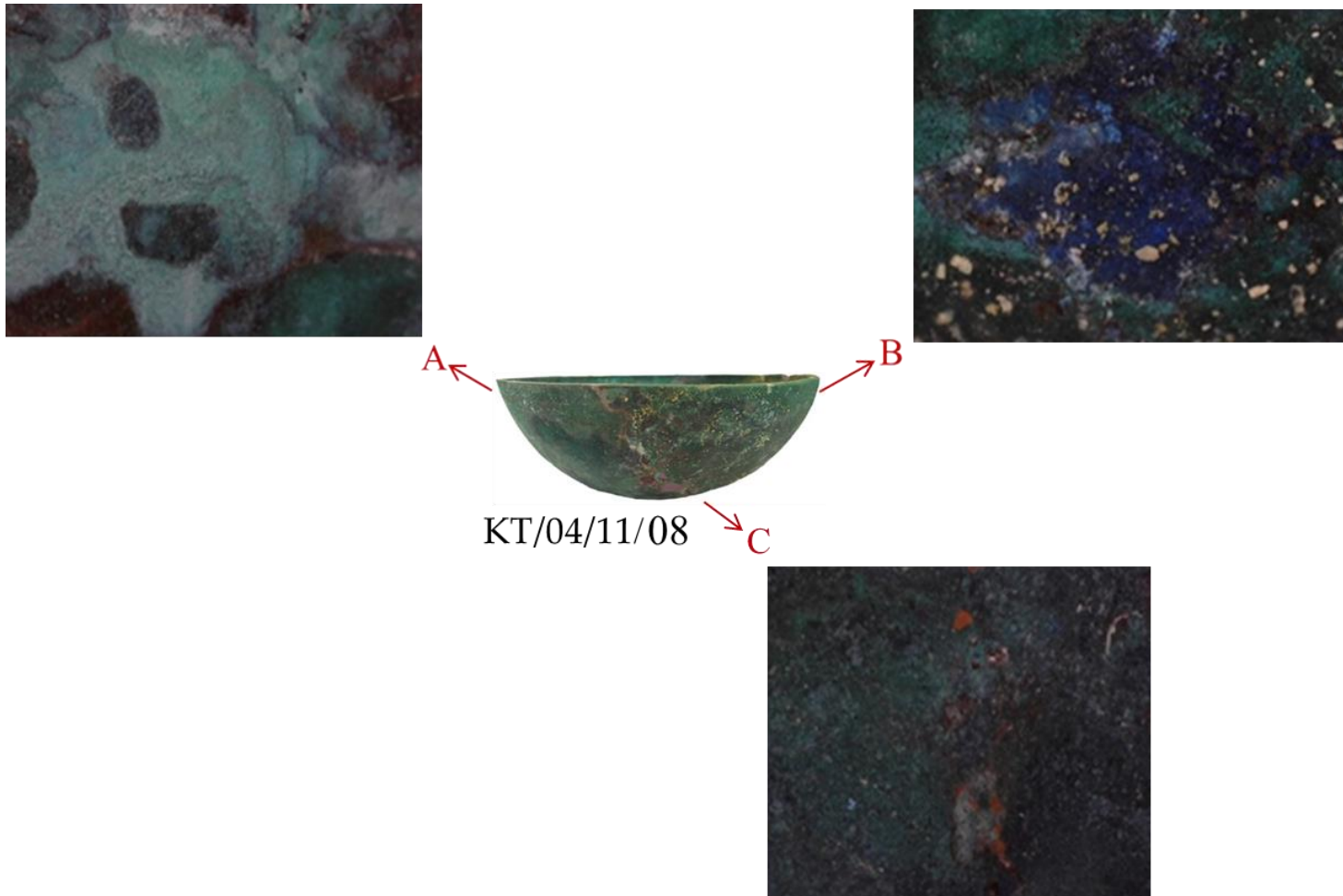


Figure 9: 3 samples of KT/04/11/08's locations and their microscopic images

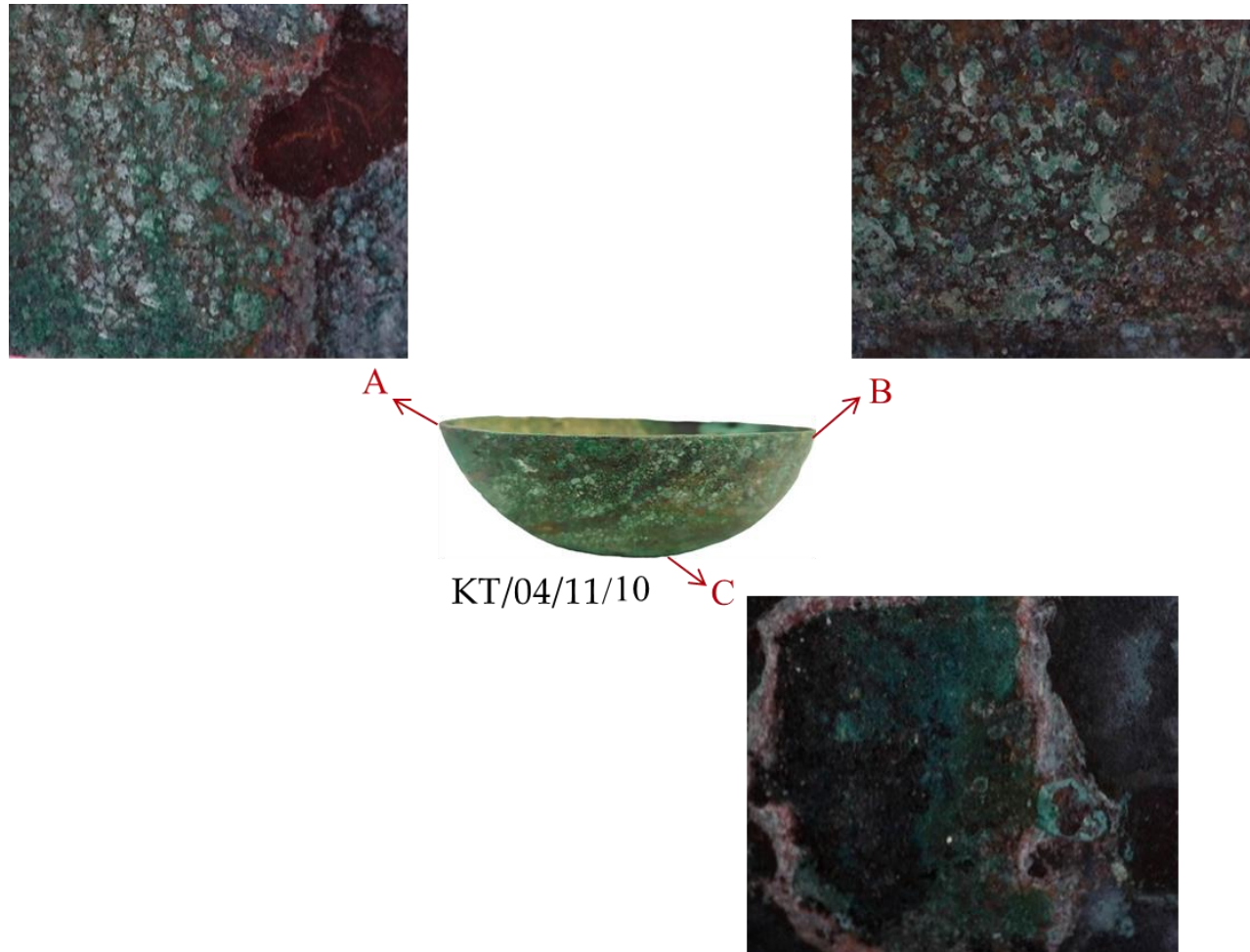


Figure 10: 3 samples of KT/04/11/10's locations and their microscopic images

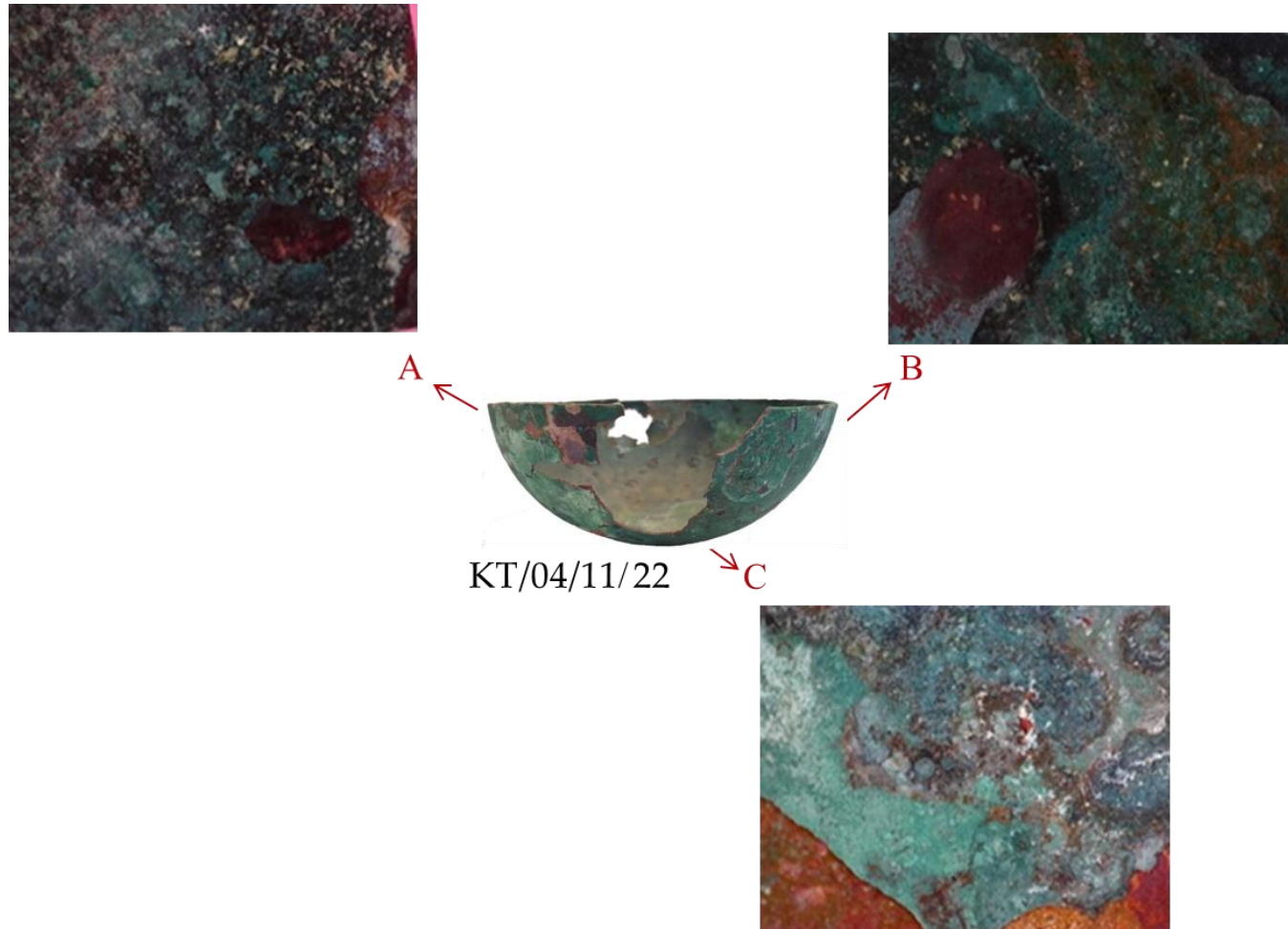


Figure 11: 3 samples of KT/04/11/22's locations and their microscopic images

3.2 Instruments

Mattson (USA) satellite was used to record the Infrared Spectra of the samples.

REFERENCE 600 computer controlled Potentiostat/Galvanostat/ZRA was utilized to analyzed the electrochemical properties.

3.3 Methods

3 samples were analyzed from each of the chosen 6 bowls and the samples were taken from 2 cm² regions because it was predicted that the bowl would show different corrosions within itself. 18 samples were investigated for infrared spectroscopy and 15 samples were investigated for cyclic voltammetry measurements. Fourier transform infrared spectra (FTIR) were obtained in KBr pellets with high resolution using a JASCO FT/IR–6200 spectrometer. REFERENCE 600 computer controlled Potentiostat/Galvanostat/ZRA was utilized to analyzed the electrochemical properties. FT-IR spectrometer analysis were performed by preparing KBr pellets mixed with minimum amount of the samples.

Solid state cyclic voltammetry were done under argon via immobilized microparticles voltammetry technique. The reference electrode was Ag/AgCl and the counter electrode was platinum wire. Approximately 10 µg of sample was powdered in a mortar and spread on a fine paper sheet. Then, the particles were attached to the surface of the carbon paste electrode by gently rubbing the layer. Carbon paste was prepared from graphite powder and paraffin oil (0.025 mg graphite in 10 microliter paraffin oil). The electrode was polished carefully with 0.05 µm alumina slurry to a mirror finish prior to use. The supporting electrolyte, 0.1 M HCl (aq) was degassed with Argon gas for 5 minutes prior to the measurements. All measurements were

carried out at room temperature. Experiments of cyclic voltammetry were used with a potential scan rate of 100 mVs^{-1} and between the region from -1.2V to $+1.2\text{V}$ for the samples.

A new sample of the material attached to the surface on the carbon paste electrode was used in each measurements. Two voltammetric cycles were performed for each sample.

Chapter 4

DATA

4.1 FT-IR

The results of the infrared spectrum measurements of the bronze bowls' samples are given below.

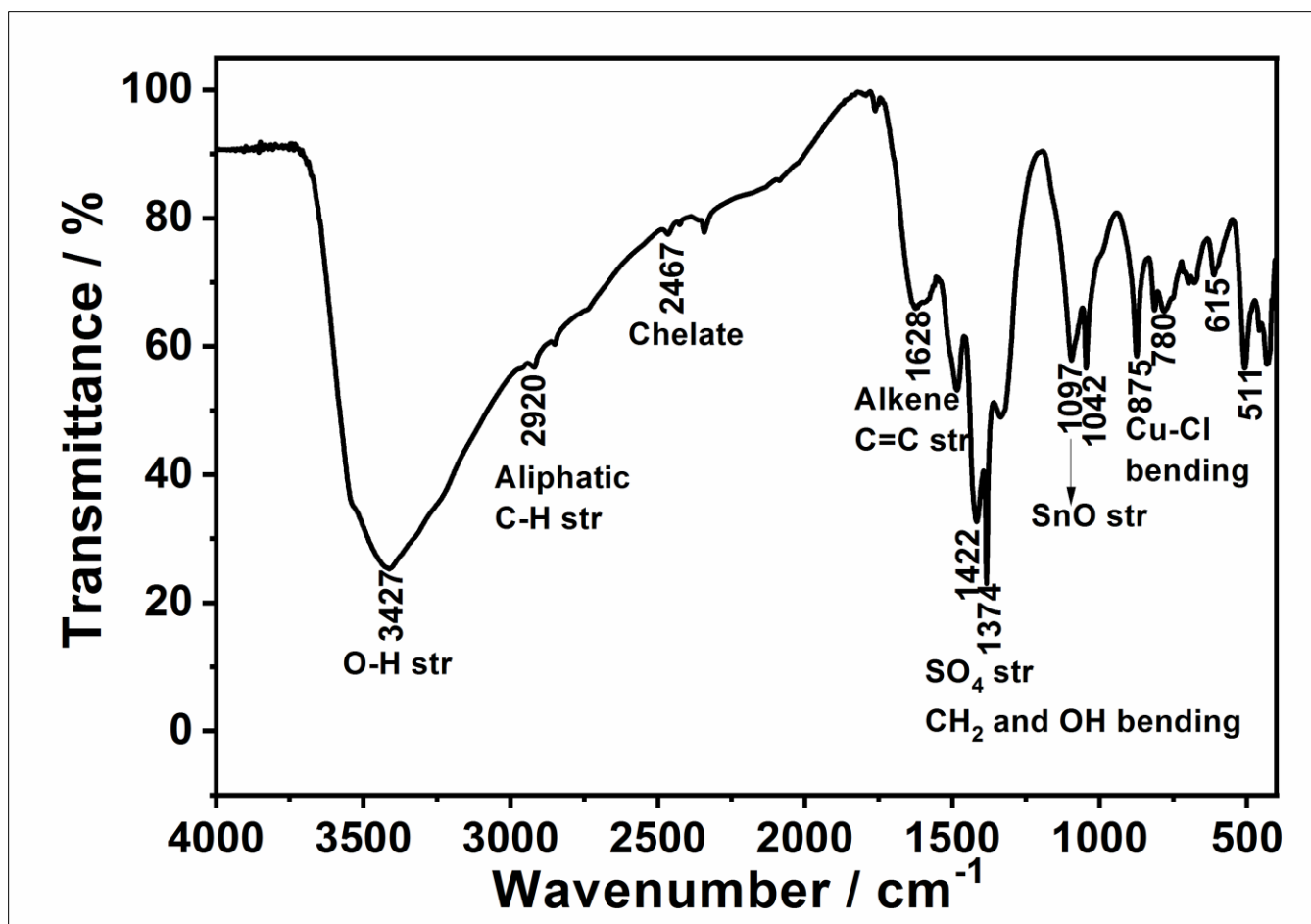


Figure 12: Infrared Spectrum of KT/04/11/05 A

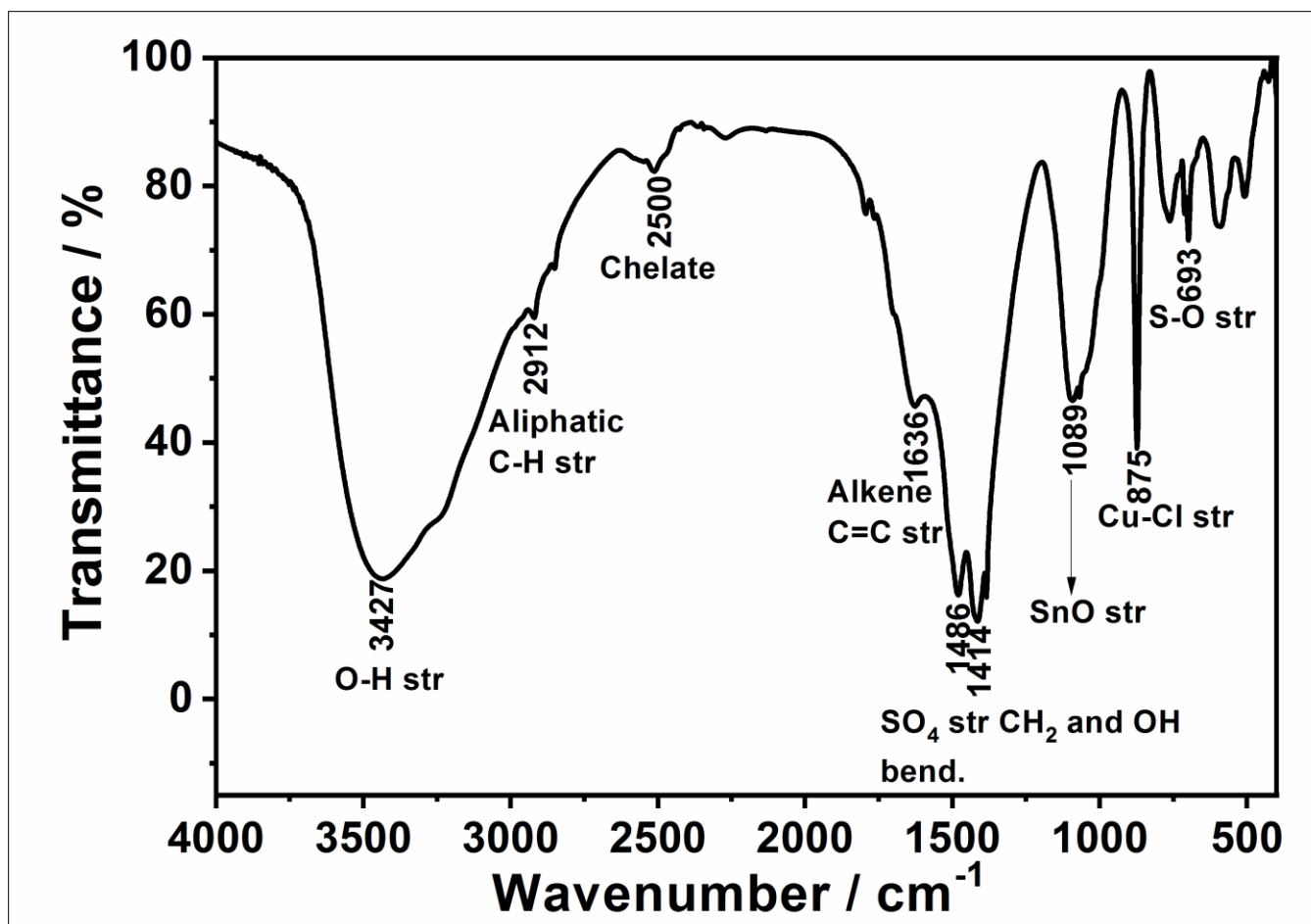


Figure 13: Infrared Spectrum of KT/04/11/05 B

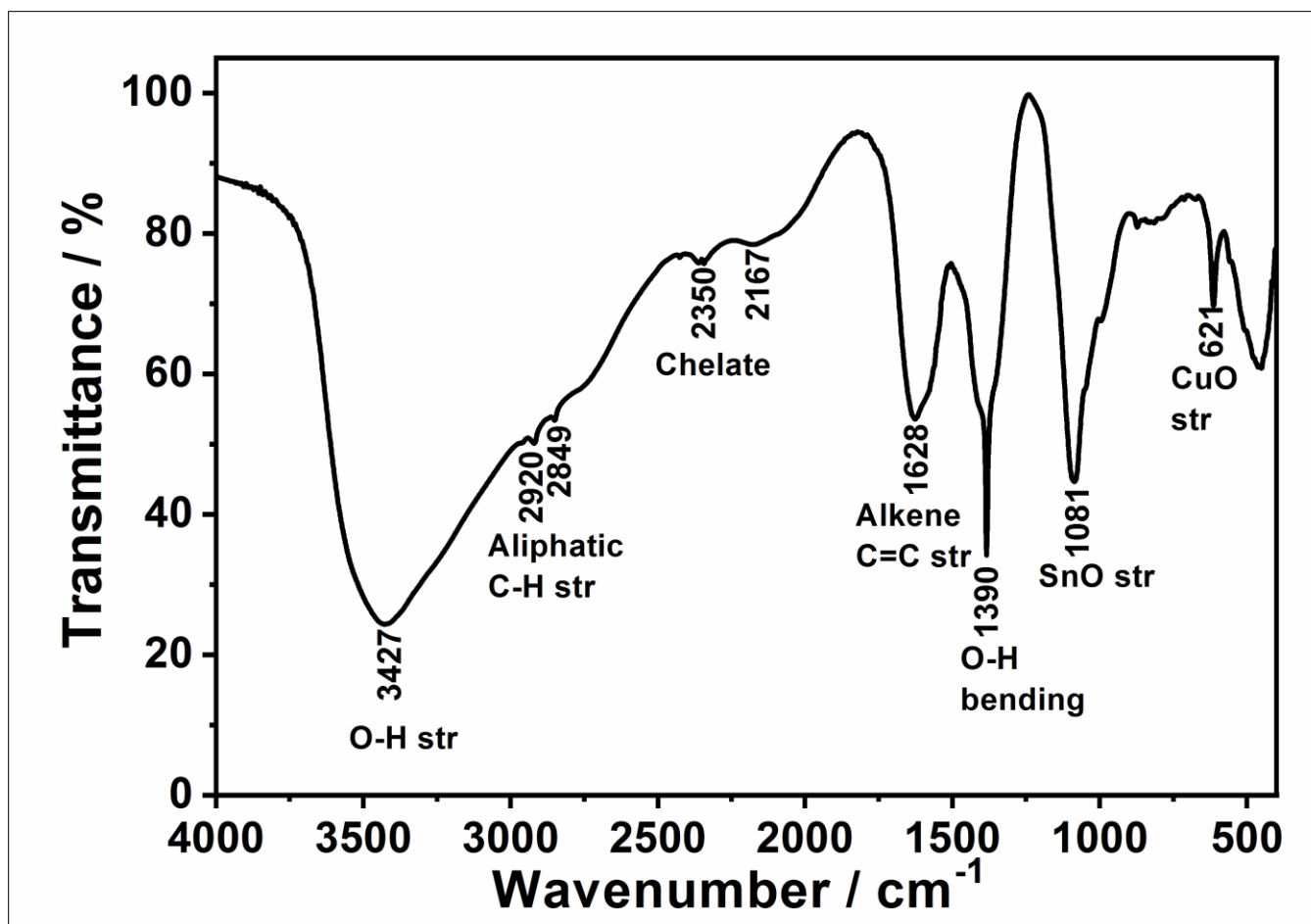


Figure 14: Infrared Spectrum of KT/04/11/06 A

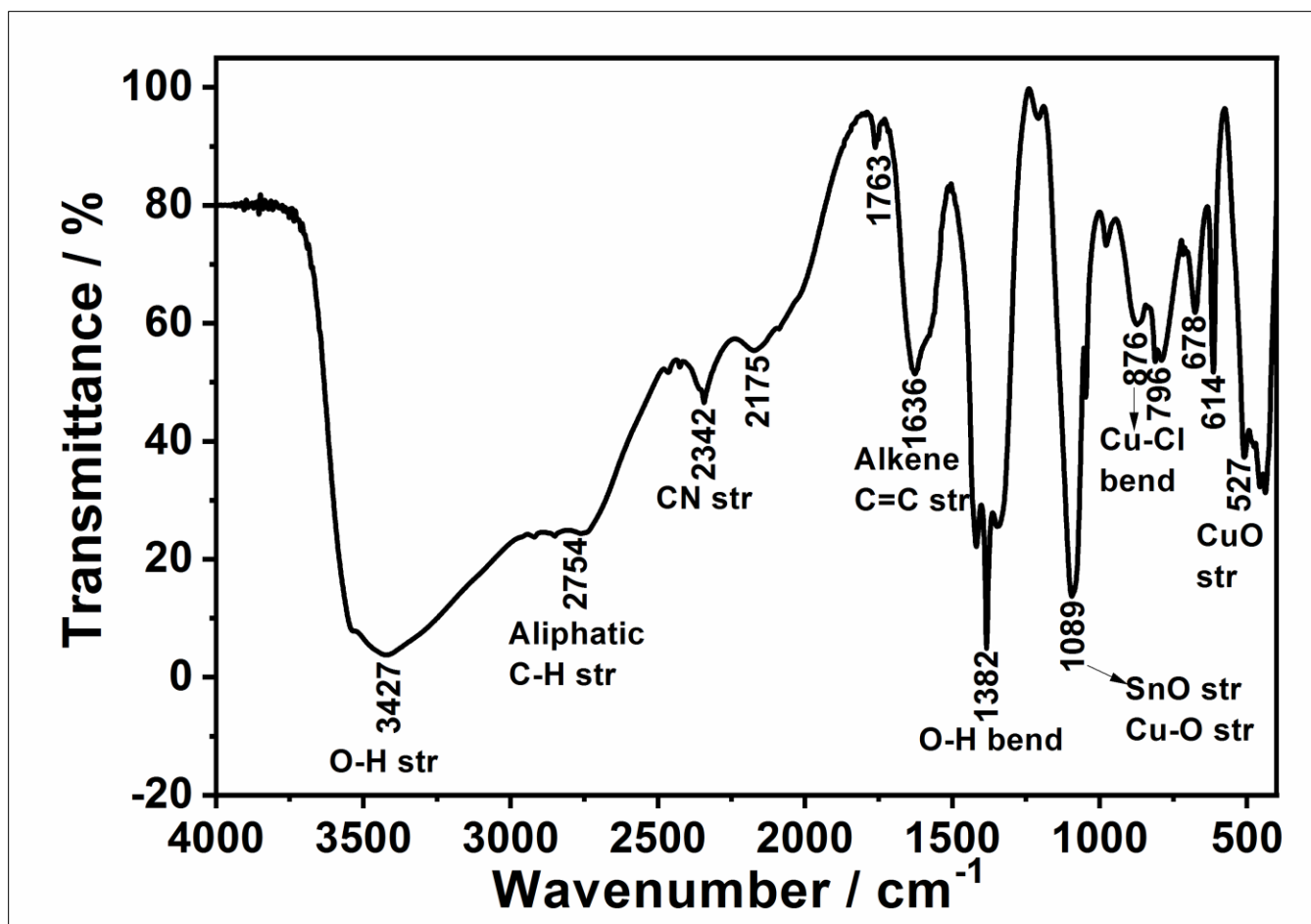


Figure 15: Infrared Spectrum of KT/04/11/06 B

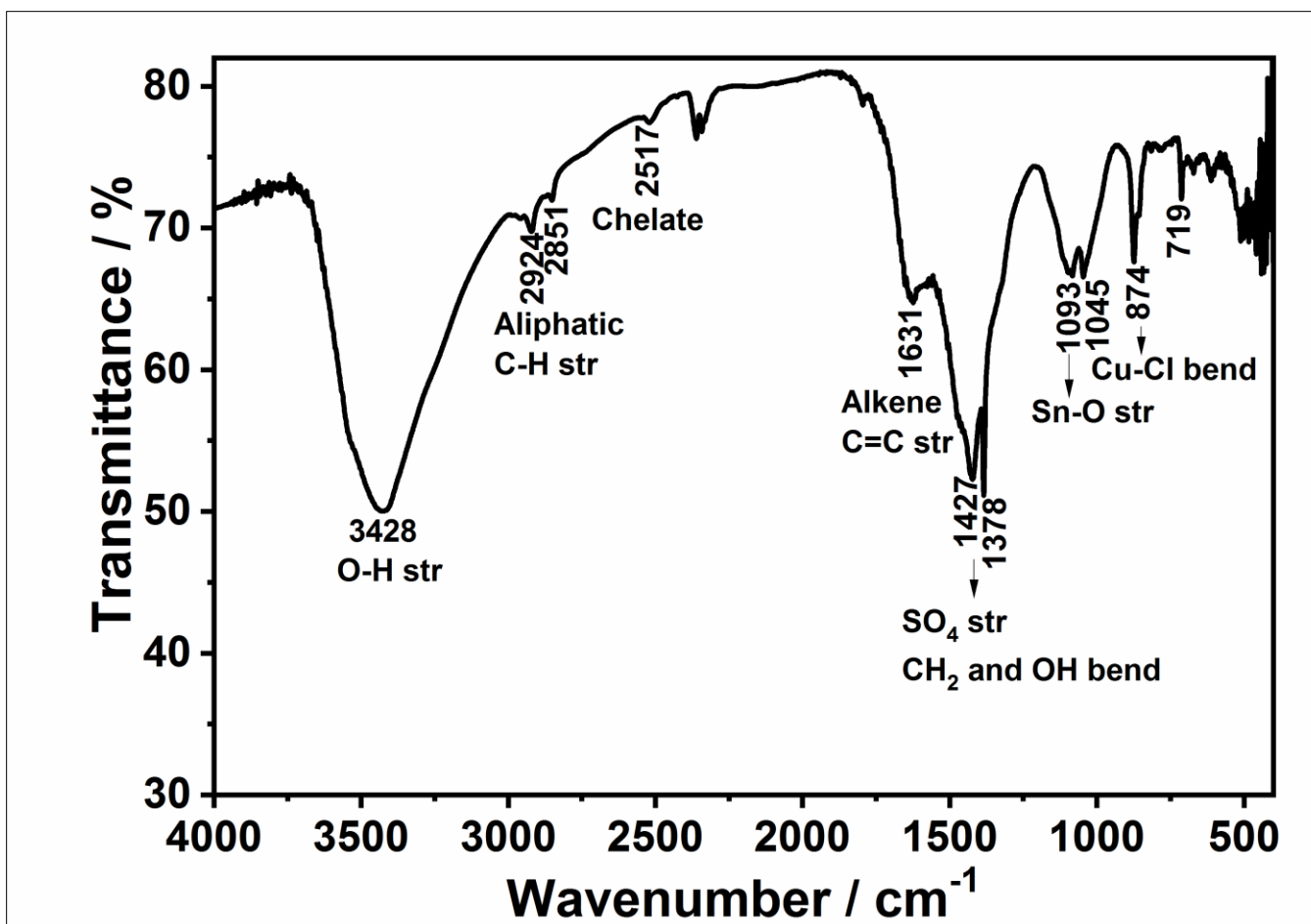


Figure 16: Infrared Spectrum of KT/04/11/06 C

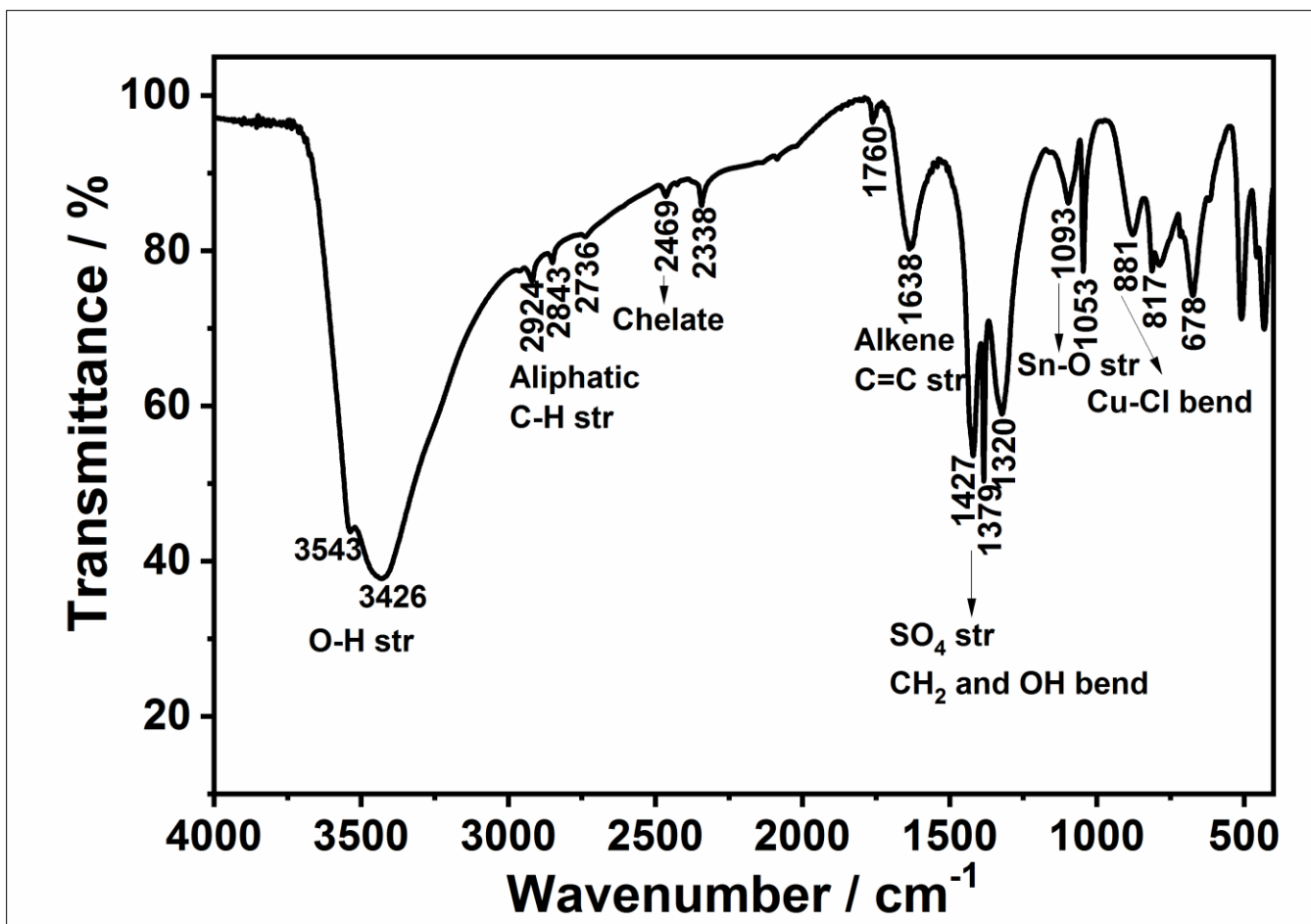


Figure 17: Infrared Spectrum of KT/04/11/07 A

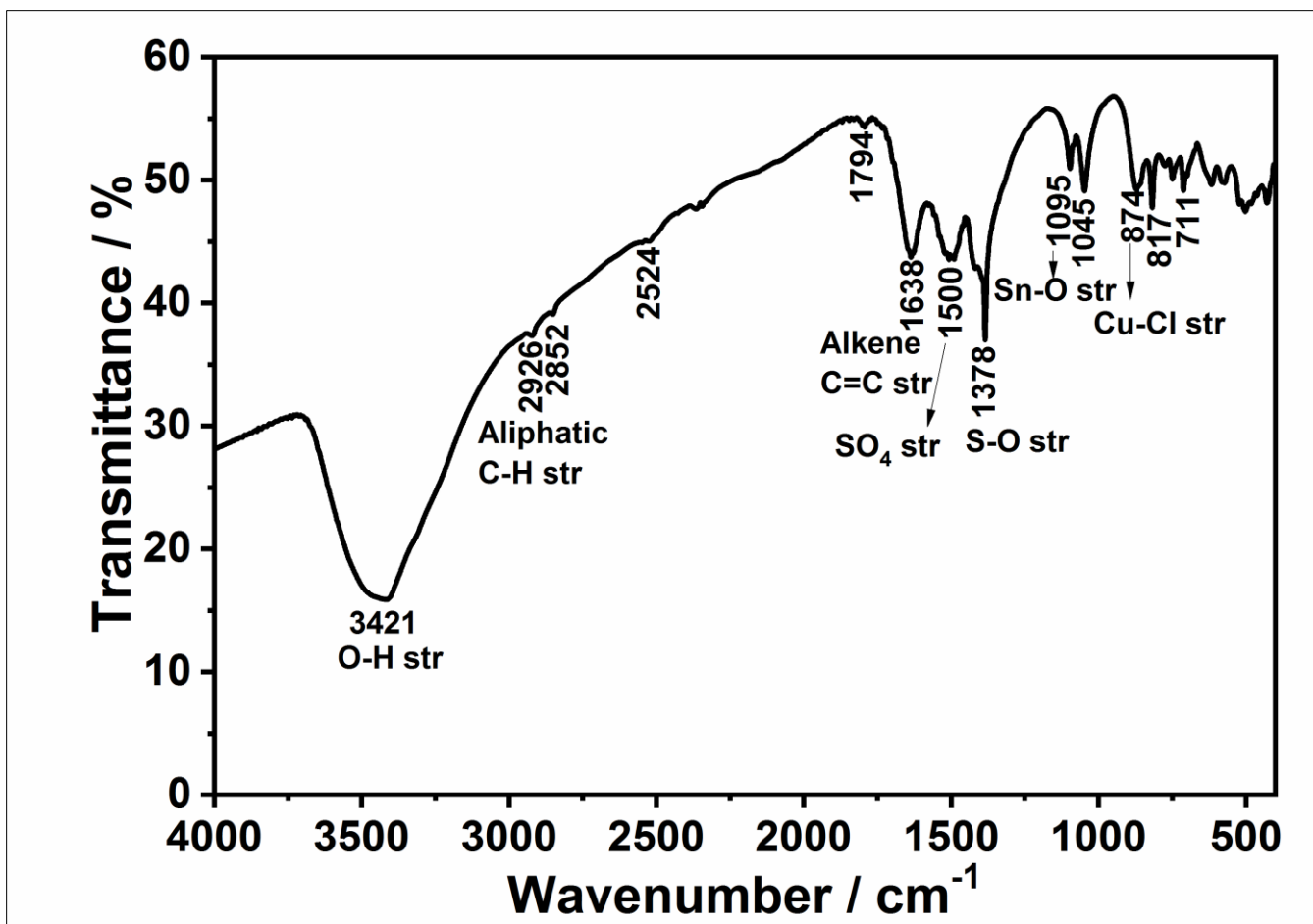


Figure 18: Infrared Spectrum of KT/04/11/07 B

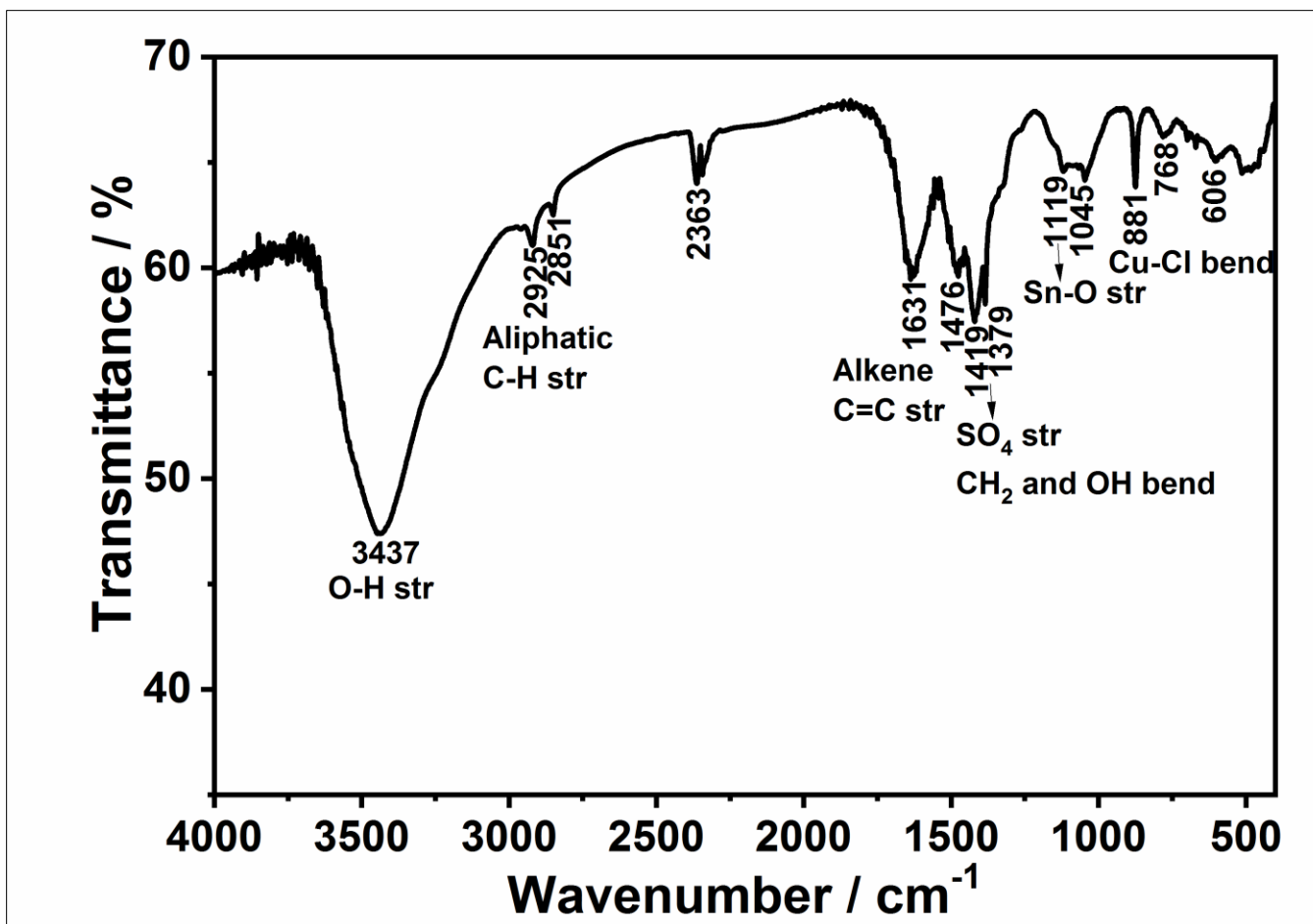


Figure 19: Infrared Spectrum of KT/04/11/07 C

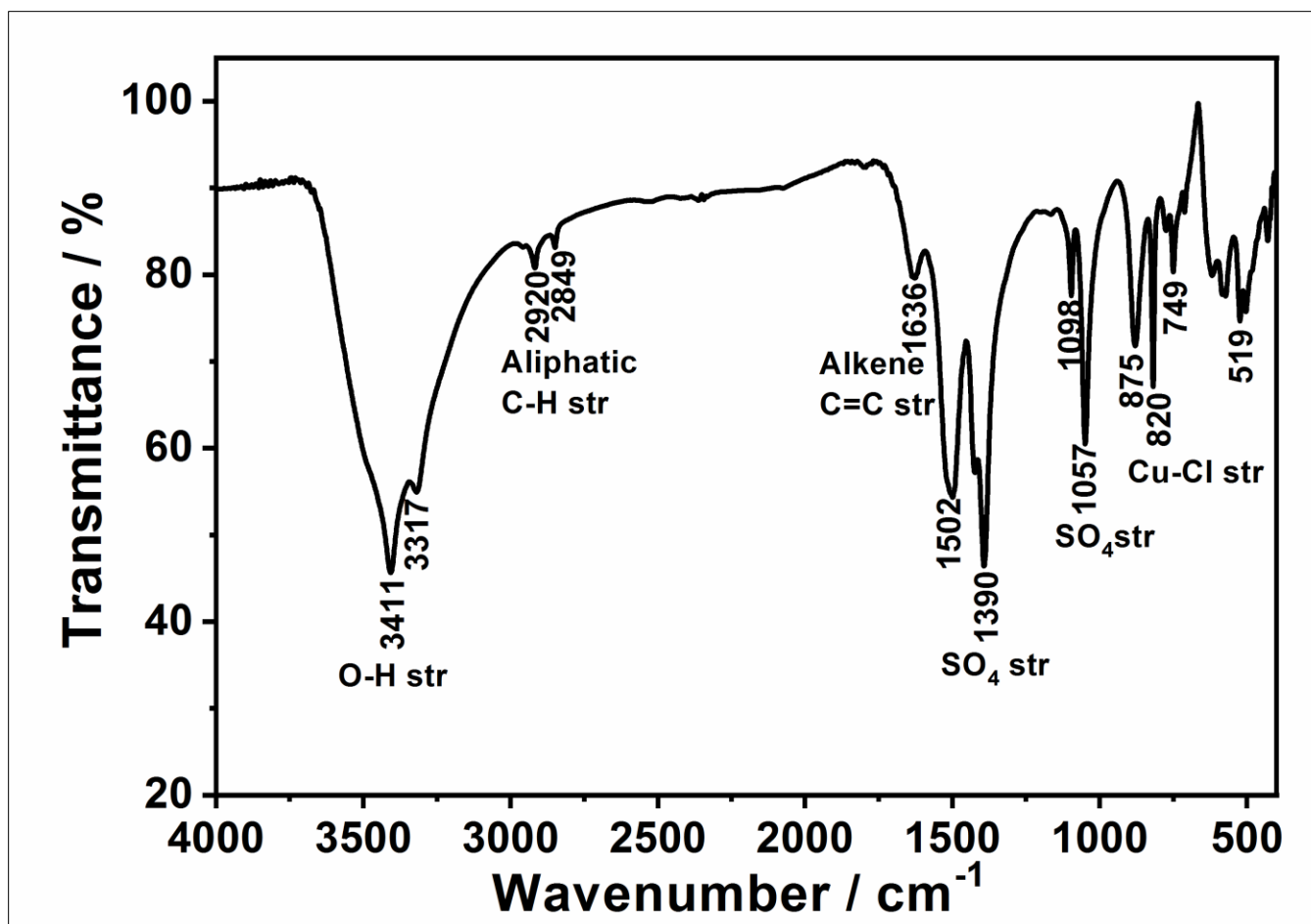


Figure 20: Infrared Spectrum of KT/04/11/08 A

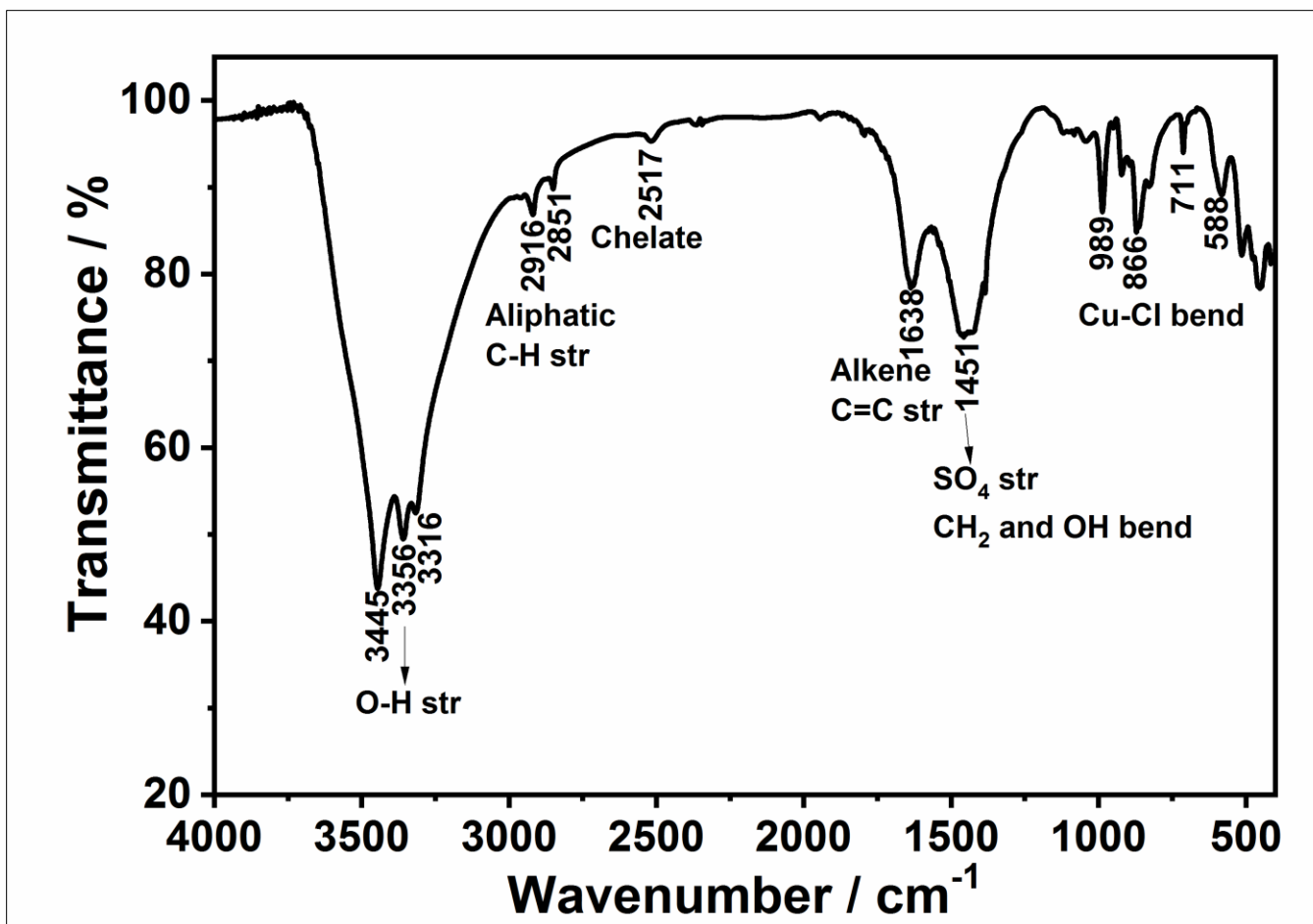


Figure 21: Infrared Spectrum of KT/04/11/08 B

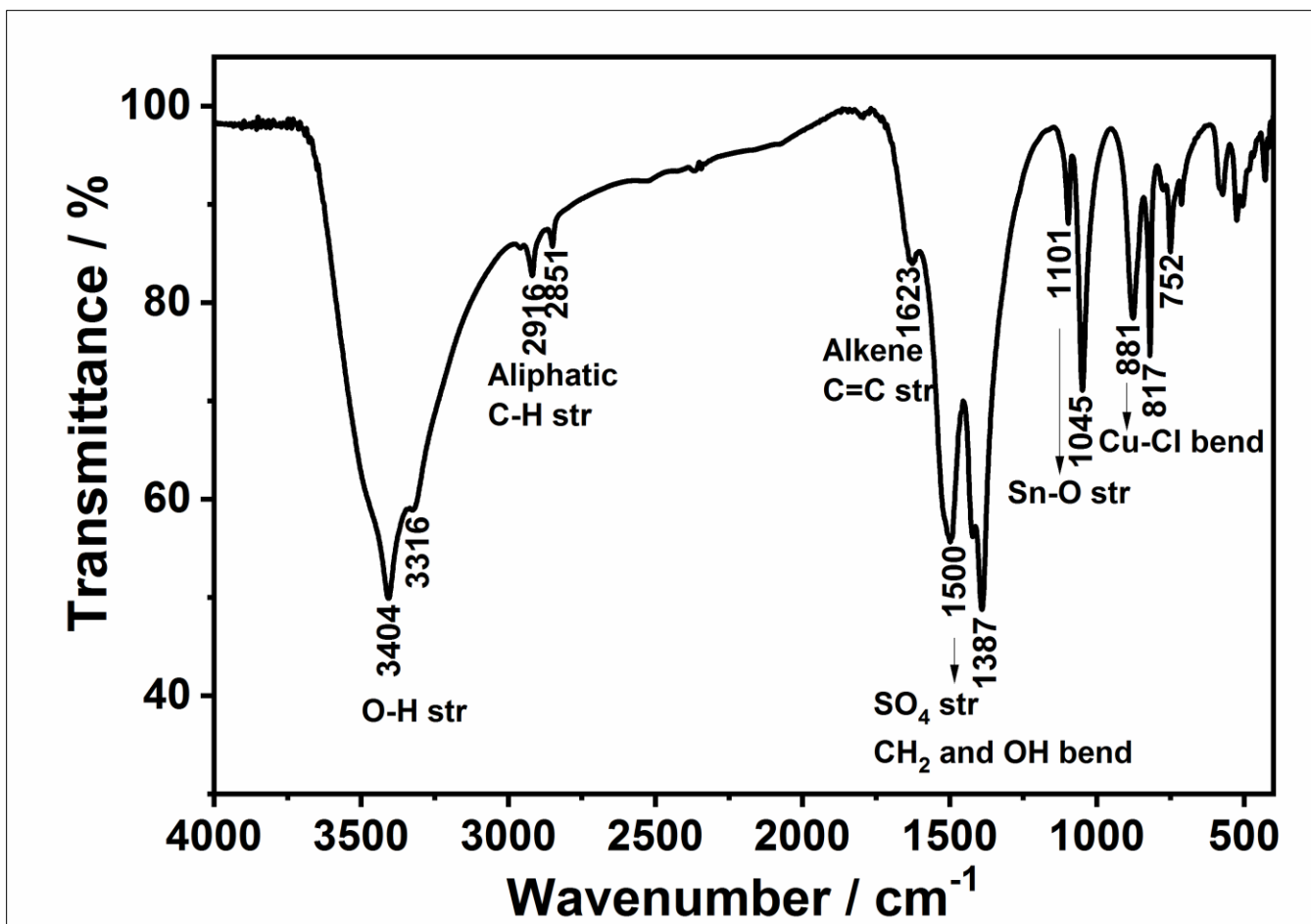


Figure 22: Infrared Spectrum of KT/04/11/08 C

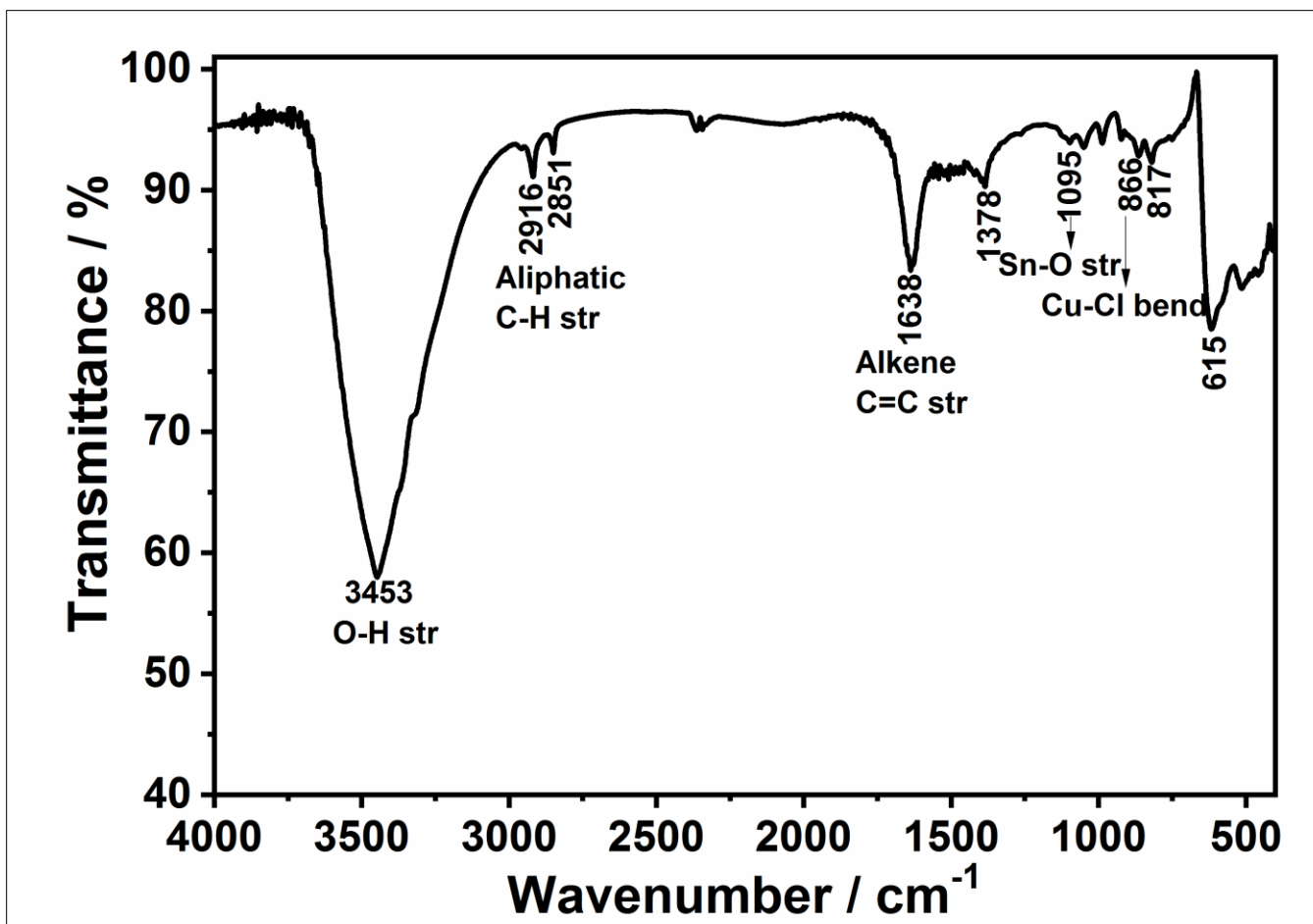


Figure 23: Infrared Spectrum of KT/04/11/10 A

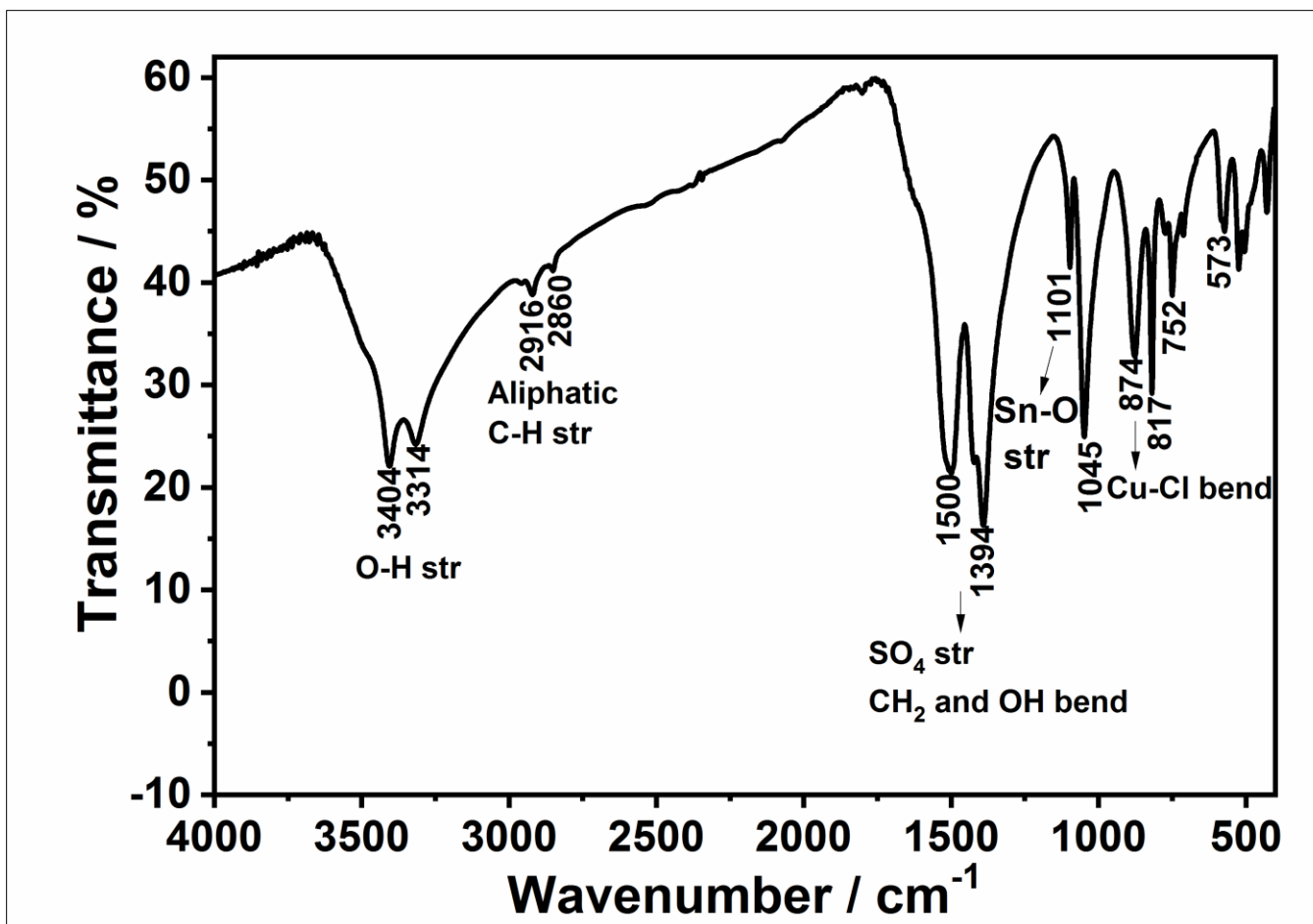


Figure 24: Infrared Spectrum of KT/04/11/10 B

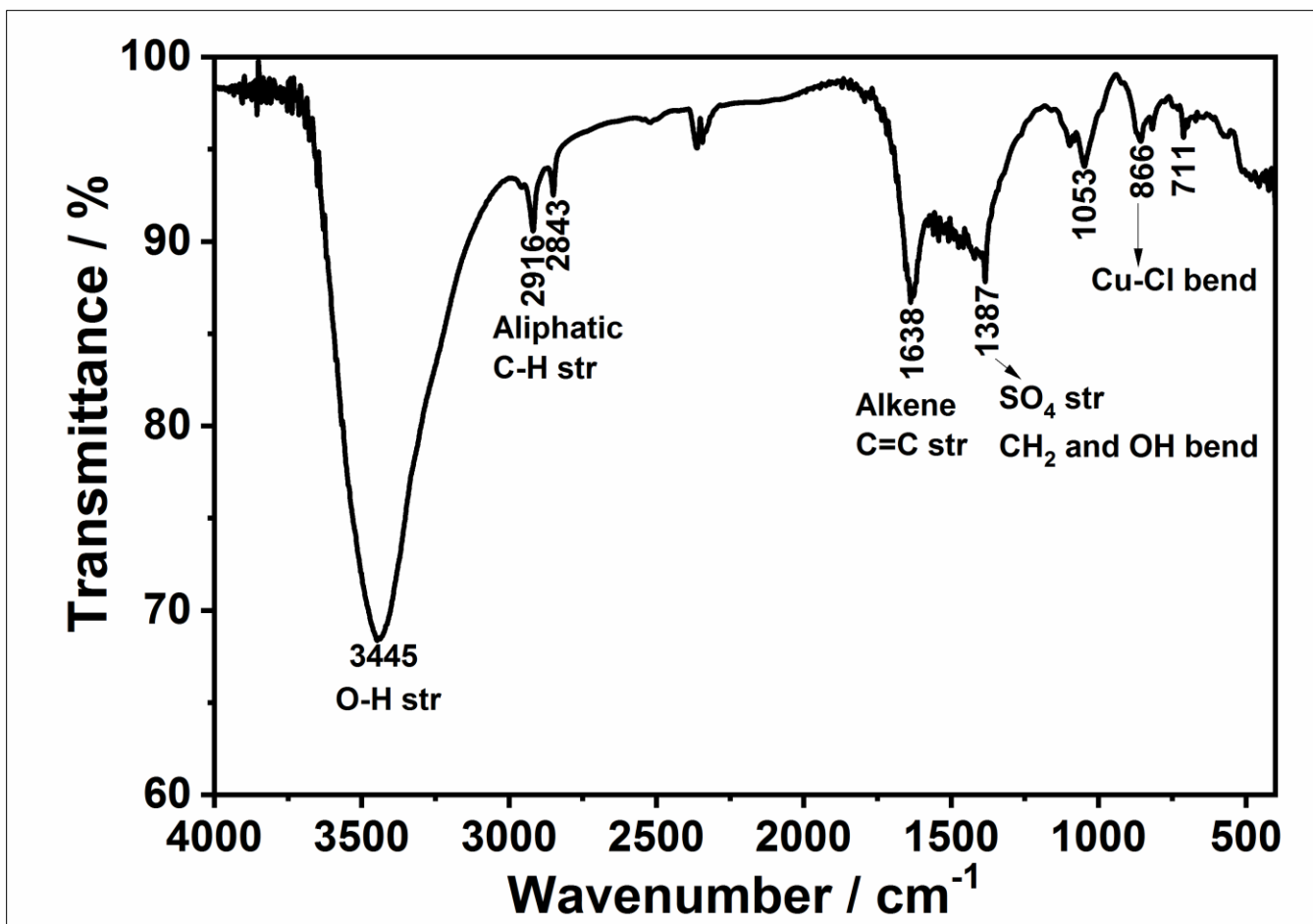


Figure 25: Infrared Spectrum of KT/04/11/10 C

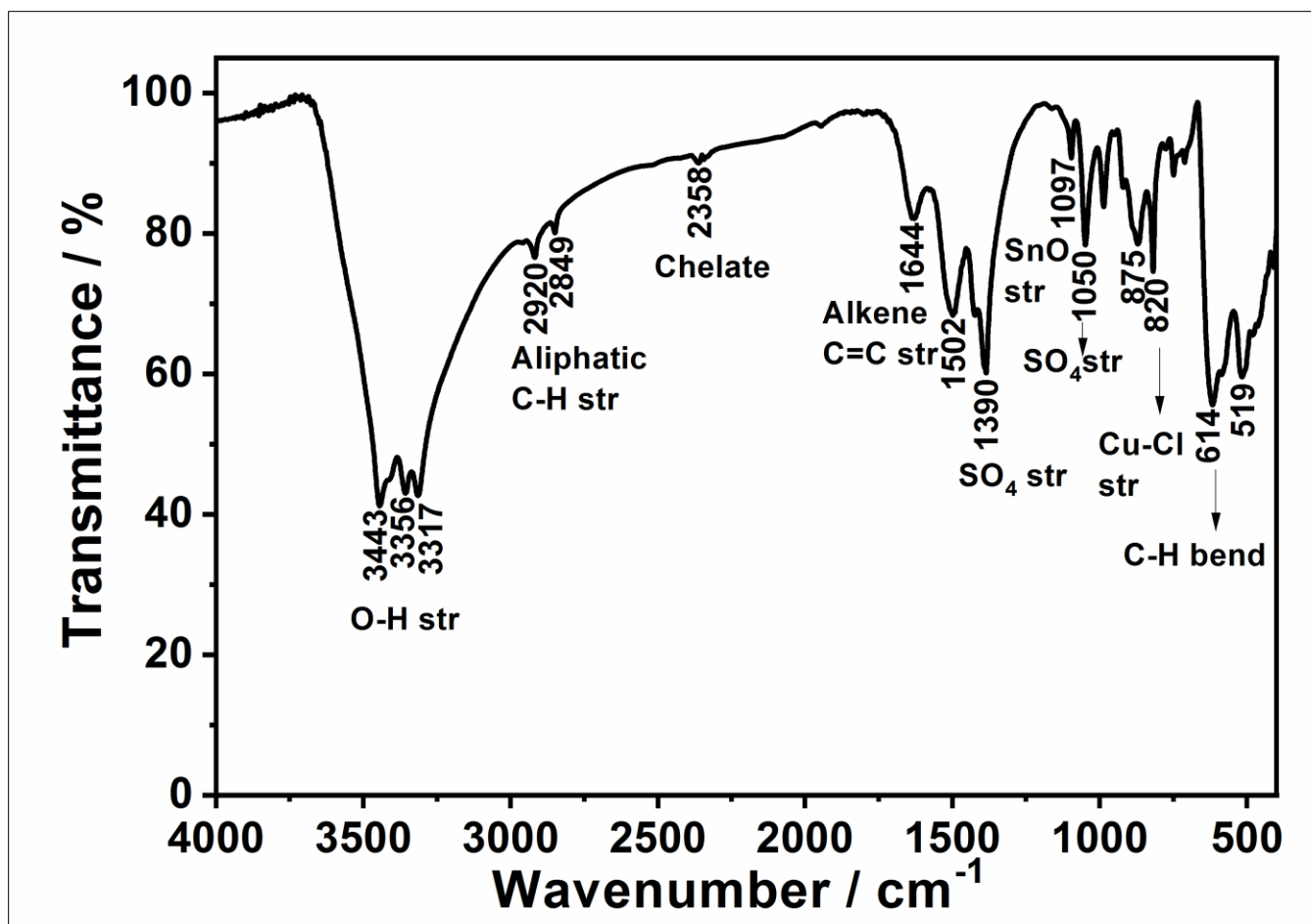


Figure 26: Infrared Spectrum of KT/04/11/22 A

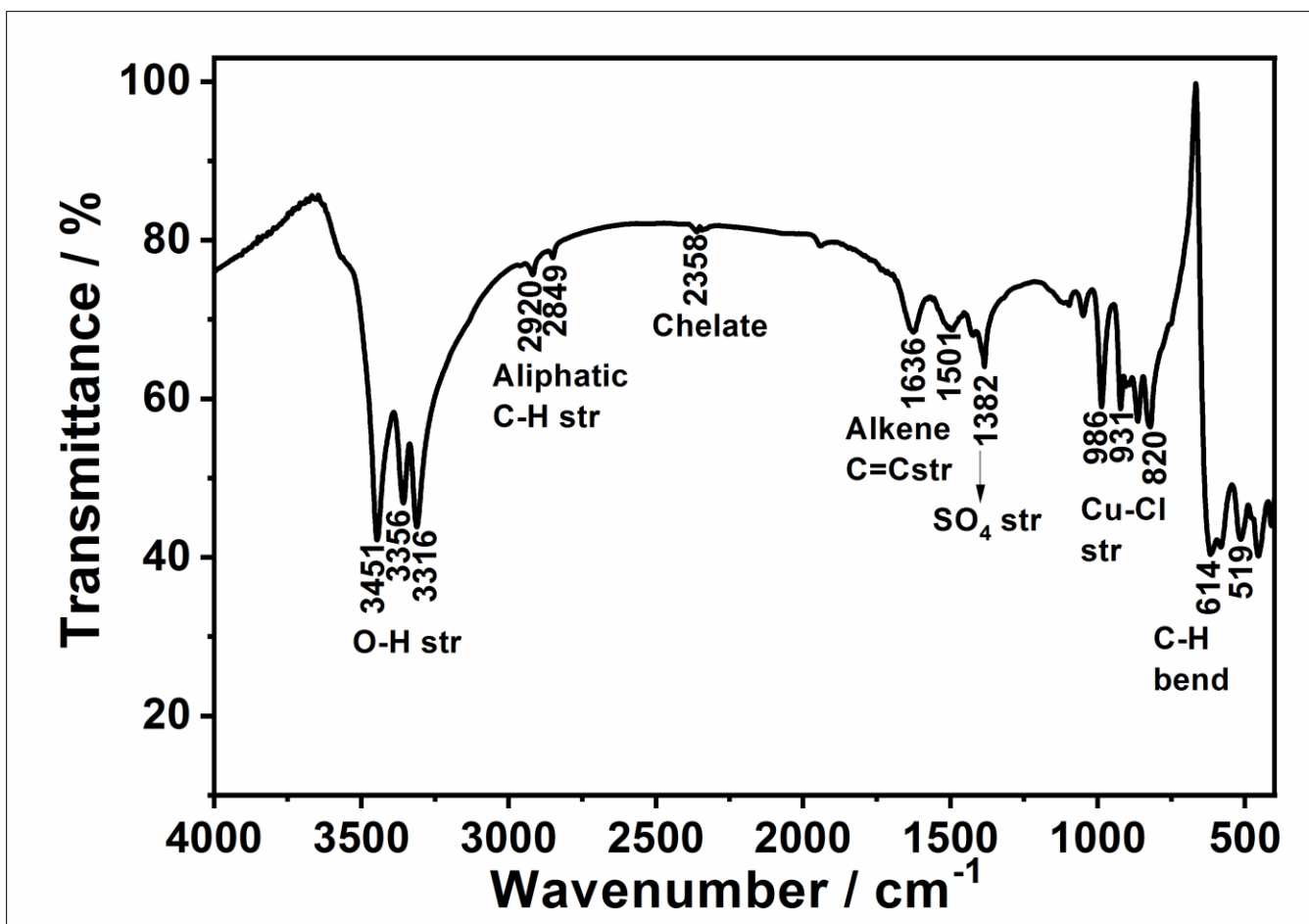


Figure 27: Infrared Spectrum of KT/04/11/22 B

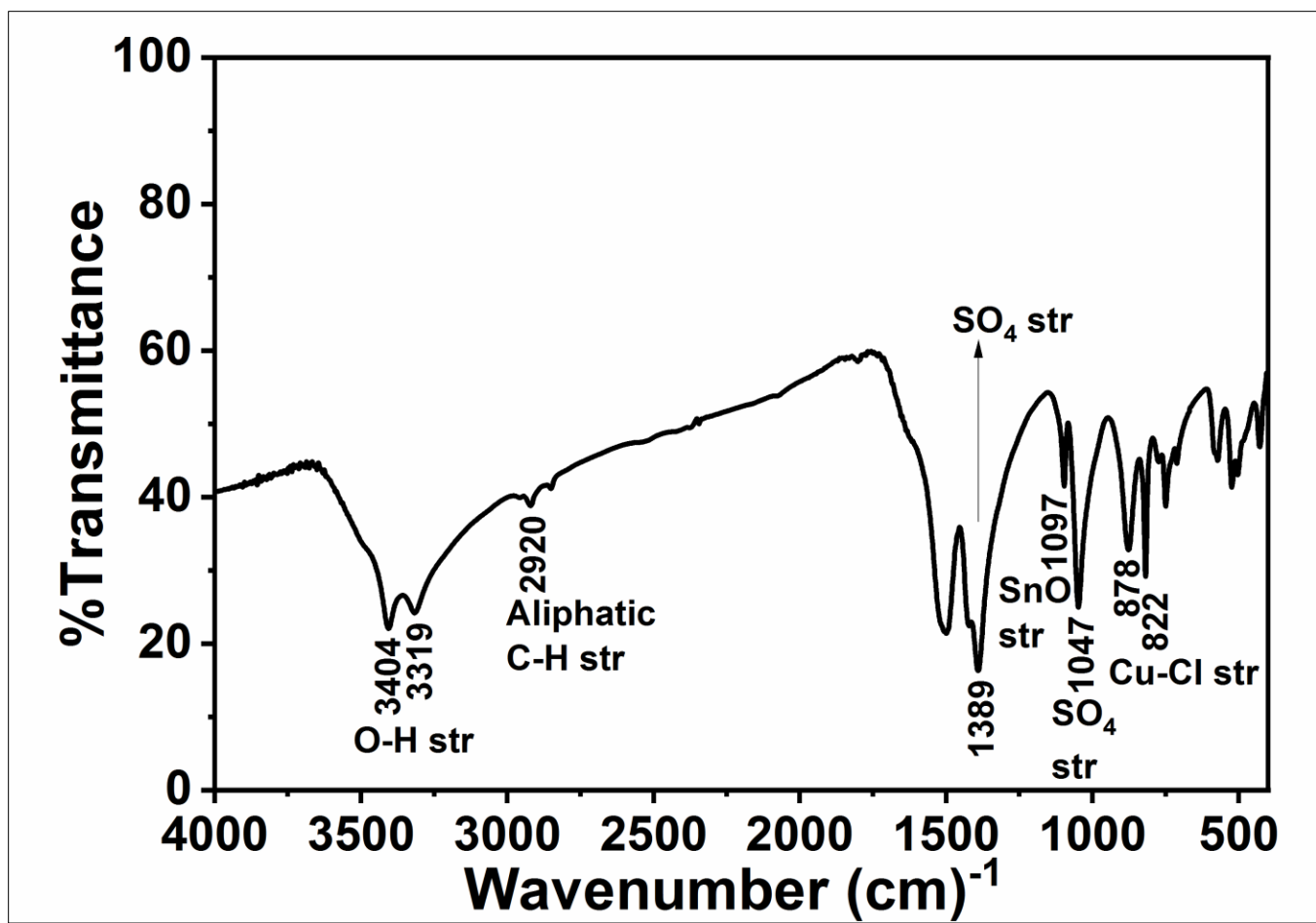


Figure 28: Infrared Spectrum of KT/04/11/22 C

4.1 CV

The results of the cyclic voltammetry measurements of the bronze bowls' samples are given below.

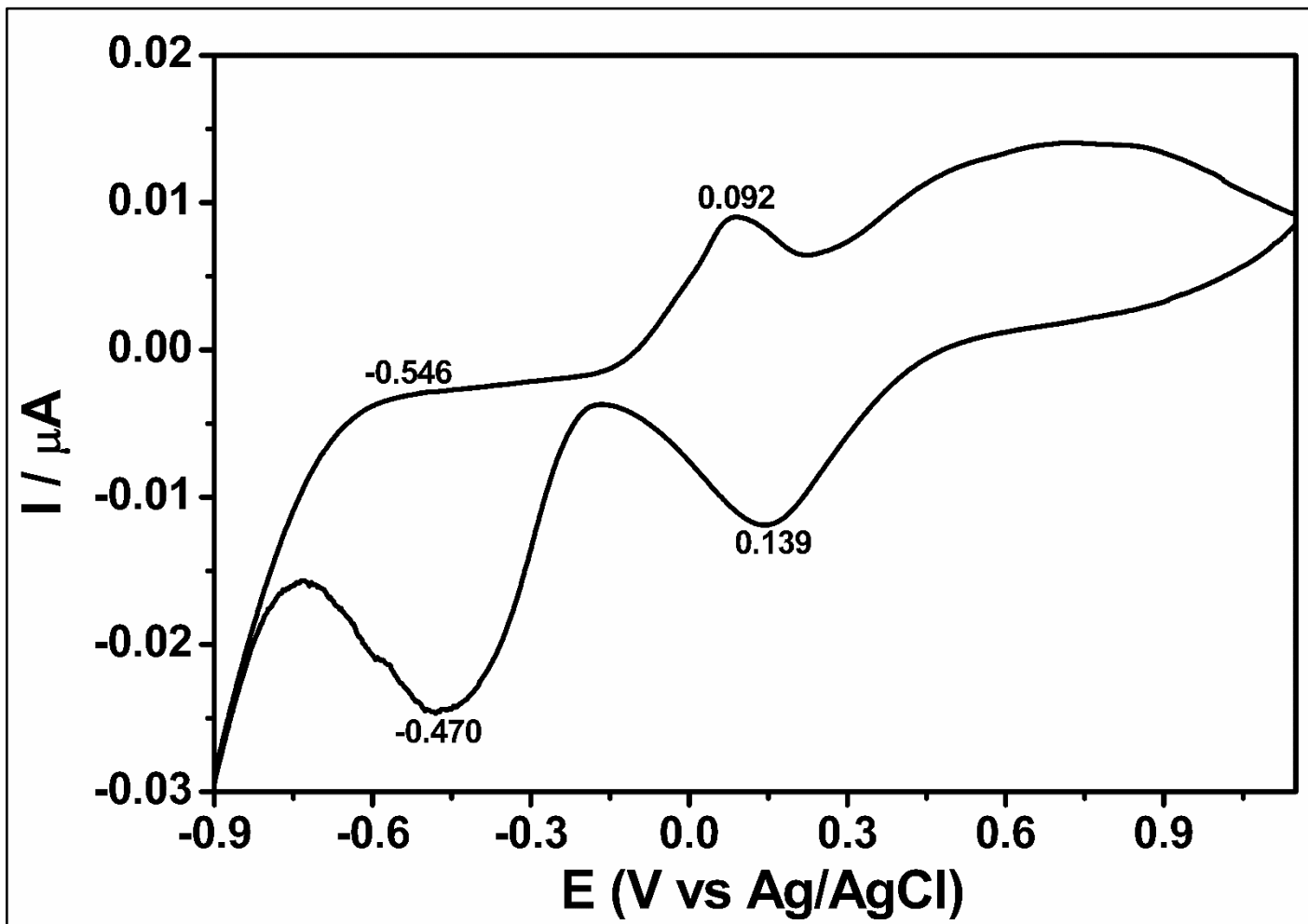


Figure 29: Cyclic voltammetry curve for KT/11/04/05 A

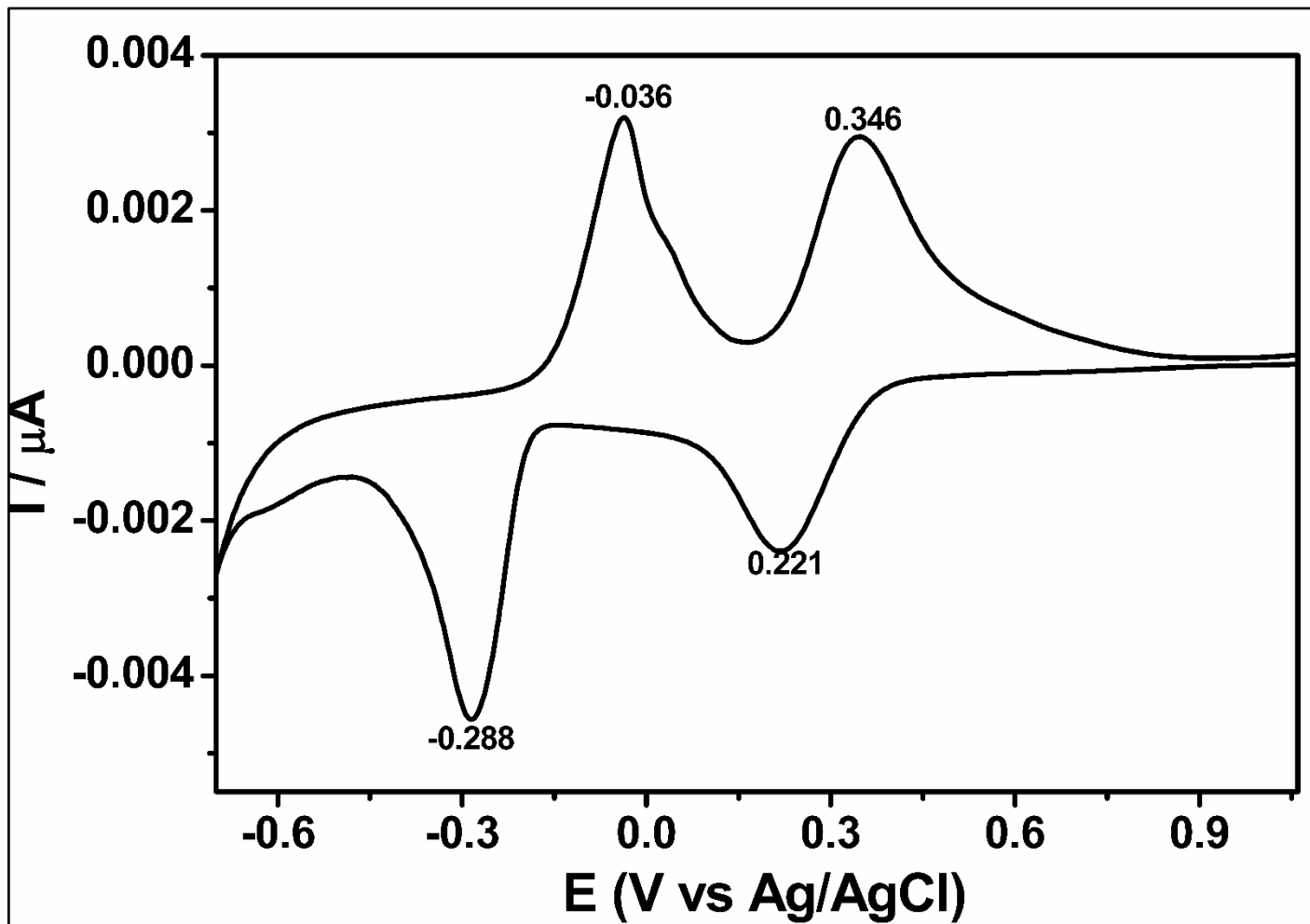


Figure 30: Cyclic voltammetry curve for KT/11/04/05B

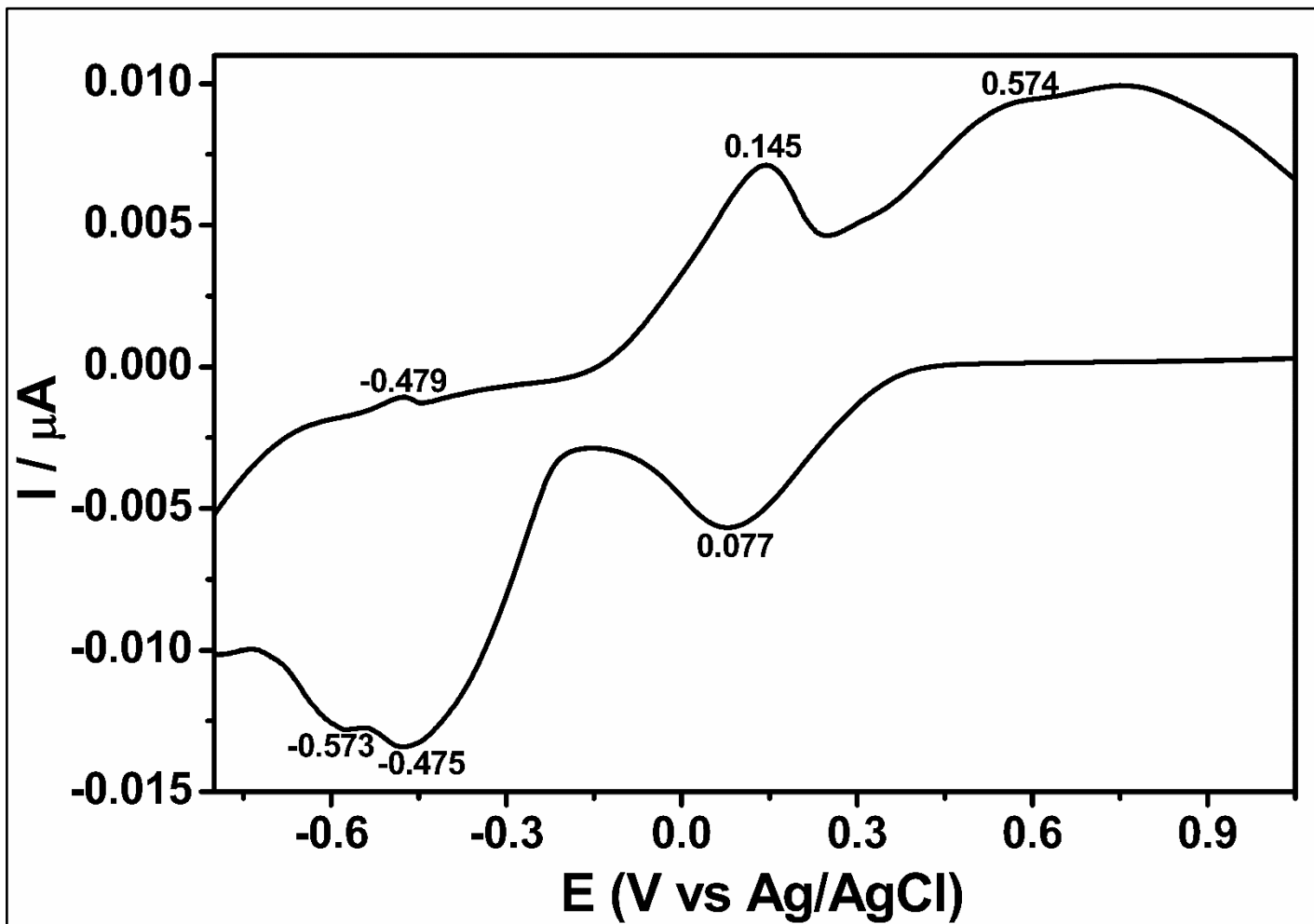


Figure 31: Cyclic voltammetry curve for KT/11/04/06 A

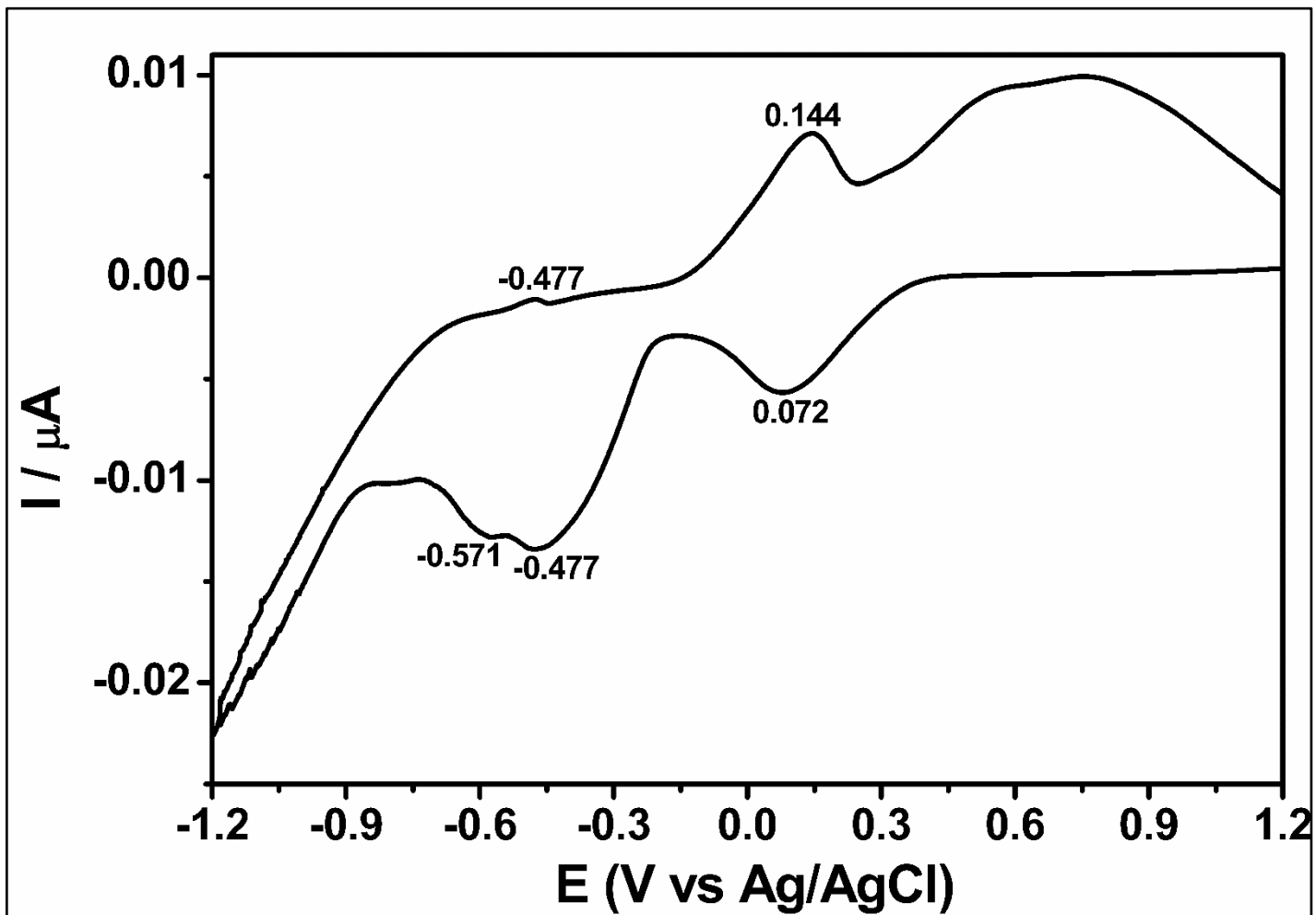


Figure 32: Cyclic voltammetry curve for KT/11/04/06 B

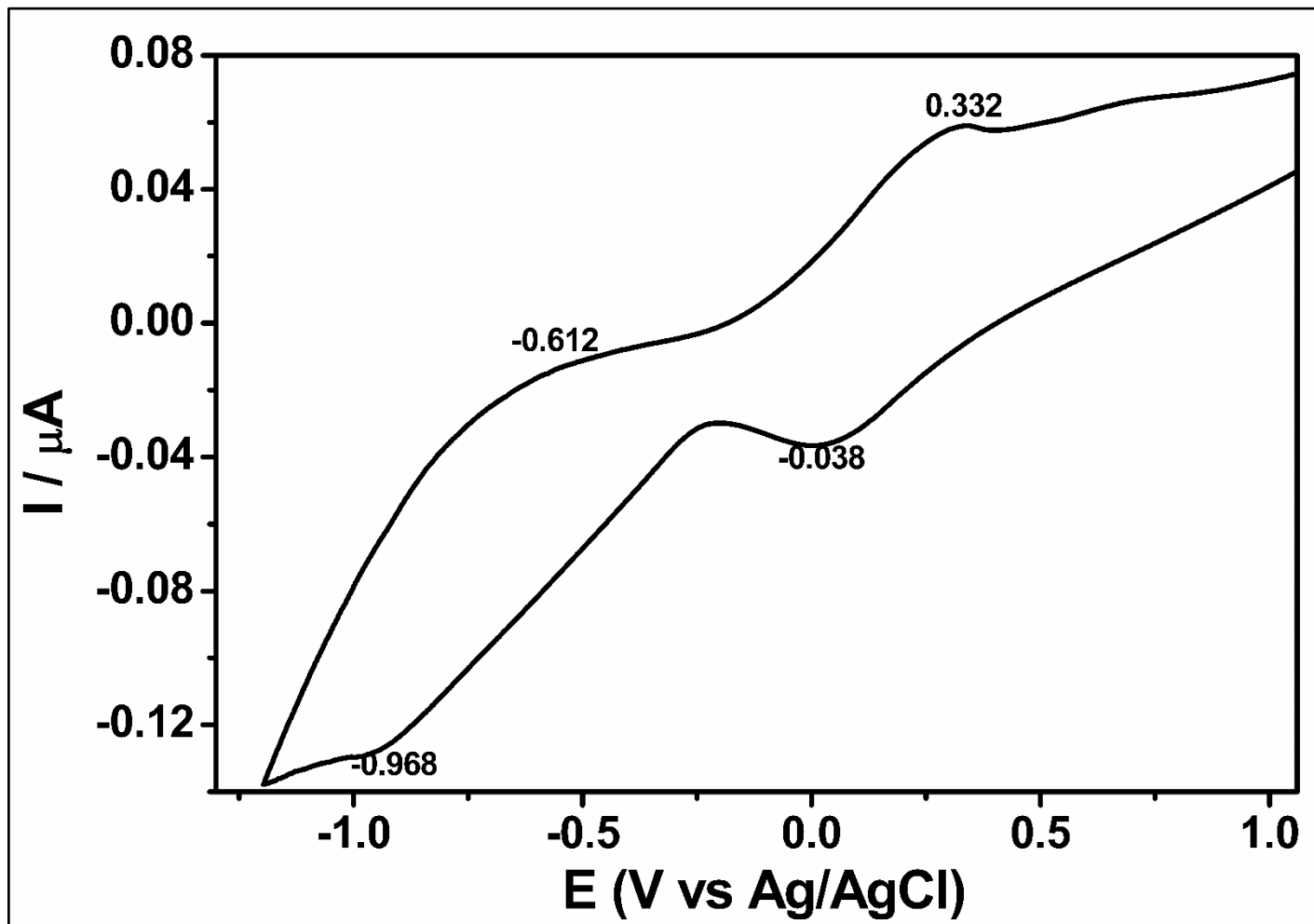


Figure 33: Cyclic voltammetry curve for KT/11/04/07 A

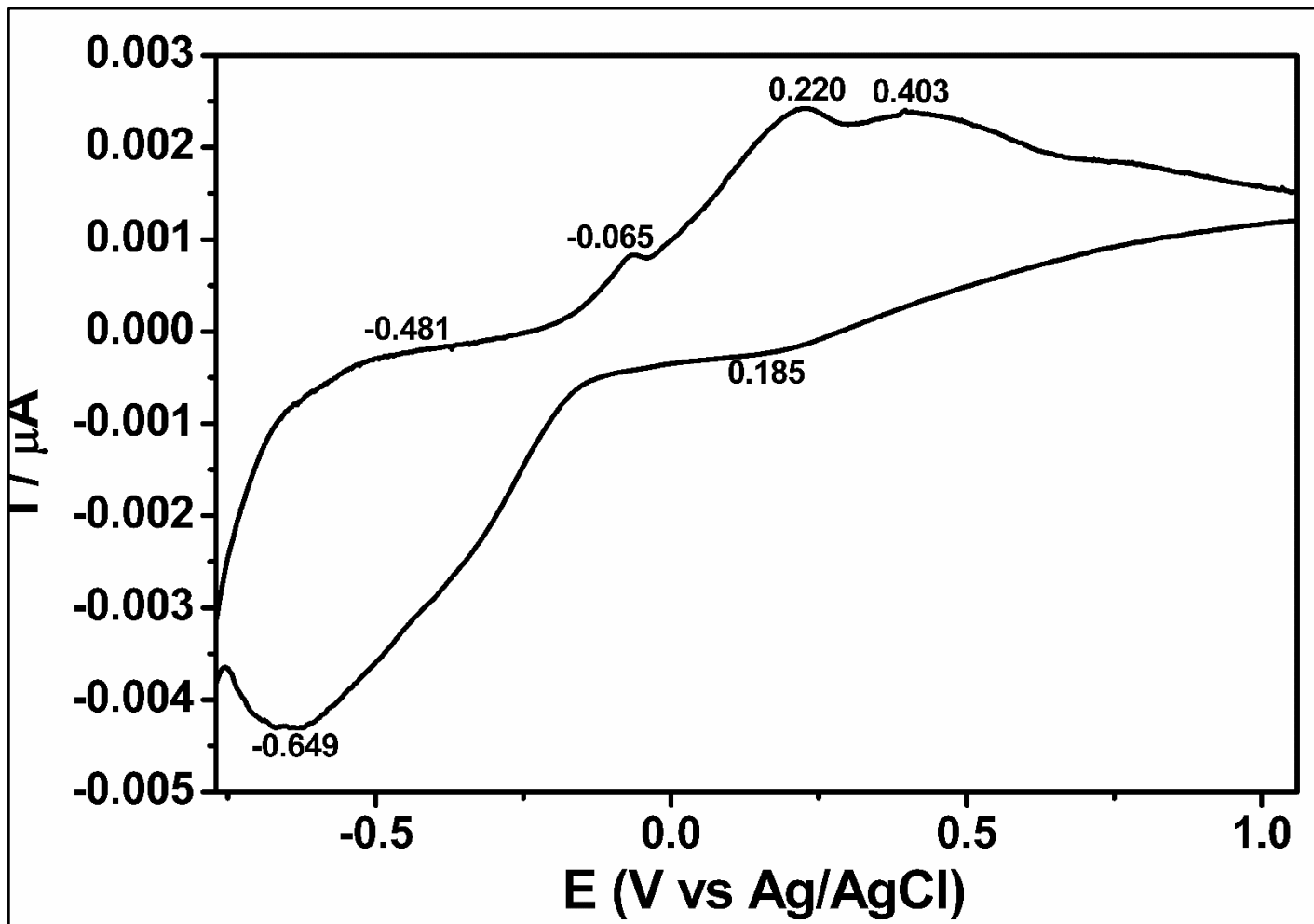


Figure 34: Cyclic voltammetry curve for KT/11/04/07 B

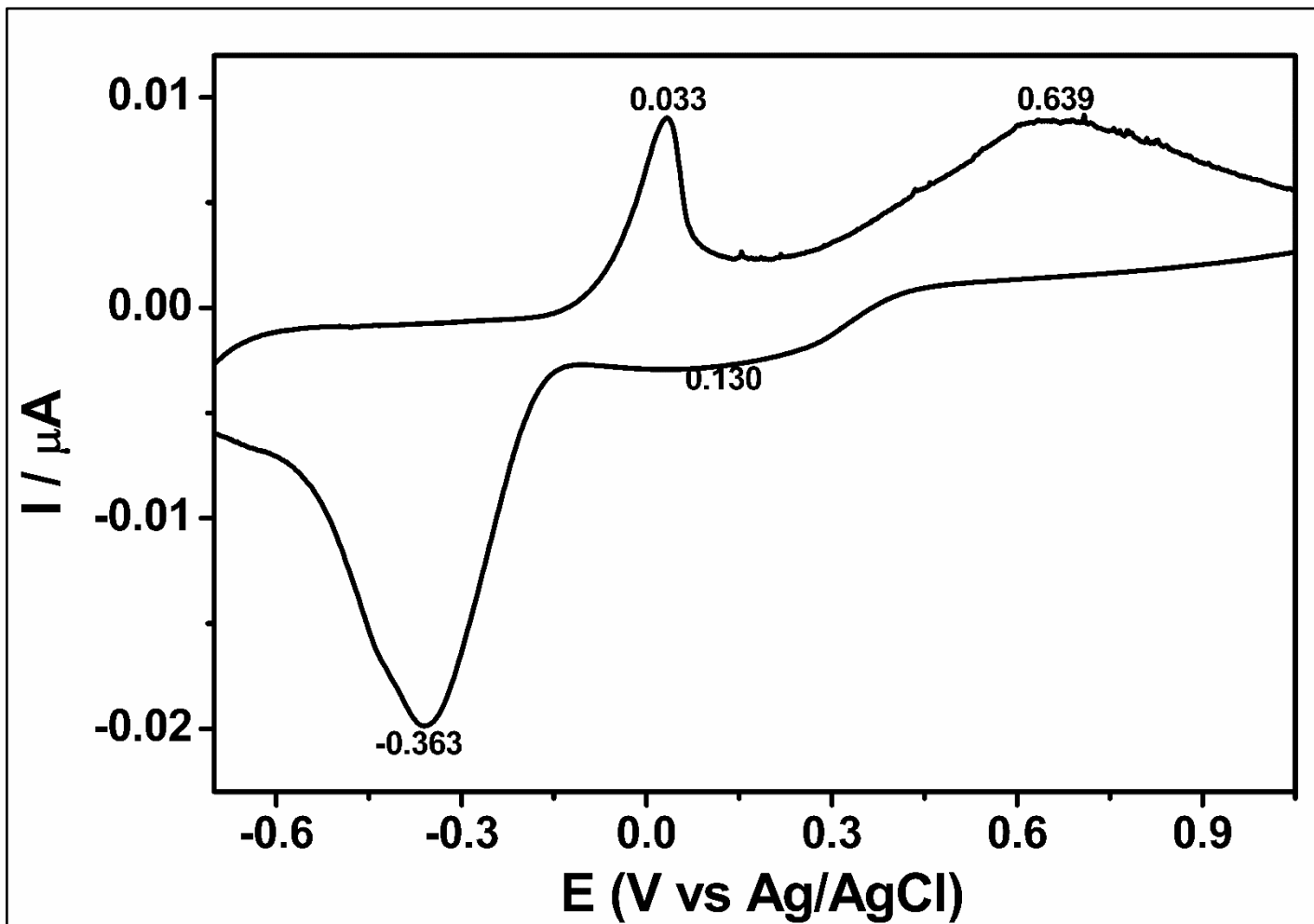


Figure 35: Cyclic voltammetry curve for KT/11/04/08 A

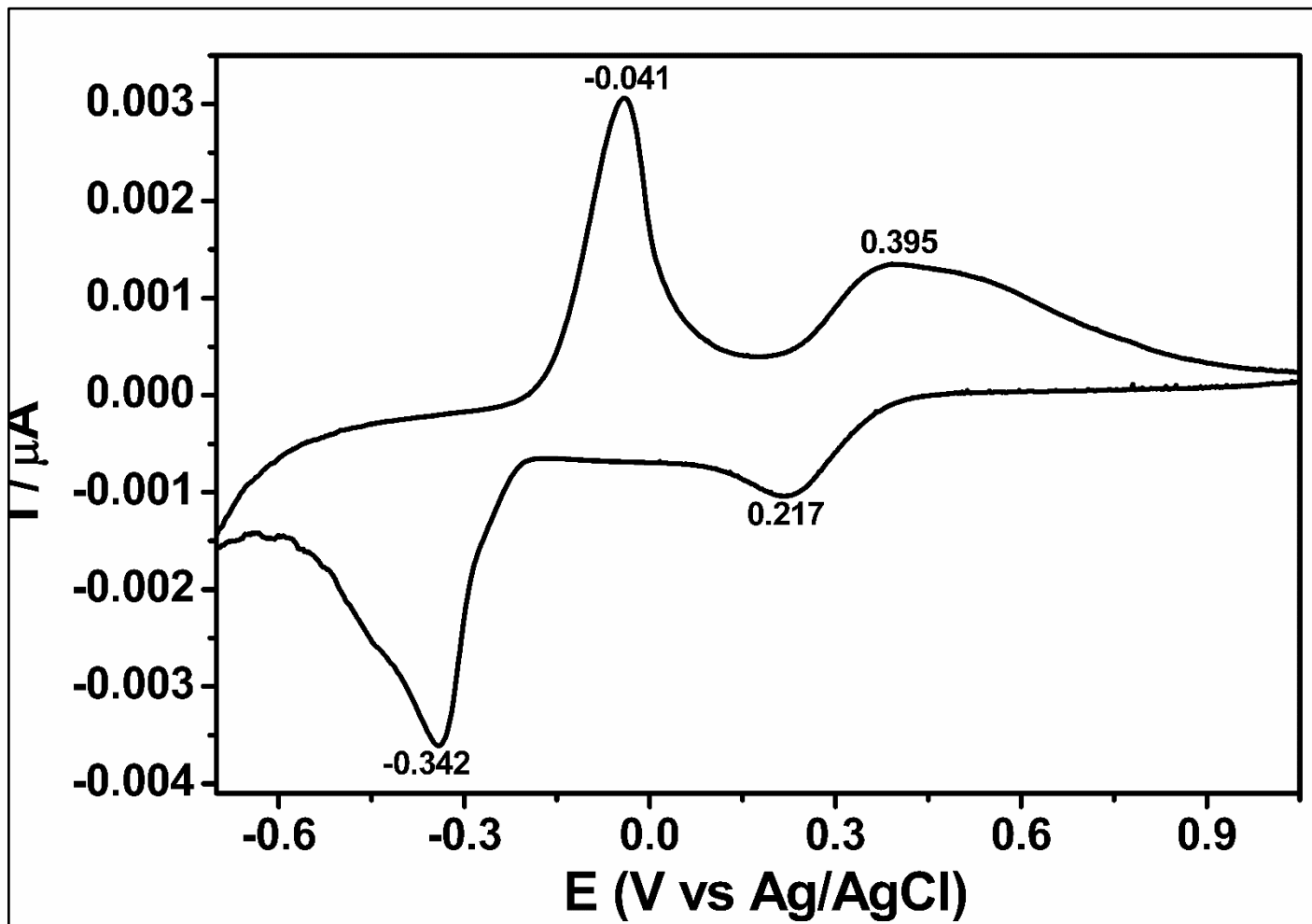


Figure 36: Cyclic voltammety curve for KT/11/04/08 B

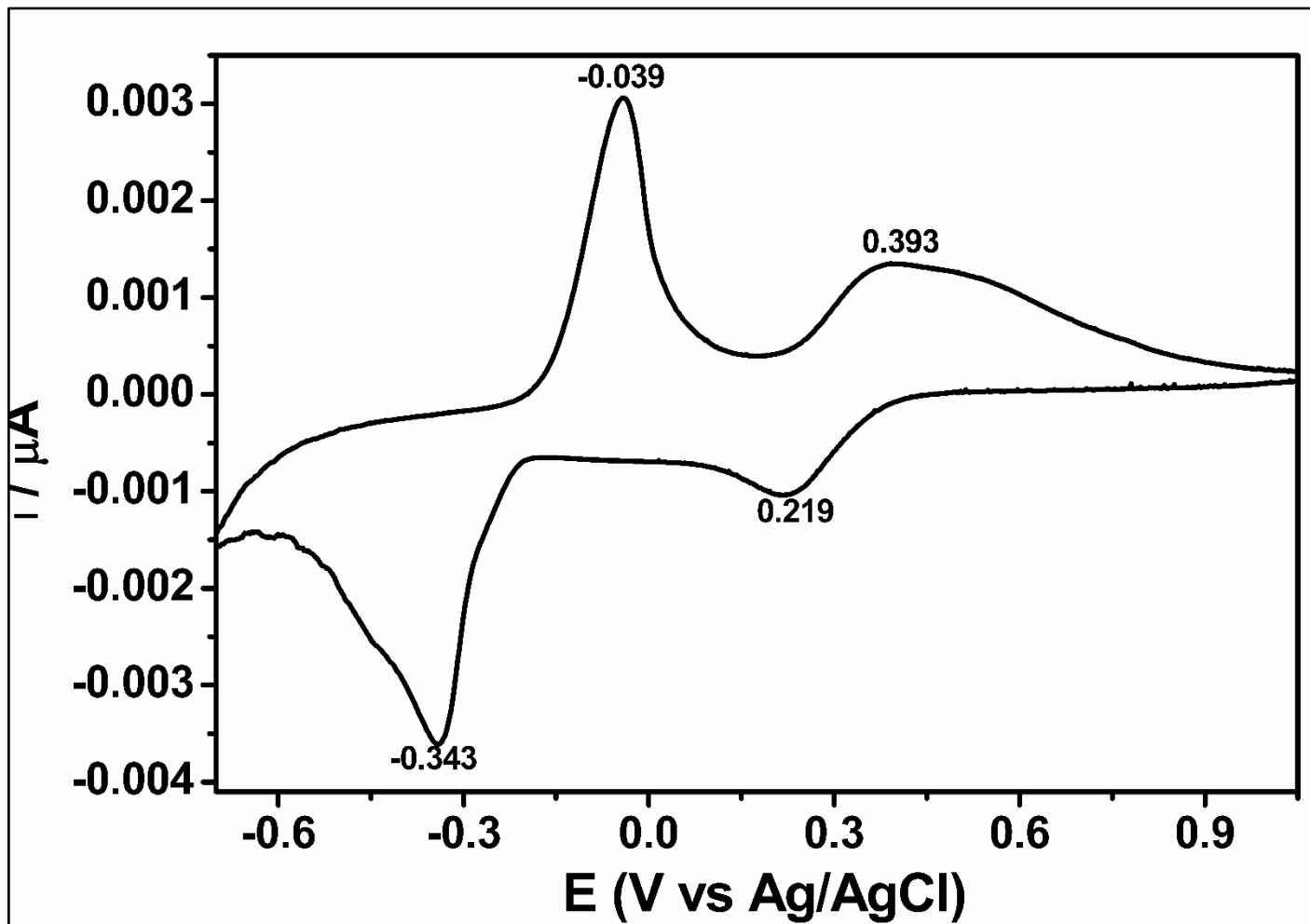


Figure 37: Cyclic voltammetry curve for KT/11/04/08 C

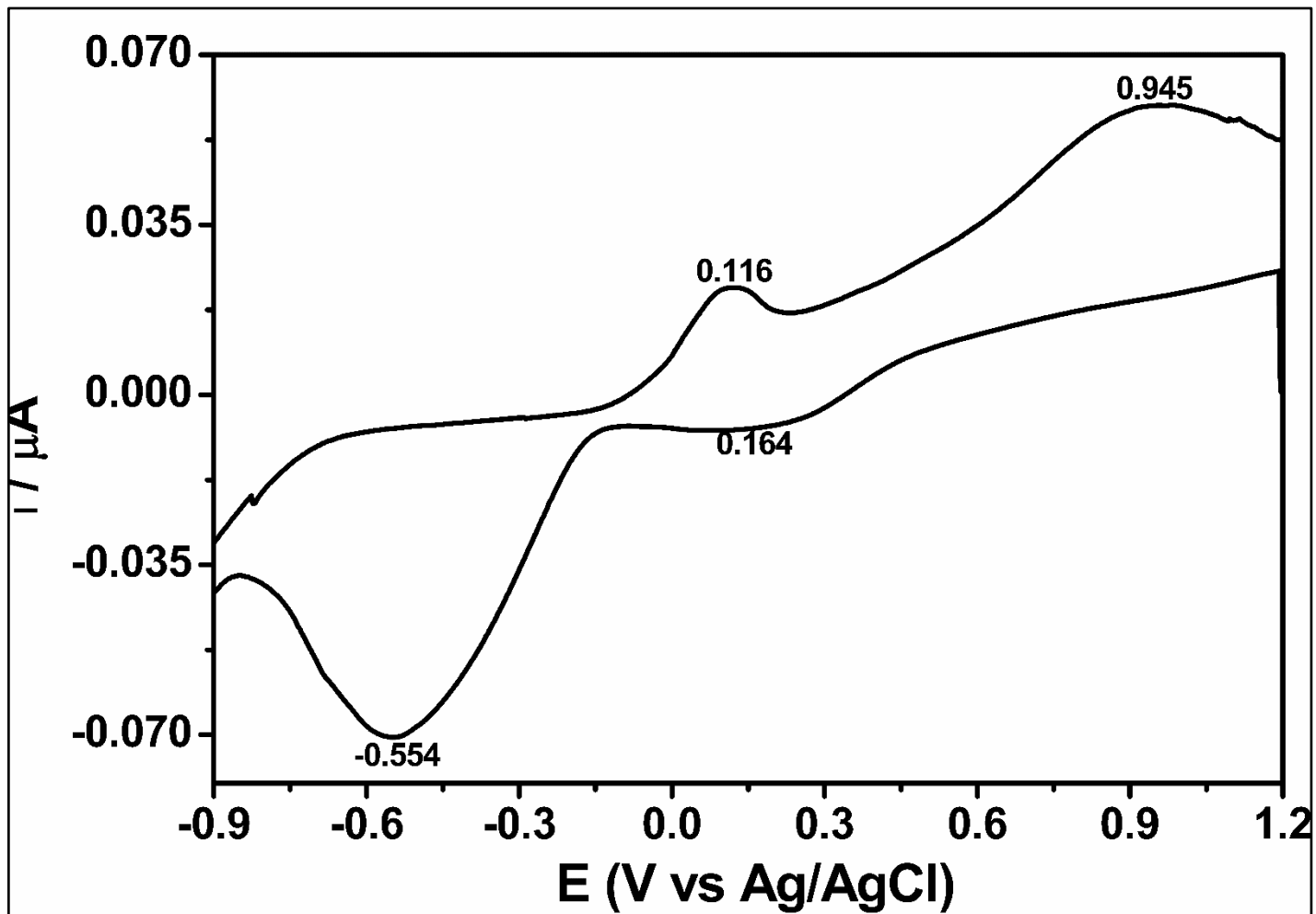


Figure 38: Cyclic voltammetry curve for KT/11/04/10 A

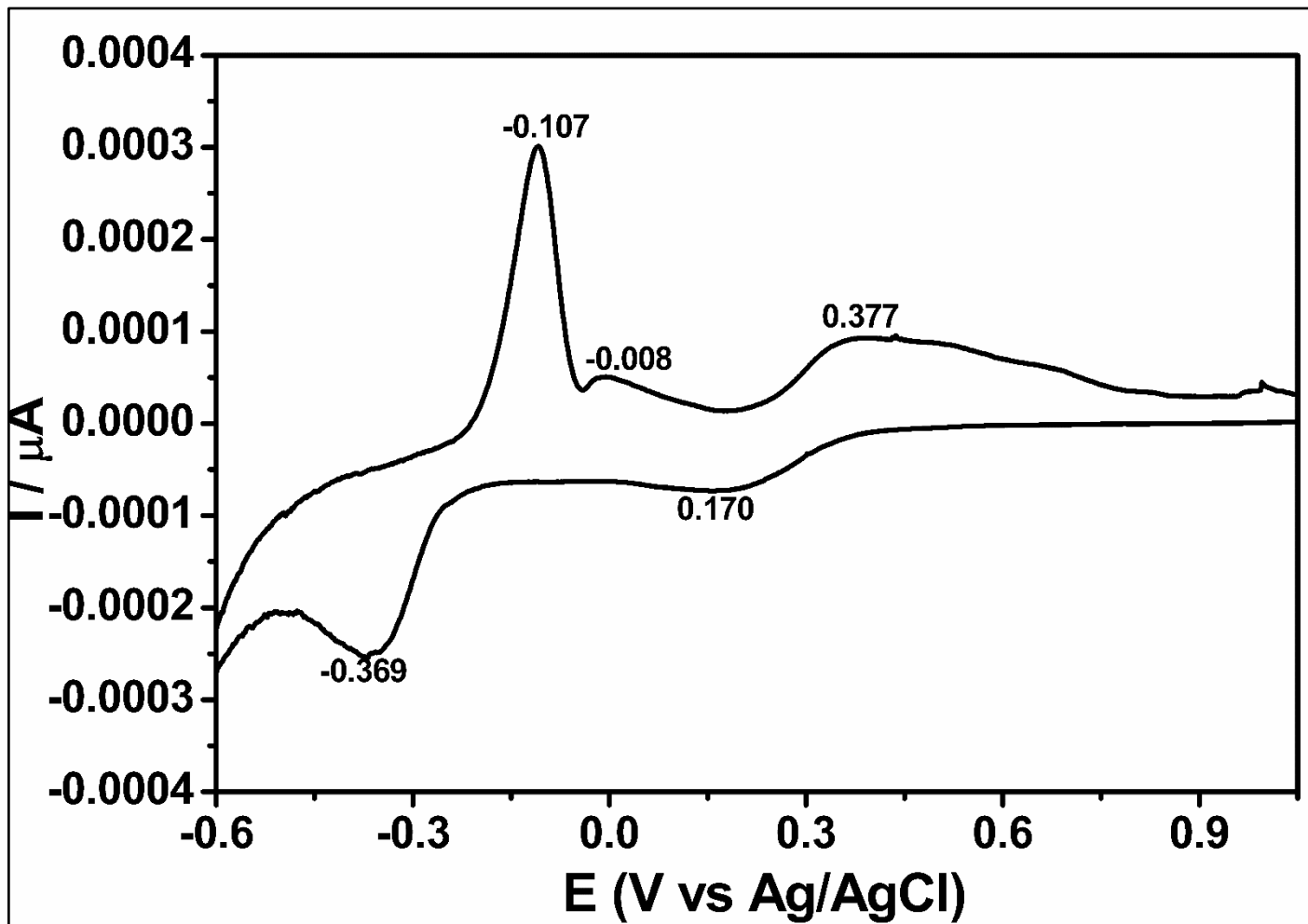


Figure 39: Cyclic voltammetry curve for KT/11/04/10 B

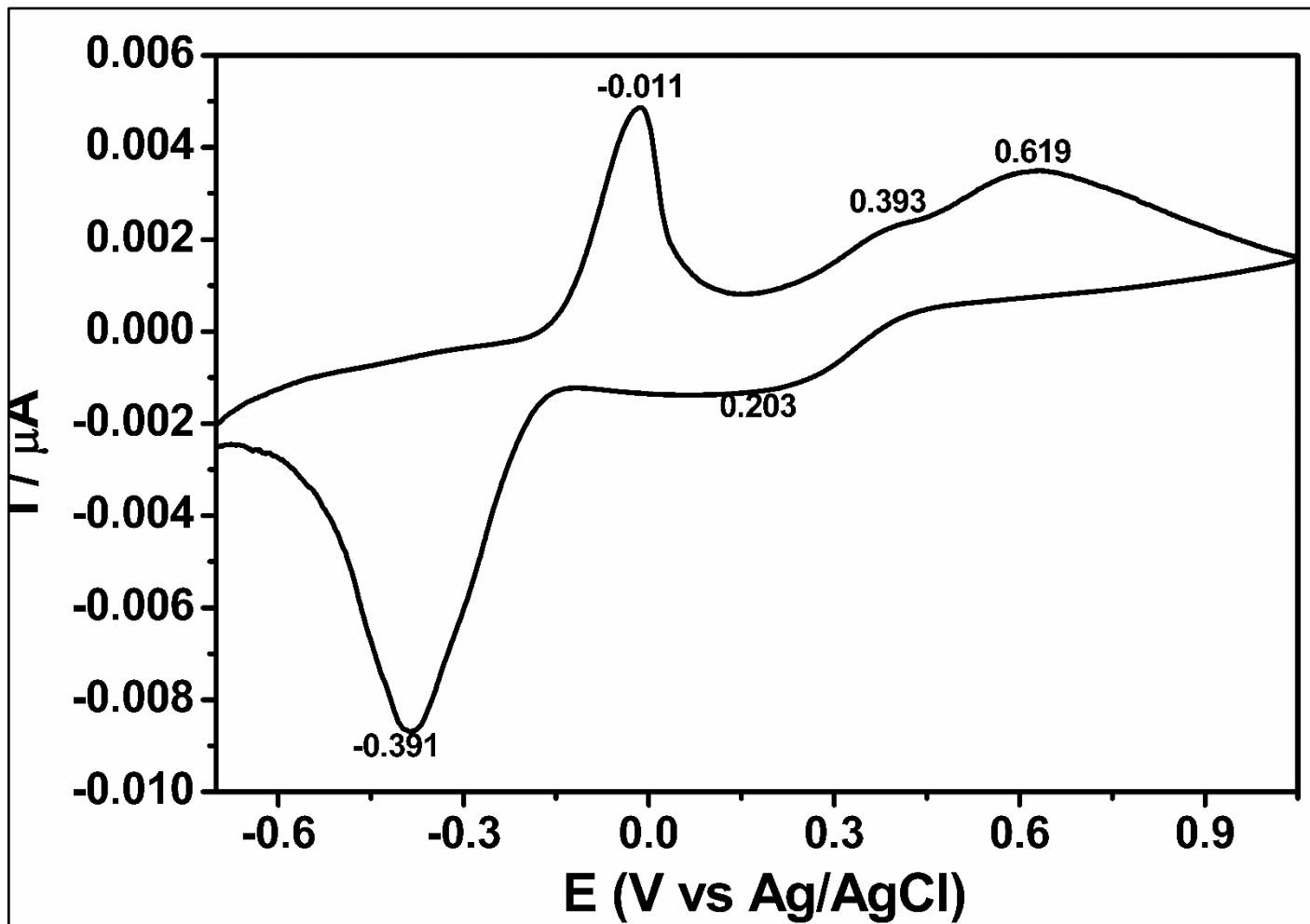


Figure 40: Cyclic voltammetry curve for KT/11/04/10 C

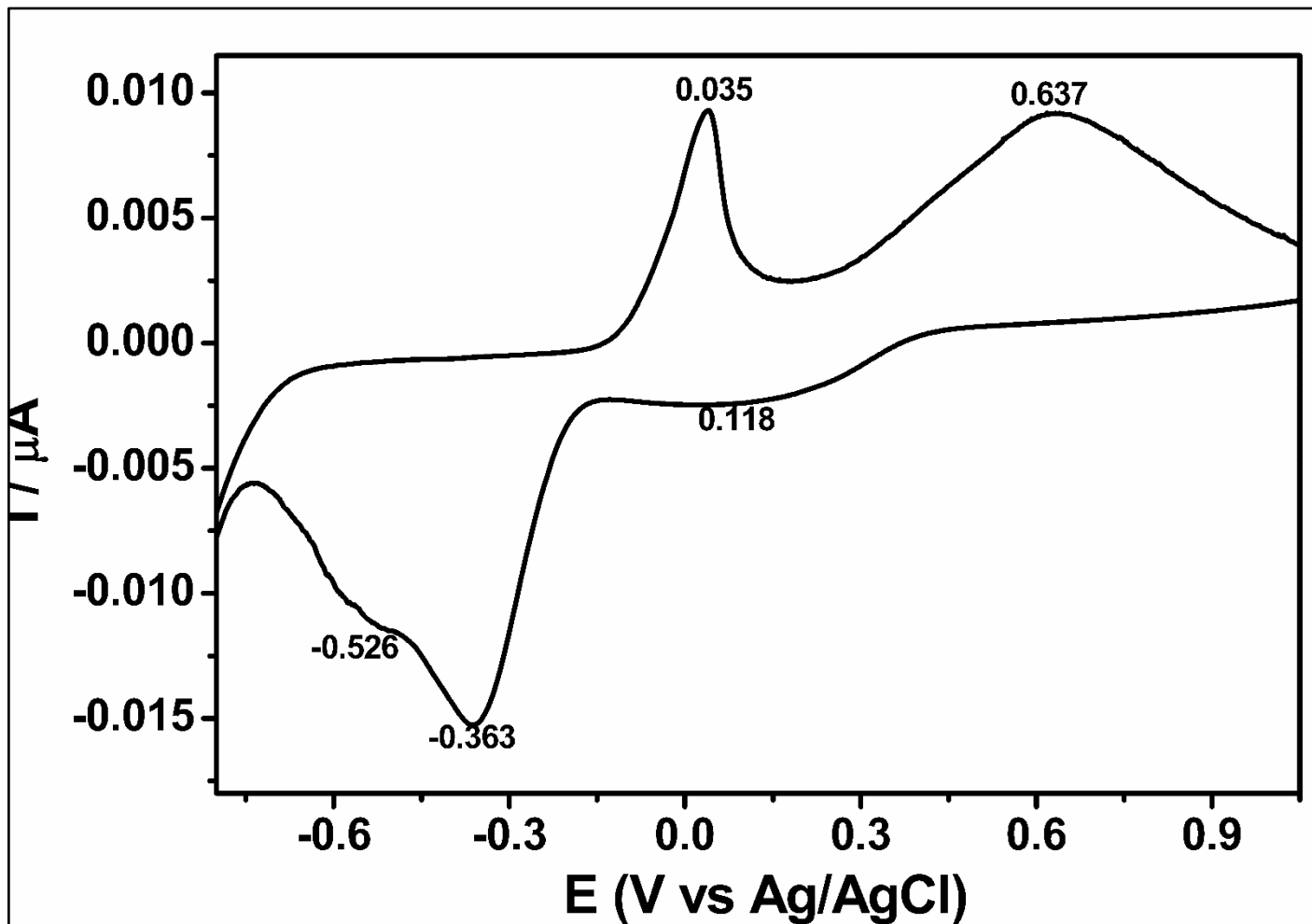


Figure 41: Cyclic voltammetry curve for KT/11/04/22 A

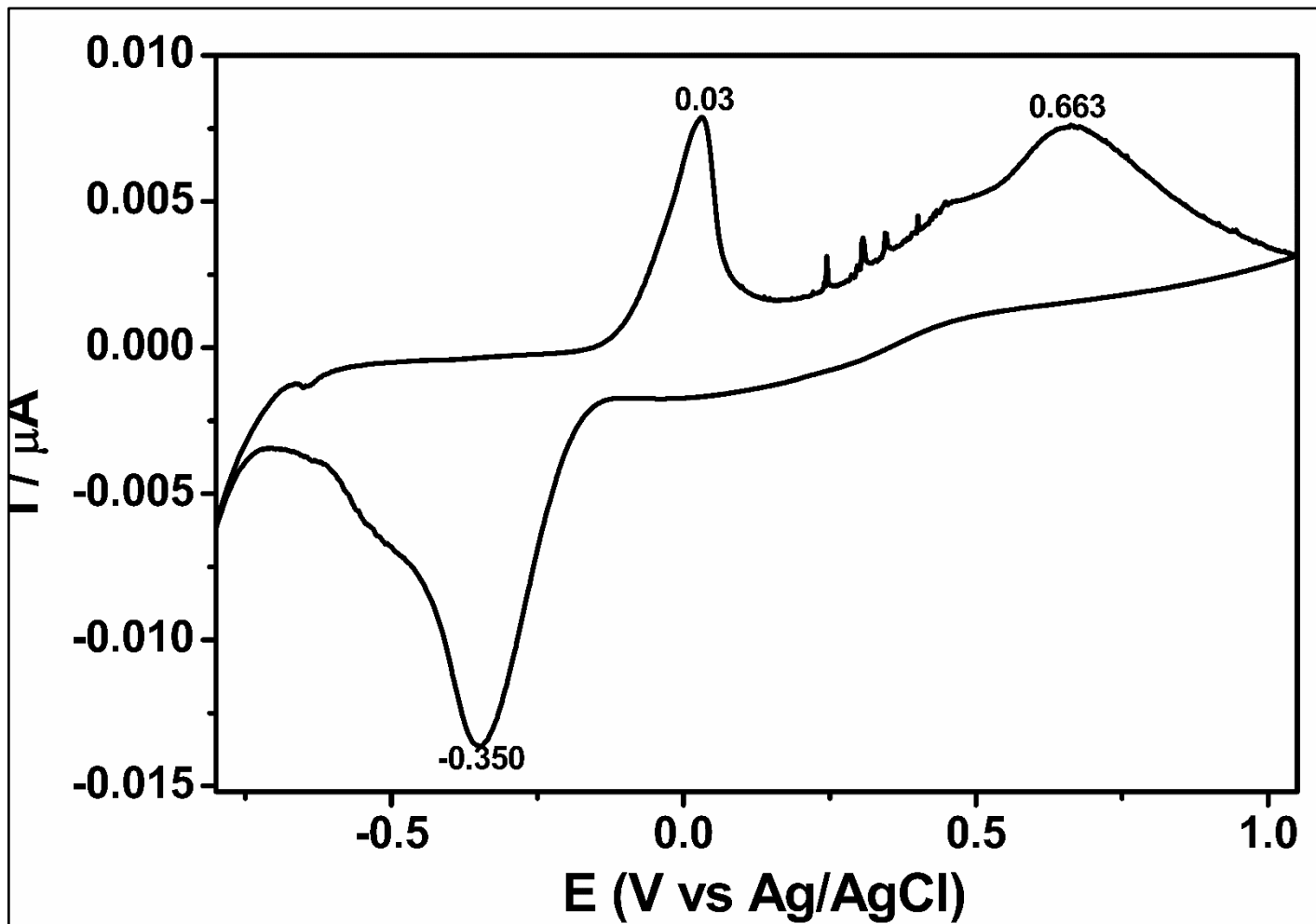


Figure 42: Cyclic voltammetry curve for KT/11/04/22 B

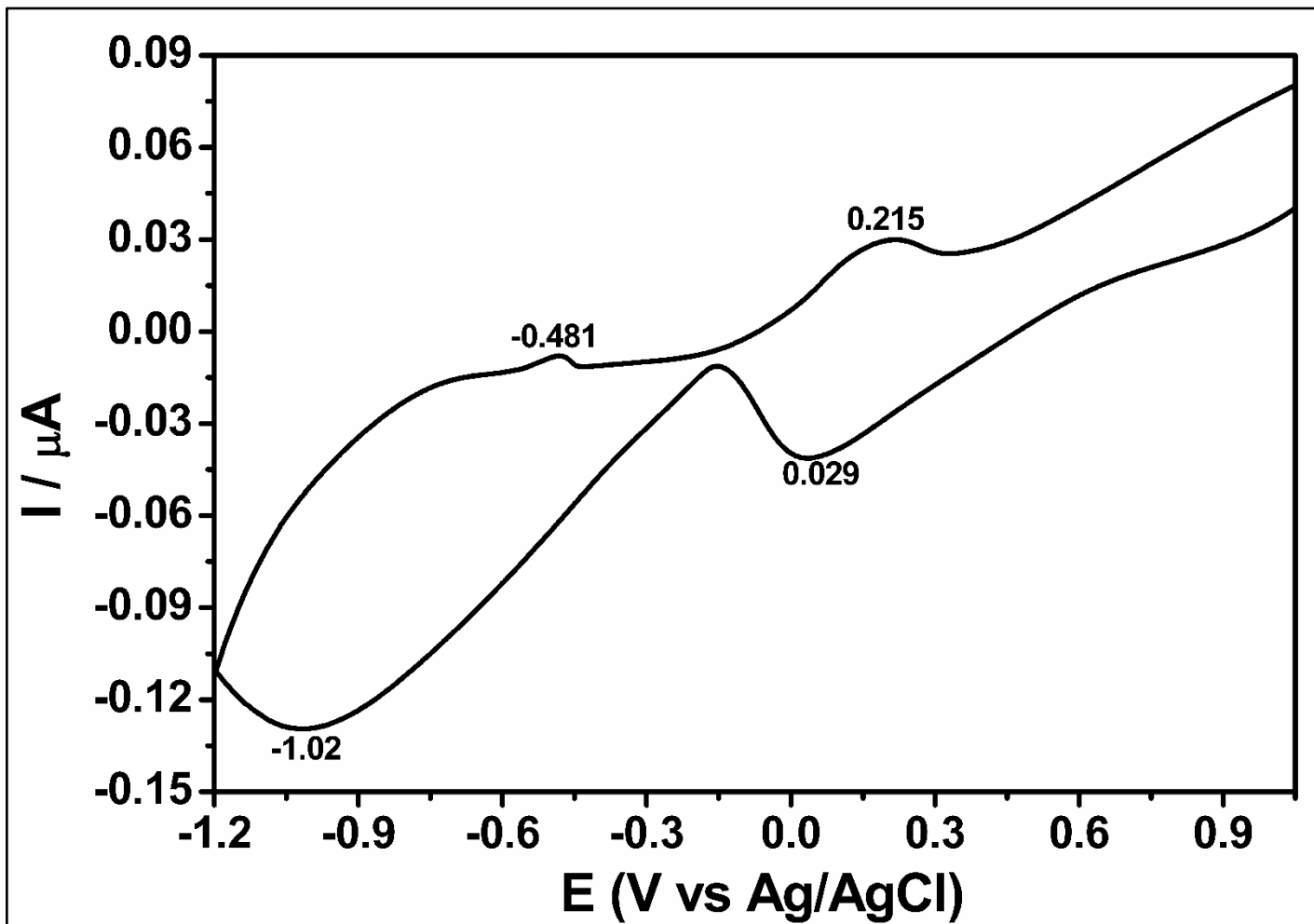


Figure 43: Cyclic voltammetry curve for KT/11/04/22 C

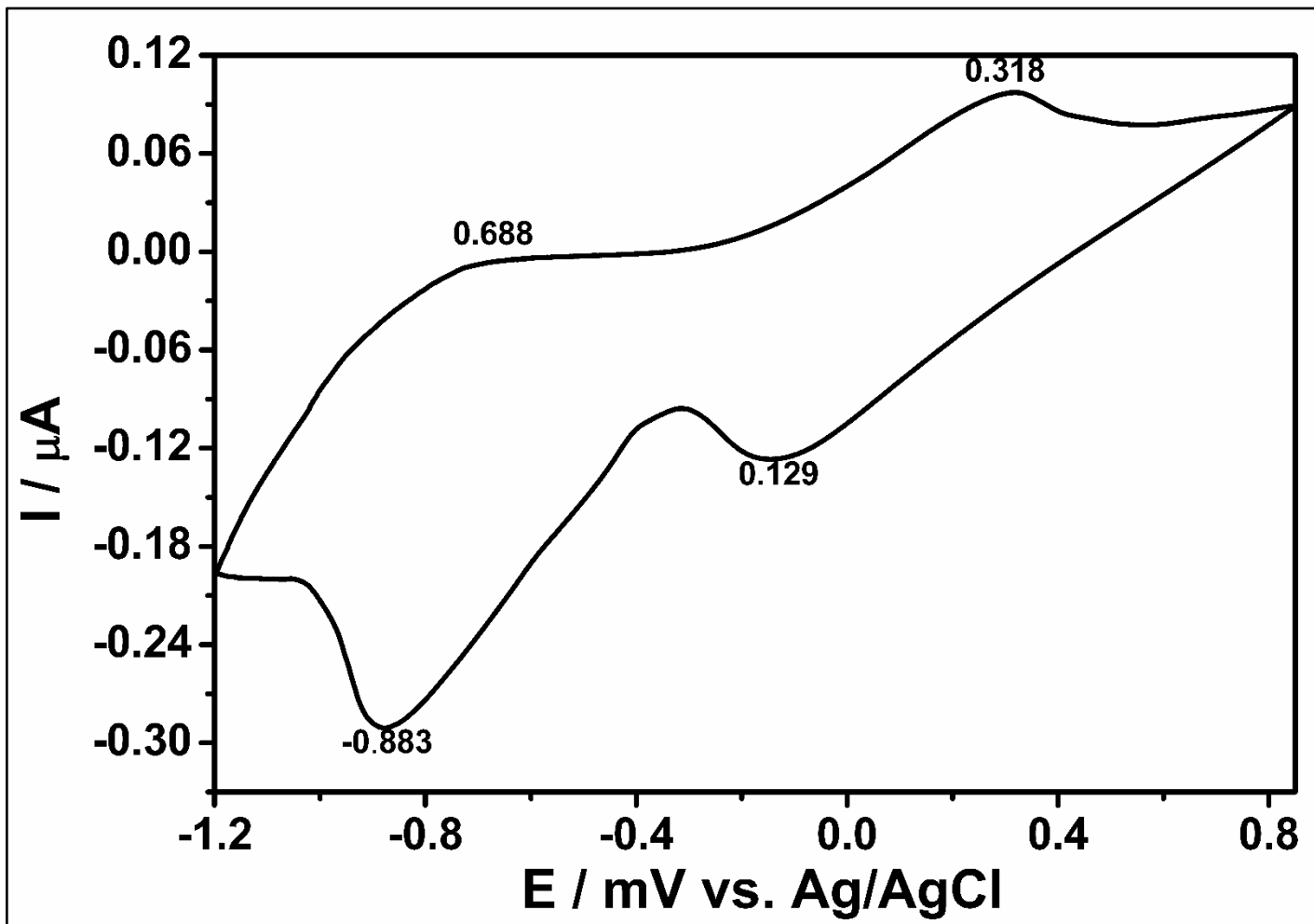


Figure 44: Cyclic voltammetry curve for CuCl

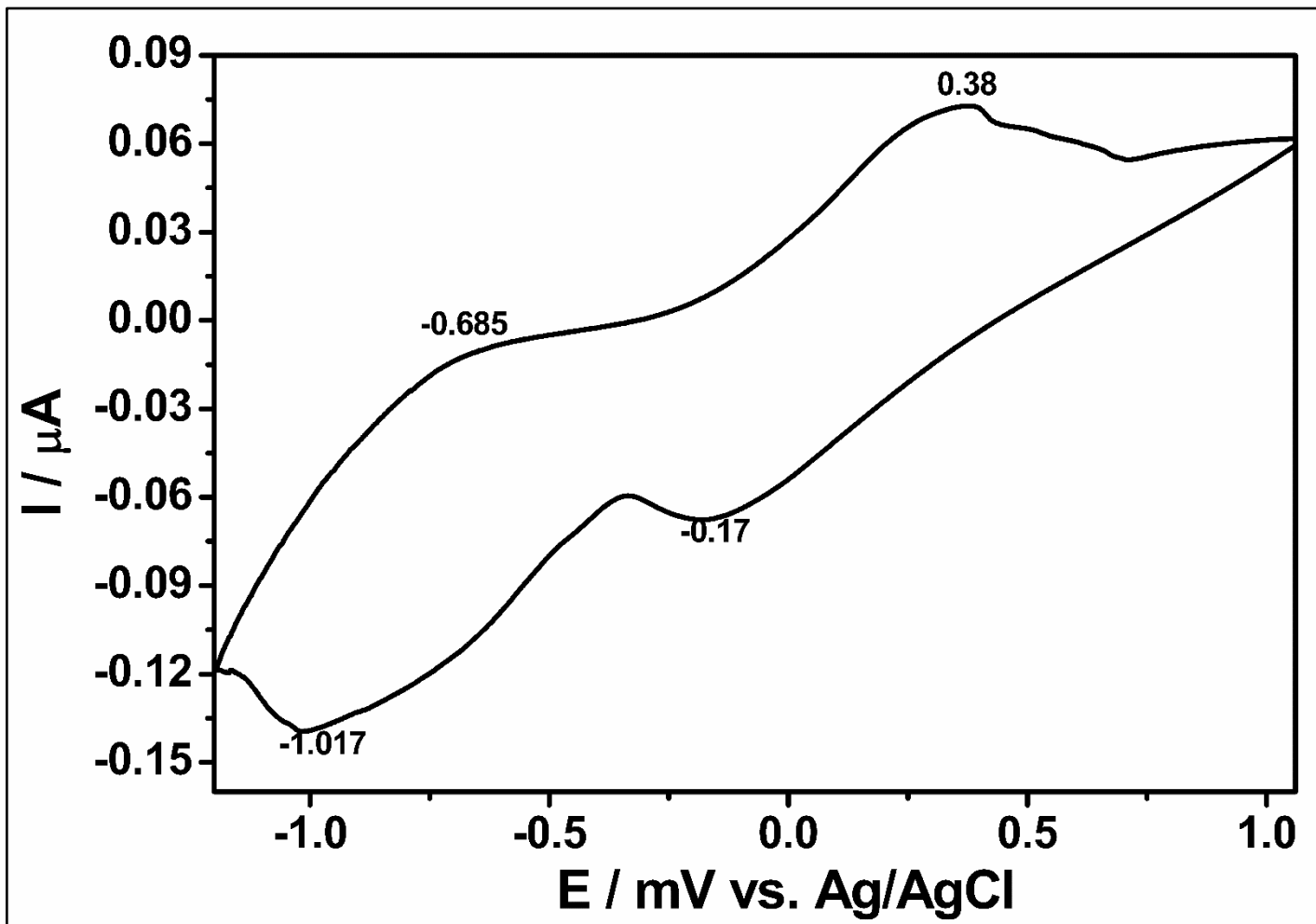


Figure 45: Cyclic voltammetry curve for CuCl_2

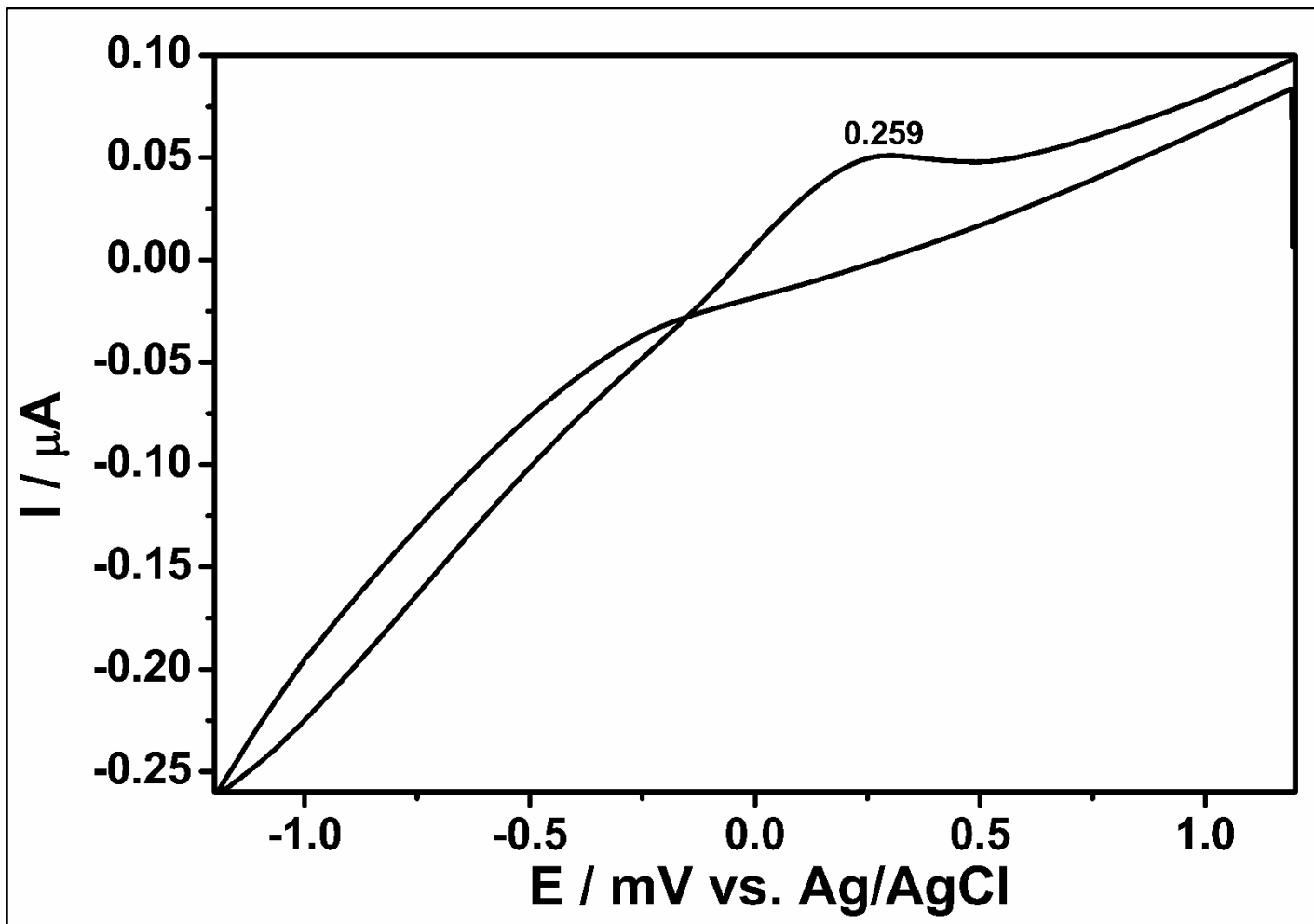


Figure 46: Cyclic voltammetry curve for CuO

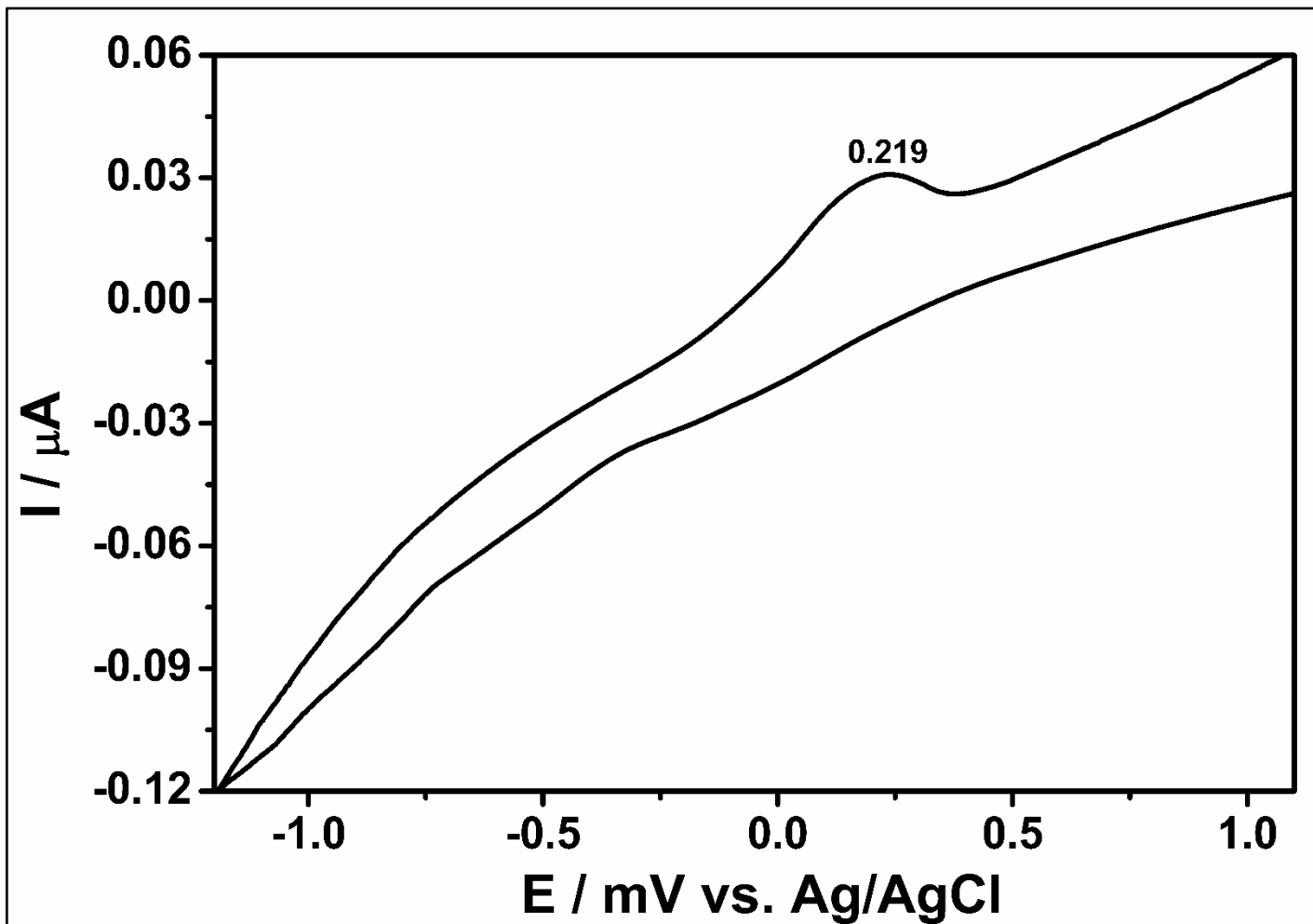


Figure 47: Cyclic voltammetry curve for CuSO_4

Chapter 5

RESULTS AND DISCUSSION

5.1 FT-IR

KT 04/11/05;

Sample A;

The adsorption at around 2920 cm^{-1} and 1628 cm^{-1} were attributed to the C-H and C=C stretching vibration. There is also a tiny dip in the spectra at 2467 cm^{-1} due to the chelate. Infrared spectra 3427 cm^{-1} represents O-H stretching of HSO_4 . Absorption peak at 875 cm^{-1} were due to the Cu-Cl bending. Peak at 1097 cm^{-1} also represents SnO stretching vibration. There is also absorbance peak at wavenumber 1374 cm^{-1} and 1422 cm^{-1} related to SO_4 stretching and it is overlapping with CH_2 and O-H bending.

Sample B;

The adsorption at around 2912 cm^{-1} and 1636 cm^{-1} represents C-H and C=C stretching vibration. In addition, absorbance peak at around 1414 cm^{-1} and 1486 cm^{-1} represents SO_4 stretching and it is overlapping with CH_2 and O-H bending. At peak 1089 cm^{-1} SnO stretching was observed. Peak at 693 cm^{-1} is related to the stretching of the S-O. Peak at 875 cm^{-1} represents Cu-Cl stretching.

Sample C;

There is no meaningful peak due to lack of sampling amount.

KT 04/11/06;

Sample A;

FT-IR spectrum of sample A shows absorbance peak at wavenumbers 3427 cm^{-1} (which is an O-H stretching), at 2920 cm^{-1} (which is C-H stretching) and 2350 cm^{-1} (which represents chelate). The peak at 1390 cm^{-1} is related to O-H bending. Absorbance peak at wavenumber 621 cm^{-1} represents CuO stretching and at 1081 cm^{-1} SnO stretching.

Sample B;

Observation of 3427 cm^{-1} , 2754 cm^{-1} , 1636 cm^{-1} peaks corresponds to the O-H stretching, C-H stretching and C=C stretching, respectively. Moreover, absorbance peak at 2342 cm^{-1} indicates the presence of CN. The sharp peak at wavenumber 1382 cm^{-1} is related to O-H bending, but at wavenumber 1089 cm^{-1} represents SnO and C-O stretching which are overlapping. In addition, occurrence of peaks at 614 cm^{-1} , 527 cm^{-1} and 447 cm^{-1} can represent presence of CuO .

Sample C;

The adsorption at around 3428 cm^{-1} , 2924 cm^{-1} and 1631 cm^{-1} were attributed to the O-H, C-H and C=C stretching vibration, respectively. Absorbance of tiny peak at 2517 cm^{-1} represents chelate. Peak at 1427 cm^{-1} is related to SO_4 stretching vibration. Absorbance at peak 1093 cm^{-1} SnO stretching was observed. The peaks at 874 cm^{-1} represent Cu-Cl bending.

KT/04/11/07;

Sample A;

Absorbance peaks at wavenumbers 3426 cm^{-1} , 2924 cm^{-1} and 1638 cm^{-1} are related to O-H, C-H and C=C double bond stretching, respectively. In addition,

absorbance peak at 2469 cm^{-1} represents chelate. In addition, absorbance peaks at 1379 cm^{-1} and 1093 cm^{-1} represents SO_4 and SnO stretching, respectively. Absorbance at peak 1053 cm^{-1} is related to asymmetric SO_4 stretching where peaks at 878 cm^{-1} and 816 cm^{-1} are related to Cu-Cl bending. Finally, absorbance peak at 678 cm^{-1} represents SO_4 bending.

Sample B;

Absorbance peak at wavenumber 3421 cm^{-1} and 1638 cm^{-1} related to O-H and C=C stretching, respectively. In addition, peaks at 1500 cm^{-1} and 1045 cm^{-1} corresponded to SO_4 and asymmetric SO_4 stretching, respectively. In addition, absorbance peak at wavenumber 874 cm^{-1} represents Cu-Cl stretching.

Sample C;

Absorbance peaks at wavenumbers 3437 cm^{-1} , 2925 cm^{-1} and 1631 cm^{-1} are related to O-H, C-H and C=C double bond stretching, respectively. In addition, absorbance peak at 2363 cm^{-1} represents chelate. Furthermore, peak at wavenumber 1419 cm^{-1} represents SO_4 stretching. Absorbance peaks at 1109 cm^{-1} is related to Sn-O stretching where peak at 881 cm^{-1} represents Cu-Cl bending.

KT/04/11/08

Sample A;

Observation of peak at 3411 cm^{-1} corresponds to the O-H stretching, while absorbance peaks are 2920 cm^{-1} and 1636 cm^{-1} revealed stretching vibration of C-H and C=C. In addition, peak at wavenumber 1390 cm^{-1} shows the existence of SO_4 stretching. Peak at 1057 corresponded to asymmetric SO_4 stretching. Sample C has also Cu-Cl stretching bands between 875 cm^{-1} and 820 cm^{-1} .

Sample B;

Absorbance peaks at wavenumbers 3445 cm^{-1} , 2916 cm^{-1} and 1638 cm^{-1} are related to O-H, C-H and C=C double bond stretching, respectively. In addition, absorbance peak at 2317 cm^{-1} represents chelate. Furthermore, peak at wavenumber 1457 cm^{-1} represents SO_4 stretching. Absorbance peaks at 989 cm^{-1} and 866 cm^{-1} are related to Cu-Cl bending.

Sample C;

Absorbance peaks at wavenumbers 3404 cm^{-1} , 2916 cm^{-1} and 1623 cm^{-1} are related to O-H, C-H and C=C double bond stretching, respectively. Furthermore, peak at wavenumber 1500 cm^{-1} and 1387 cm^{-1} represents SO_4 stretching whereas peak at 1045 cm^{-1} is related to SO_4 asymmetric stretching. Absorbance peaks at 881 cm^{-1} and 817 cm^{-1} are related to Cu-Cl bending.

KT/04/11/10;

Sample A;

Observation of peaks at 3453 cm^{-1} , 2916 cm^{-1} and 1638 cm^{-1} are related to O-H, C-H and C=C double bond stretching, respectively. Finally, peak at wavenumbers 1095 cm^{-1} and 866 cm^{-1} represents Sn-O stretching and Cu-Cl bending, respectively.

Sample B;

Absorbance peaks at wavenumbers 3404 cm^{-1} and 2916 cm^{-1} are related to O-H and C-H stretching, respectively. In addition, absorbance peaks at 1394 cm^{-1} and 1045 cm^{-1} are related to SO_4 and asymmetric SO_4 stretching. Absorbance peak at wavenumber 1101 cm^{-1} corresponds to Sn-O stretching. Finally, 874 cm^{-1} and 817 cm^{-1} wavenumber peaks are related to Cu-Cl bending.

Sample C;

Absorbance peaks at wavenumbers 3445 cm^{-1} , 2916 cm^{-1} and 1638 cm^{-1} are related to O-H, C-H and C=C double bond stretching, respectively. Furthermore, peak at wavenumber 1387 cm^{-1} corresponds to SO_4 stretching whereas peak at 1053 cm^{-1} is related to SO_4 asymmetric stretching. Absorbance peak at 866 cm^{-1} is related to Cu-Cl bending.

KT/04/11/22;

Sample A;

Observation of peaks at 3443 cm^{-1} and 3356 cm^{-1} related to O-H stretching. Furthermore, absorbance peaks at 2920 cm^{-1} , 1644 cm^{-1} and 1390 cm^{-1} corresponds to C-H, C=C double bond and SO_4 stretching, respectively. In addition, absorbance peak at 2358 cm^{-1} represents chelate. Peak at wavenumber 1050 cm^{-1} is related to asymmetric SO_4 stretching whereas 1097 cm^{-1} represents SnO stretching. Finally, absorbance peaks at 875 cm^{-1} and 820 cm^{-1} signifies Cu-Cl stretching and 614 cm^{-1} and 519 cm^{-1} wavenumber peaks indicate C-H bending.

Sample B;

Absorbance peaks at wavenumbers 3451 cm^{-1} , 3356 cm^{-1} and 3316 cm^{-1} are all associated to O-H stretching. Furthermore, absorbance peaks at 2920 cm^{-1} , 1636 cm^{-1} and 1382 cm^{-1} corresponds to C-H, C=C double bond and SO_4 stretching, respectively. In addition, absorbance peak at 2358 cm^{-1} represents chelate. Absorbance peaks at wavenumbers 986 cm^{-1} , 931 cm^{-1} and 820 cm^{-1} are all related to Cu-Cl stretching. Finally, peaks at 614 cm^{-1} , 519 cm^{-1} and 519 cm^{-1} wavenumbers specify C-H bending.

Sample C;

Absorbance peaks at wavenumbers 3404 cm^{-1} and 3319 cm^{-1} are all associated to O-H stretching. Furthermore, peaks at 2920 cm^{-1} and 1389 cm^{-1} wavenumbers correspond to C-H and SO_4 stretching, respectively. Furthermore, peak at wavenumber 1097 cm^{-1} corresponds to Sn-O stretching whereas peak at 1047 cm^{-1} is related to SO_4 asymmetric stretching. Finally, peaks at wavenumbers 878 cm^{-1} and 822 cm^{-1} are all related to Cu-Cl stretching.

5.2 Cyclic Voltammetry

The electrochemical properties of the samples were explored through electrochemical reduction and oxidation measurements using cyclic (CV) solid-state. Electrochemical properties of all the samples in solid-state were investigated using Gamry instruments workstation equipped with a PC computer monitoring Reference 600 Potentiostat/Galvanostat/ZRA system. Redox data from cyclic (CV) voltammetry measurements were recorded using three-electrode system throughout the work, which are working-glassy carbon, counter-platinum wire, and reference-Ag/AgCl electrodes. Prior to use, the surface of the working electrode was polished carefully with 0.05 mm alumina slurry for better precision. Solid-state redox potentials of the samples were recorded in 1 M HCl solution by immobilized microparticles voltammetry technique. All the solid-state electrochemical results were described in Figures 24-45, and Table 10.

The cyclic voltammograms of sample KT/04/11/05 B showed one quasireversible reduction wave (Figure 30), implying the formation of anion at -0.162 V (vs. Ag/AgCl, scan rate: 100 mV s^{-1} , $\Delta E_p = 252\text{ mV}$) and one reversible oxidation peak at 0.284 V (vs. Ag/AgCl, scan rate: 100 mV s^{-1} , $\Delta E_p = 125\text{ mV}$).

The cyclic voltammograms of sample KT/04/11/06 A showed one reversible reduction wave (Figure 31), implying the formation of anion at -0.526 V (vs. Ag/AgCl, scan rate: 100 mV s^{-1} , $\Delta E_p = 94 \text{ mV}$) and one reversible oxidation peak at 0.111 V (vs. Ag/AgCl, scan rate: 100 mV s^{-1} , $\Delta E_p = 68 \text{ mV}$). It is important to note that two more irreversible oxidation peaks are observed for the sample KT/04/11/6 A at 0.574 and 0.752 V (vs. Ag/AgCl, scan rate: 100 mV s^{-1}).

The cyclic voltammograms of sample KT/04/11/07 B showed one irreversible reduction waves (Figure 34), implying the formation of anion at -0.565 V (vs. Ag/AgCl, scan rate: 100 mV s^{-1} , $\Delta E_p = 168 \text{ mV}$) and -0.065 V (vs. Ag/AgCl, scan rate: 100 mV s^{-1}), respectively. Similarly, one reversible and one irreversible oxidation waves observed at 0.203 V (vs. Ag/AgCl, scan rate: 100 mV s^{-1} , $\Delta E_p = 35 \text{ mV}$) and 0.403 V (vs. Ag/AgCl, scan rate: 100 mV s^{-1}), respectively.

The cyclic voltammograms of sample KT/04/11/08 B showed one quasireversible reduction wave (Figure 36), implying the formation of anion at -0.192 V (vs. Ag/AgCl, scan rate: 100 mV s^{-1} , $\Delta E_p = 301 \text{ mV}$) and one quasireversible oxidation wave at 0.306 V (vs. Ag/AgCl, scan rate: 100 mV s^{-1} , $\Delta E_p = 178 \text{ mV}$) s^{-1}), respectively.

The cyclic voltammograms of sample KT/04/11/10 C showed one quasireversible reduction wave (Figure 40), implying the formation of anion at -0.675 V (vs. Ag/AgCl, scan rate: 100 mV s^{-1} , $\Delta E_p = 290 \text{ mV}$) and one quasireversible oxidation wave at 0.393 V (vs. Ag/AgCl, scan rate: 100 mV s^{-1} , $\Delta E_p = 190 \text{ mV}$) s^{-1}),

respectively. Additionally one irreversible oxidation wave is obtained at 0.619 V (vs. Ag/AgCl, scan rate: 100 mV s⁻¹).

The cyclic voltammograms of sample KT/04/11/22 A showed two quasireversible oxidation wave (Figure 41), implying the formation of cation at 0.200 V (vs. Ag/AgCl, scan rate: 100 mV s⁻¹, ΔE_p = 328 mV) and 0.376 V (vs. Ag/AgCl, scan rate: 100 mV s⁻¹, ΔE_p = 519 mV s⁻¹), respectively.

The solid state voltammetry of pure samples CuCl, CuSO₄, CuO and CuCl₂ were investigated carefully. The cyclic voltammograms of CuCl showed one quasireversible reduction wave (Figure 44), implying the formation of anion at -0.785 V (vs. Ag/AgCl, scan rate: 100 mV s⁻¹, ΔE_p = 195 mV) and one quasireversible oxidation wave at 0.223 V (vs. Ag/AgCl, scan rate: 100 mV s⁻¹, ΔE_p = 189 mV s⁻¹), respectively. The cyclic voltammograms of CuSO₄ showed one irreversible oxidation wave (Figure 47), implying the formation of cation at 0.219 V (vs. Ag/AgCl, scan rate: 100 mV s⁻¹). The cyclic voltammograms of CuO showed one irreversible oxidation wave (Figure 44), implying the formation of cation at 0.259 V (vs. Ag/AgCl, scan rate: 100 mV s⁻¹). The cyclic voltammograms of CuCl₂ showed one quasireversible reduction wave (Figure 45), implying the formation of anion at -0.851 V (vs. Ag/AgCl, scan rate: 100 mV s⁻¹, ΔE_p = 332 mV) and one quasireversible oxidation wave at 0.275 V (vs. Ag/AgCl, scan rate: 100 mV s⁻¹, ΔE_p = 275 mV). We couldn't measure the cyclic voltammetry of pure SnO. Importantly, one sharp cathodic peak at -0.807 V in the negative scan with shoulders at 0.585 V and -0.927 V has been confirmed in the literature for SnO (Šatović et al., 2010).

Table 10: Cyclic voltammetry data of samples and reference compounds in solid state

SAMPLE	E_{pc}^a (V) vs.		E_{pa}^b (V)	ΔE_p^c (mV)	$E_{1/2}^d$ (V) vs. Ag/AgCl ^f	Corrosion products
	Ag/AgCl ^f	SCE ^g				
KT 04/11/05B	-0.036	(-0.081)	-0.288	252	-0.162	CuCl₂
	0.346	(0.301)	0.221	125	0.284	
KT 04/11/06A	-0.479	(-0.521)	-0.573	94	-0.526	Cu₂O SnO
	0.145	(0.100)	0.077	68	0.111	
	0.574	(0.529)	-	-	0.574	
	0.751	(0.706)	-	-	0.751	
KT 04/11/07B	-0.481	(-0.526)	-0.649	168	-0.565	CuSO₄ CuCl
	-0.065	(-0.110)	-	-	-0.065	
	0.220	(0.175)	0.185	35	0.203	
	0.403	(0.358)	-	-	0.403	
KT 04/11/08B	-0.041	(-0.086)	-0.342	301	-0.192	CuCl
	0.395	(0.350)	0.217	178	0.306	
KT 04/11/10C	-0.011	(-0.056)	-0.391	290	-0.675	CuCl₂ SnO
	0.393	(0.348)	0.203	190	0.298	
	0.619	(0.574)	-	-	-	
KT 04/11/22A	0.035	(-0.010)	-0.363	328	0.200	SnO
	0.637	(0.592)	0.118	519	0.376	
CuCl	-0.688	(-0.733)	-0.883	195	-0.785	
	0.318	(0.273)	0.129	189	0.223	
CuSO ₄	0.219	(0.174)	-	-	0.219	
CuO	0.259	(0.214)	-	-	0.259	
CuCl ₂	-0.685	(-0.730)	-1.017	332	-0.851	
	0.380	(0.335)	-0.17	210	0.275	

^a E_{pc} : cathodic potential.

^b E_{pa} : anodic potential.

^c ΔE_p : peak potential separations.

^e $E_{red, onset}$: reduction potential onset.

^d $E_{1/2, red}$: reduction half wave potential (reversible)

^f Ag/AgCl: silver/silver chloride reference electrode.

^g $E(Ag/AgCl) + (-0.045) = E(SCE)$

We couldn't measure the cyclic voltammetry of pure SnO. Importantly, one sharp cathodic peak at -0.807 V in the negative scan with shoulders at 0.585 V and -0.927 V has been confirmed in the literature for SnO (Šatović et al., 2010).

In summary, we have compared the similarities of the pure compounds with our samples in order to decide for the corrosion compounds. At the same time we have used the flowchart given in the literature (Šatović et al., 2010).



In addition, infrared spectrum results of, KT 04/11/05 B (Figure 13) where the wavenumber 875 cm^{-1} represents Cu-Cl stretching; KT 04/11/06 A (Figure 14) where the absorbance peak at wavenumber 621 cm^{-1} represents CuO and at 1081 cm^{-1} SnO stretching; KT 04/11/07 B (Figure 18) where peaks at 1378 cm^{-1} and 1045 cm^{-1} corresponded to SO_4 and asymmetric SO_4 stretching and 874 cm^{-1} represents Cu-Cl stretching; KT 04/11/08 B (Figure 21) where the absorbance peaks at 989 cm^{-1} and 866 cm^{-1} are related to Cu-Cl stretching; KT 04/11/22 A (Figure 26) where the peak at 1097 cm^{-1} represents SnO stretching have provided verifying of corrosion products has given in Table 10.

Finally, we have identified the corrosion compounds based on CuCl_2 (in KT/04/11/05 B and KT/04/11/10 C), Cu_2O (in KT/04/11/06 A), SnO (in KT/04/11/06 A), CuSO_4 (in KT/04/11/07 B), CuCl (in KT/04/11/07 B and KT/04/11/08 B) and SnO in (KT/04/11/10 C and KT/04/11/22 A).

Results of corrosion product types of all samples were performed by cyclic voltammetry and/or infrared spectroscopy is given in Table 11.

Table 11: Corrosion product types of all samples ⁵

Sample No.	A	B	C
KT 04/11/05	Copper sulphate Copper chloride	<i>CuCl₂</i>	—
KT 04/11/06	<i>Cu₂O</i> <i>SnO</i>	Tin oxide Copper oxide	Tin oxide Copper sulphate
KT 04/11/07	Tin oxide Copper chloride Copper sulphate	<i>CuSO₄</i> <i>CuCl</i>	Copper sulphate Copper chloride
KT 04/11/08	Copper chloride Copper sulphate	<i>CuCl</i>	Tin oxide Copper chloride Copper sulphate
KT 04/11/10	Tin oxide	Tin oxide Copper sulphate Copper chloride	<i>CuCl₂</i> <i>SnO</i>
KT 04/11/22	<i>SnO</i>	Copper sulphate Copper chloride	Copper sulphate Copper chloride

⁵  cyclic voltammetry
 infrared spectroscopy

In summary, 4 different corrosion product types (copper chloride, copper sulphate, copper oxide and tin oxide) is detected on selected 6 bronze bowls according to the infrared spectroscopy and cyclic voltammetry results (Figure 48).

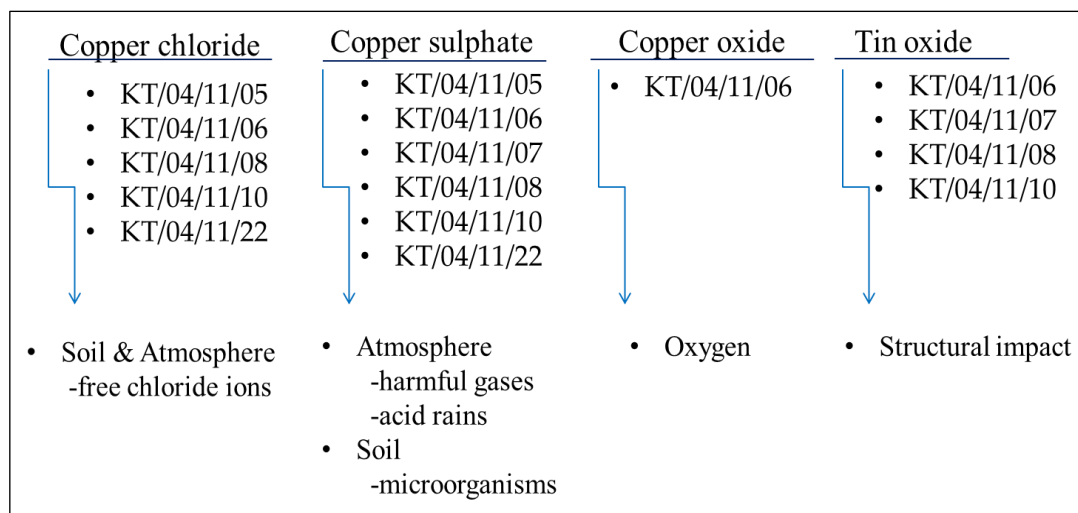


Figure 48: Selected bowls' main corrosion types and possible causes

Ph, humidity and temperature affect all kind of corrosion process. However, existing of copper chloride corrosion products depend on free chloride ions and these free chloride ions are caused by soil and/or atmosphere. Copper sulphates are mostly seen on the artifacts which exposed directly atmosphere and rarely seen bronzes which are buried. Generally, sulphate reducing bacterias are causes of copper sulphate corrosion products for buried artifacts. Oxygen is one of the reason copper oxides and tin oxides although tin oxides are result of structural impact, especially for high tin bronzes.

When Kral Tepesi Late Bronze Age Hoard was found in 2004, it was almost at the surface due to the constant erosion on soil of the location. According to this circumstances, it is known that the hoard went through period below ground and after that a period near the surface. Moreover, the absence of soil in the pithos where

hoard is located indicates that the artifacts were exposed to soil affect indirectly, not directly. In addition, the proximity of the Kral Tepesi settlement to the sea indicates the artifacts are exposed to free chloride and sulphate ions in the surface period and in the buried period they exposed to the water-soluble salts which in the soil affected the artifacts with rainwater. Furthermore, copper sulphate products are also likely to occur in period when the bronzes are in direct contact with the atmosphere.

Chapter 6

CONCLUSION

This study investigated the degradation of bronze artifacts and their possible causes. For this aim, material characterization of bronze samples obtained from Kaleburnu Bronze Hoard 2004 was performed on cyclic voltammetry and infrared spectroscopy.

Analysis results prove that deterioration of copper alloy artifacts on every and each sample, even taken from same bowl, has different structure. Electrochemical investigations were done by cyclic voltammetry to understand the degradation of copper and copper alloy artifacts as the most observed corrosion process is formed by electrochemical corrosion types.

Material characterization and corrosion elements of patinas were evaluated by FTIR analysis results. FTIR analysis results performed on copper and copper alloy samples has shown the degradation type of complex structured corrosion products. Moreover, each type of patina will continue to perform different reactions depending on its chemical structure.

Importance of investigating the characterizations of copper and copper alloys with different chemical ways that are confirmative of each other is to determine protection methods.

REFERENCES

- Bachmann, H. G. (2016). *The identification of slags from archaeological sites*.
London: Institute of Archaeology.
- Barnard, N. (1961). *Bronze casting and bronze alloys in ancient China*. Canberra:
Australian National University.
- Bartelheim, M., Kizilduman, B., Müller, U., Pernicka, E., & Tekel, H. (2008). The
Late Bronze Age Hoard of Kaleburnu/Galinoporni on Cyprus. *Památky*
Archeologické, 99, 161-188.
- Bartelheim, M., Behrendt S., Kizilduman, B., Müller, U., Pernicka, E. (2011). *The*
Treasure from King's Mountain, Kaleburnu/Galinoporni, Cyprus. A
Manifestation of International Bronze Age Sea Trade in the Eastern
Mediterranean. International Symposium Anatolian Metal V. Frühe
Rohstoffgewinnung in Anatolien und seinen Nachbarländern. Deutsches
Bergbau-Museum Bochum. Anatolian Metal V, Der Anschnitt, Beiheft
24: 91-110.
- Berger, D. (2012). *Bronzezeitliche Färbetechniken an Metallobjekten nördlich der*
Alpen: Eine archäometallurgische Studie zur prähistorischen Anwendung von
Tauschierung und Patinierung anhand von Artefakten und Experimenten.
Halle an der Saale: Landesamt für Denkmalpflege und Archäologie Sachsen-
Anhalt, Landesmuseum für Vorgeschichte.

Bettembourg, J. M. (1993). *Examen et analyse des processus de corrosion des vitraux anciens. In 2nd international conference on non-destructive testing, microanalytical methods and environment evaluation for study and conservation of works of art, Perugia 17-20 April 1988.* (1.1-1.15). Rome: Comas Grafica.

Biestek, T., & Drys, M. (1974). *Corrosion products formed on copper in various corrosive environments.* *Powloki Ochronne*, 6 (3), 21-27.

Buchholz, H. (1967). *Analysen prihistorischer Metallfunde aus Zypern und den Nachbarländern.* *Berliner Jahrbuch für Vor- und Frühgeschichte* 7: 189- 256.

Caley, E. R., Chang, I. S. M., & Woods, N. P. (1979). *Gravimetric and Spectrographic Analysis of Some Ancient Chinese Copper Alloys.* *Ars orientalis*, 11, 183-193.

Chase, W. T. (1994). *Chinese bronzes: casting, finishing, patination and corrosion.* In D. A. Scott., J. Podany & B. B. Considine, *Ancient and historic metals: conservation and scientific research. Proceedings of a symposium on Ancient and Historic Metals organized by the J. Paul Getty Museum and the Getty Conservation Institute, November 1991 (85-11), Marina del Rey, Calif: Getty Conservation Institute.*

Courcier, A. (2014). *Ancient metallurgy in the Caucasus from the sixth to the third millennium BCE.* In B. W. Roberts & C. P. In Thornton, *Archaeometallurgy*

in global perspective: Methods and syntheses (579-664). New York: Springer.

Cramer, S. D., & Covino, B. S. (1992). *ASM Handbook Volume 13 Corrosion*. ASM International Handbook Committee. Ohio: Materials Park.

Cronyn, J. (1990). *Elements of Archaeological Conservation*. London: Routledge.
<https://doi.org/10.4324/9780203169223> (Original Work 1990).

Dana, J.D. (1951). *Dana's Manuel of Mineralogy*. 7ed., John Wiley and Sons Inc. New York

Daubree, M. (1875). *Exemples de formation contemporaine de la pyrite de fer, dans des sources thermales et dans de l'eau de mer*. CR Acad. Sci., Paris, 81, 854-859.

Davy, J. (1826). *III. Observations on the changes which have taken place in some antient alloys of copper*. By John Davy, MDFRS In a letter to Sir Humphry Davy. Philosophical Transactions, 116, 55-59.

Derrick, M. R., Stulik, D., & Landry, J. M. (2000). *Infrared spectroscopy in conservation science*. Los Angeles: Getty Conservation Institute.

Di Carlo, G., Giuliani, C., Riccucci, C., Pascucci, M., Messina, E., Fierro, G., Lavorgna, M. & Ingo, G. M. (2017). *Artificial patina formation onto copper-*

based alloys: chloride and sulphate induced corrosion processes. Applied Surface Science, 421 (Part A), 120-127.

Dillmann, P., Béranger, G., Piccardo, P., & Matthiessen, H. (2014). *Corrosion of metallic heritage artefacts: investigation, conservation and prediction of long term behaviour* (Vol. 48). Elsevier:Woodhead Publishing.

Doménech-Carbó, A., Doménech-Carbó, M. T., & Costa, V. (2009). *Electrochemical methods in archaeometry, conservation and restoration*. Springer Science & Business Media.

Eggert, G., Weichert, M., Euler, H., & Barbier, B. (2004). *Some news about 'black spots'*. Proceedings of Metals.Canberra, Australia, 142 – 148.

Ehsani, A. *Anadolu'da Bakır Madenciliği ve Kullanımının Kısa Tarihçesi*. (2016).MT Bilimsel, 9, 43-48.

Escalante, E. (1989). *Concepts of underground corrosion*. In V. Chaker and J. Palmer, *Effects of Soil Characteristics on Corrosion* (81-94), West Conshohocken, PA: ASTM International.

Esin, U. (1969). *Kuantitatif spektral analiz yardımıyla Anadolu'da başlangıcından Asur kolonileri çağına kadar Bakır ve Tunç madenciliği:(metin, kataloglar, resim ve haritalar)*. İstanbul: İstanbul Üniversitesi Edebiyat Fakültesi Yayınları.

European Federation of Corrosion, & Institute of Materials (London. (1992). *A Working party report on microbiological degradation of materials--and methods of protection*. (No. 9). Woodhead Pub Ltd.

Faltermeier, R. (1995). *The evaluation of corrosion inhibitors for application to copper and copper alloy archaeological artefacts*.(unpublished doctoral dissertation). University of London, London.

Feitknecht, W., & Maget, K. (1949). *Zur Chemie und Morphologie de basischen Salze zweiwertiger Metalle XIV. Die Hydroxychloride des Kupfers*. *Helvetica Chimica Acta*, 32 (5), 1639-1653.

Forbes, R. J. (1950). *Metallurgy in antiquity: a notebook for archaeologists and technologists*. Leiden: Brill.

Franey, J. P., & Davis, M. E. (1987). *Metallographic studies of the copper patina formed in the atmosphere*. *Corrosion Science*, 27 (7), 659-668.

Frost, R. L. (2003). *Raman spectroscopy of selected copper minerals of significance in corrosion*. *Spectrochimica acta Part A: molecular and biomolecular spectroscopy*, 59 (6), 1195-1204.

Gadzhiev, M. G., & Korenevskii, S. N. (1984). *Metall Velikentskoi katakomby. Drevnie Promysly, Remeslo i Torgovyla v Dagestane*, 7-27.

- Gale, N. H. (1991). *Metals and metallurgy in the Chalcolithic period*. Bulletin of the American Schools of Oriental Research, 282 (1), 37-61.
- Gale, N. H., & Stos-Gale, Z. A. (1985). *Lead isotope analysis and Alashiya: 3*. Report of the Department of Antiquities Cyprus, 83-99.
- Gale, N. H., & Stos Gale, Z. A. (1982). *Bronze Age Copper Sources in the Mediterranean: A New Approach*. Science 216. No:4541
- Gettens, R. J. (1970). *Patina: noble and vile*. In Art and technology. A symposium on classical bronzes. Cambridge: MIT Press.
- Ghoniem, M. (2011). *The Characterization Of A Corroded Egyptian Bronze Statue And A Study Of The Degradation Phenomena*. International Journal of Conservation Science, 2 (2), 95-108.
- Gnesin, G. G. (2015). *Metals and alloys of the Bronze Age: from middle to modern times. I. Copper and its alloys*. Powder Metallurgy and Metal Ceramics, 53 (9-10), 610-618.
- Graedel, T. E. (1987). *Copper patinas formed in the atmosphere—II. A qualitative assessment of mechanisms*. Corrosion Science, 27 (7), 721-740.

- Graedel, T. E. (1987). *Copper patinas formed in the atmosphere—III. A semi-quantitative assessment of rates and constraints in the greater New York metropolitan area*. *Corrosion Science*, 27 (7), 741-769.
- Greenwood, N. N., & Earnshaw, A. (2012). *Chemistry of the Elements*. Elsevier.
- Heritage, E. (2008). *Investigative Conservation: Guidelines on How the Detailed Examination of Artefacts From Archaeological Sites can Shed Light on Their Manufacture and Use*. Swindon: English Heritage Publishing.
- Hodges, H. W. (1964). *Artifacts. An introduction to early materials and technology*. John Baker. London, United Kingdom.
- Holden, N. E., & Holden, N. E. (2019). *History of the origin of the chemical elements and their discoverers* (No. BNL-211891-2019-COPA). Brookhaven National Lab.(BNL), Upton, NY (United States).
- Kassianidou, V. (2012). *Natural Resources and the Importance of Copper*. *Ancient Cyprus: Cultures in Dialogue*, 76-77.
- Kızılduman, B. (2000). *Erken-Orta Kıbrıs Çağı Madenciliği Işığında İncesu Kurtarma Kazısı Tunç Eserleri*. Yüksek Lisans Tezi, Hacettepe Üniversitesi.
- Kızılduman, B. (2017). *Kıbrıs'ta Kaleburnu-Kral Tepesi/ Galinoporni-Vasılı'de Dikkate Değer Bir Geç Tunç Çağı Yapısı*. *Olba*, 25, 113.

- Knapp, A. B. (1985). *Alashiya, Caphtor/Keftiu, and Eastern Mediterranean Trade: Recent Studies in Cypriote Archaeology and History*. *Journal of Field Archaeology*, 12, 2, 231-250.
- Knapp, A. B. (1986). *Production, Exchange, And Socio-Political Complexity On Bronze Age Cyprus 1*. *Oxford Journal of Archaeology*, 5 (1), 35-60.
- Knapp, A. B. (2003). *The Archaeology of Community on Bronze Age Cyprus: Politiko" Phorades" in Context*. *American Journal of Archaeology*, 107 (4), 559-580.
- Knotkova, D., & Kreislova, K. (2007). *Atmospheric corrosion and conservation of copper and bronze. Environmental deterioration of materials*. WIT Press, Southampton, 107-142.
- Koltai, O. (1984). *Római kori hagymafejes exüst fibula restaurálása*. *Muzeumi Műtárgyvédelem*, 13, 275-284.
- Komkov, A. I., & Nefedov, E. I. (1967). *Posnjakite, a new mineral*. *Zapiski Vsesoyuznogo Mineralogicheskogo Obschestva*, 96, 58-62.
- Krapchev, T. A. (1976). *Literary survey on corrosion and corrosion products of copper and bronze observed in ancient artifacts* (Unpublished doctoral dissertation). Cambridge: Massachusetts Institute of Technology.

- La-Niece, S. (Ed.). (2013). *Metal plating and patination: cultural, technical and historical developments*. Elsevier.
- Little, B. J., & Lee, J. S. (2007). *Microbiologically influenced corrosion* (Vol. 3). John Wiley & Sons.
- MacLeod, I. D. (1981). *Bronze disease: an electrochemical explanation*. ICCM Bulletin, 7 (1), 16-26.
- Marabelli, M. (1994). *The monument of marcus aurelius: Research and conservation*. In D. A. Scott., J. Podany & B. B. Considine, Ancient and historic metals: conservation and scientific research. Proceedings of a symposium on Ancient and Historic Metals organized by the J. Paul Getty Museum and the Getty Conservation Institute, November 1991 (1-19). Marina del Rey, Calif: Getty Conservation Institute.
- Mattsson, E., Nord, A. G., Tronner, K., Fjaestad, M., Lagerlof, A., Ullen, I., & Borg, G. C. (1996). *Deterioration of Archaeological Material in soil, Rik 10*. Central Board of National Antiquities), Stockholm, Sweden, 50.
- Mazzeo, R., & Joseph, E. (2005). *The Use Of Ftir Micro-Atr Spectroscopy And Ftir-Mapping For The Surface Characterisation Of Bronze Corrosion Products*. In Proceedings of Art'05, 8th International Conference on Non-Destructive Investigation and Microanalysis for the Diagnostics and Conservation of Cultural and environmental Heritage.

- McNeil, M. B., & Little, B. J. (1999). *The use of mineralogical data in interpretation of long-term microbiological corrosion processes: sulfiding reactions*. *Journal of the American Institute for Conservation*, 38 (2), 186-199.
- Meeks, N. (1993). *Patination phenomena on Roman and Chinese high-tin bronze mirrors and other artefacts*. In *Metal plating and patination* (63-84). Butterworth-Heinemann.
- Memet, J. B. (2007). *The corrosion of metallic artefacts in seawater: descriptive analysis*. In *Corrosion of Metallic Heritage Artefacts* (152-169). Woodhead Publishing.
- Moncmanová, A. (2007). *Environmental factors that influence the deterioration of materials*. *Environmental Deterioration of Materials* (1-21). Southampton, Boston: WITPress.
- Moorey, P. R. S. (1994). *Ancient mesopotamian materials and industries: the archaeological evidence*. Oxford: Clarendon Press.
- Muros, V., & Scott, D. A. (2018). *The occurrence of brochantite on archaeological bronzes: a case study from Lofkënd, Albania*. *Studies in Conservation*, 63 (2), 113-125.
- Novák, P. (2007). *Environmental deterioration of metals*. *Environmental Deterioration of Materials* (21-27). Southampton, Boston: WITPress.

- Organ, R. M. (1963). *Aspects of bronze patina and its treatment*. *Studies in conservation*, 8 (1), 1-9.,
- Özen, L. (1999). “*Bronz Kanseri Hastalığı*”, 1. Ulusal Taşınabilir Kültür Varlıkları Konservasyonu ve Restorasyonu Kolokyumu, 177-184, Ankara.
- Quaranta, M. (2009). *On the degradation mechanisms under the influence of pedological factors through the study of archeological bronze patina* (Unpublished doctoral dissertation). Alma Mater Studiorum Università di Bologna.
- Panayiotou, A. (1980). *Cu-Ni-Co-Fe sulphide mineralization, Limassol Forest, Cyprus*. Ophiolites: Proceedings, International Ophiolite Symposium, Cyprus, 1979. Nicosia], Cyprus: Republic of Cyprus, Ministry of Agriculture and Natural Resources, Geological Survey Dept.
- Payer, J. H. (1992). *Bronze corrosion: rates and chemical processes*. In Terry Drayman-Weisser, *The conservation of bronze sculpture in the outdoor environment: a dialogue among conservators, curators, environmental scientists, and corrosion engineers* (103-121).
- Piccardo, P., Mille, B., & Robbiola, L. (2007). *Tin and copper oxides in corroded archaeological bronzes*. In P. Dillmann et al., *Corrosion of Metallic Heritage Artefacts* (239-262). Cambridge: Woodhead Publishing.

- Rapp Jr, G. (1982). *Native copper and the beginning of smelting: chemical studies*. Early metallurgy in Cyprus, 4000-500 BC. Nicosia: publisher not identified.
- Reale, R., Plattner, S. H., Guida, G., Sammartino, M. P., & Visco, G. (2012). *Ancient coins: cluster analysis applied to find a correlation between corrosion process and burial soil characteristics*. Chemistry Central Journal, 6 (2), S9.
- Revie, R. W. (2008). *Corrosion and corrosion control: an introduction to corrosion science and engineering*. New Jersey: John Wiley & Sons.
- Robbiola, L., & Portier, R. (2006). *A global approach to the authentication of ancient bronzes based on the characterization of the alloy–patina–environment system*. Journal of Cultural Heritage, 7 (1), 1-12.
- Rodgers, B. A. (2004). *The archaeologist's manual for conservation: a guide to non-toxic, minimal intervention artifact stabilization*. Springer Science & Business Media.
- Rotaru, I., Mada, M., & Fazecaş, M. (2010). *Corrosion And Anti- Corrosion Protection Of Archeological Bronze Artifacts*. Annals Of The Oradea University. Fascicle of Management and Technological Engineering, IX (XIX), NR2, 3.237 -3.241.
- Sawada, M. (1979). *Non-destructive X-ray fluorescence analysis of ancient bronze mirrors excavated in Japan*. Ars Orientalis, 195-213.

- Schweizer, F. (1994). *Bronze objects from lake sites: from patina to " biography."*. In D. A. Scott., J. Podany & B. B. Considine, Ancient and historic metals: conservation and scientific research: proceedings of a symposium organized by the J. Paul Getty Museum and the Getty Conservation Institute, November 1991 (33-50). Marina del Rey, Calif: Getty Conservation Institute.
- Scott, D. A. (1997). *Copper compounds in metals and colorants: Oxides and hydroxides*. *Studies in conservation*, 42 (2), 93-100.
- Scott, D. A. (2002). *Copper and bronze in art: corrosion, colorants, conservation*. Getty publications.
- Scott, D. A., & Maish, J. P. (2010). *A Lydian Bed of Iron, Bronze and Copper- Technical Examination of a Metallurgical Masterpiece*. *Studies in conservation*, 55(1), 3-19.
- Serghini-Idrissi, M., Bernard, M. C., Harrif, F. Z., Joiret, S., Rahmouni, K., Srhiri, A., Takenouti, H., Vivier, V. & Ziani, M. (2005). *Electrochemical and spectroscopic characterizations of patinas formed on an archaeological bronze coin*. *Electrochimica Acta*, 50 (24), 4699-4709.
- Souissi, N., Bousselmi, L., Khosrof, S., & Triki, E. (2004). *Voltammetric behaviour of an archeological bronze alloy in aqueous chloride media*. *Materials and Corrosion*, 55 (4), 284-292.

- Stambolov, T., & Stambolov, T. (1985). *The corrosion and conservation of metallic antiquities and works of arts*. Amsterdam: Central research laboratory for objects of art and Science.137-146
- Steel, L. (2014). *Cyprus during the Late Bronze Age*. In Margreet L. & Ann E. Killebrew, *The Oxford Handbook of the Archaeology of the Levant c.8000-332 BCE (577-595)*. Oxford: Oxford University Press.
- Šatović, D., Martinez, S., & Bobrowski, A. (2010). Electrochemical identification of corrosion products on historical and archaeological bronzes using the voltammetry of micro-particles attached to a carbon paste electrode. *Talanta*, 81(4-5), 1760-1765.
- Stos-Gale, Z. A., & Gale, N. H. (2010). *Bronze Age metal artefacts found on Cyprus-metal from Anatolia and the Western Mediterranean*. *Trabajos de prehistoria*, 67 (2).
- Tansuğ, G. (2016). *Bronz Yapıtların Atmosferik Korozyonunda Hava Kirleticilerin Etkisi ve İnhibitörle Korunması*. Çukurova Üniversitesi Mühendislik-Mimarlık Fakültesi Dergisi, 31(2), 401-414.
- Tennent, N. H., & Antonio, K. M. (1981). *Bronze disease: synthesis and characterisation of botallackite, paratacamite and atacamite by infra-red spectroscopy*. In Icom committee for conservation. 6th triennial meeting, Ottawa, 21-25 September 1981. Preprints (11-11).

- Toumazou, M. K., Yerkes, R. W., & Kardulias, P. N. (1998). *Athienou Archaeological Project: Investigations in the Mallowra Valley, Cyprus, 1990–1995*. *Journal of Field Archaeology*, 25 (2), 163-182.
- Tylecote, R. F. (1979). *The effect of soil conditions on the long-term corrosion of buried tin-bronzes and copper*. *Journal of Archaeological Science*, 6 (4), 345-368.
- Tylecote, R. F. (1982). *The Late Bronze Age: copper and bronze metallurgy at Enkomi and Kition*. *Early metallurgy in Cyprus, 4000-500*.
- Ullmann, F., Gerhartz, W., Yamamoto, Y. S., Campbell, F. T., Pfefferkorn, R., & Rounsaville, J. F. (1985). *Ullmann's encyclopedia of industrial chemistry*. VCH publishers.
- Vernon, W. H. J., & Whitby, L. (1929). *The open-air corrosion of copper: A chemical study of the surface patina*. *The journal of the Institute of Metals*, 42 (2), 181-202.
- Watkinson, D. (2010). *Preservation of metallic cultural heritage*. *Shreir's Corrosion*. (4), 3307-3340
- Weil, P. D. (2007). *Technical Art History And Archeometry I Patina: Historical Scientific And Practical Considerations*. *Revista Brasileira de Arqueometria, Restauração e Conservação*, 1(2), 60-66.